MESENCHYMAL STEM CELLS-LIKE CELLS FROM PLURIPOTENT STEM CELLS

DERIVING MESENCHYMAL STEM CELLS-LIKE CELLS WITH IMPROVED ADIPOGENIC CAPACITY FROM PLURIPOTENT STEM CELL SOURCES

By: RUPAL HATKAR, B.Sc

A Thesis Submitted to the School of Graduate Studies in Partial Fulfillment of the Requirements for the Degree Master of Science

McMaster University MASTER OF SCIENCE (2016) Hamilton, Ontario

(Biochemistry & Biomedical Sciences)

TITLE: Deriving Mesenchymal Stem Cell-like Cells with Improved Adipogenic Capacity from the Pluripotent Stem Cell Sources

AUTHOR: Rupal Hatkar, B.Sc. (Hon., McMaster University)

SUPERVISOR: Eva Szabo, Ph.D.

NUMBER OF PAGES: xv, 104

ABSTRACT

Mesenchymal stem cells (MSCs) have been used for tissue repair, tissue regenerative purposes, to understand cell biology of various cell types, and as an in vitro model of a disease in vitro. Primary MSCs isolated from adult human tissue (i.e. adipose tissue), have been shown to have limited proliferative and differentiation capacity over passages in vitro. Due to the limited availability of tissue donors, it is difficult to obtain sufficient primary MSCs for therapeutic purposes. Therefore, pluripotent stem cells (human embryonic stem cells, hESCs, and induced pluripotent stem cells, iPSCs) have been used an alternative source to obtain the unlimited source of MSC-like cells. These cells are reported to have similar morphological and phenotypical characteristics but have lower differentiation capability compared to primary MSCs. Additionally, the protocols used for derivation of MSC-like cells from PSC sources are lengthy, expensive, and labour intensive.

In this study, I established a method for derivation of MSC-like cells from the cells surrounding H9 hESCs and a-iPSCs (iPSC-derived by reprogramming adipose tissue-derived stem cells (ADSCs)) through a simple trypsinization step. These MSC-like cells exhibited typical fibroblastic morphology and MSC surface marker profiles akin to bonafide adult MSCs, such as ADSCs. Compared to other studies, this protocol is more time and labour efficient, and it results in the derivation of significantly more (60%) lipid droplets forming cells. However, further characterization of these cells as adipocytes is necessary, given that their differentiation capacity remains limited when compared to ADSCs.

To improve the differentiation capacity of the MSC-like cells derived from H9 hESC or a-iPSCs, I explored: 1. the role of two transcription factors, peroxisome proliferator-activated

receptor γ2 (PPARγ2) and Krüppel-like factor 4 (Klf4), both of which have been shown to enhance adipogenesis in the murine system; and 2. the effect of culture media used for adipocyte differentiation. Through these studies, I discovered that neither Klf4 nor PPARγ2 induction improved adipocyte development in my human system. Accordingly, I did not observe an increase in the adipogenic capacity of the MSC-like cells regardless of the method by which Klf4 was induced (ectopic expression or chemical induction using IBMX), or through induction of PPARγ2 using dexamethasone. However, my studies did show a significant improvement in the appearance of lipid droplet containing cells, akin to adipocytes, upon culturing the MSC-like cells with the specific concentration of MEF (Mouse Embryonic Fibroblast)-condition media compared to well-defined media that have been used for prior differentiation protocols.

Overall, compared to ADSCs, H9-MSCs and a-iPSC-MSCs displayed a unique expression pattern of MSCs and early epithelial to mesenchymal transition (EMT) genes, suggesting further analysis of H9-MSCs and a-iPSC-MSCs at global gene expression and an epigenetic level is required to improve quality of these cells to match that of adult MSCs, such as ADSCs. Additional optimization of H9-MSCs and a-iPSC-MSCs differentiation protocols is also necessary to ensure that the MSC-like cells are following the appropriate MSC differentiation trajectory, allowing us to obtain a bona fide MSC with mature adipocyte differentiation capacity, similar to that derived from ADSCs.

ACKNOWLEDMENT

I started my thesis work in Szabo laboratory 2.5 years ago. Along the way, there are several people that I must acknowledge for contributions to this work and support in general. I would like to start by thanking Dr. Eva Szabo for the opportunity of working in her lab. In addition to being one of the most intelligent and influential role models for me, Eva has been an incredible mentor, and more importantly a great friend. It's rare to find such extremely successful scientists who are kind and generous to their students and genuinely care about them. I leave the lab with the wealth of scientific knowledge and fondest memories of my life.

I also want to thank the members of my committee, Dr. Jonathan Draper and Dr. Geoff Werstuck for taking precious time from your busy schedule in order to provide valuable input during scheduled meetings and for being very supportive and providing great guidance throughout my graduate career.

I especially like to thank my fellow lab members, Kanwaldeep Singh and Alexandria Afonso, for working alongside me, for helping to overcome obstacles through combined efforts, for editing my reports with constructive feedback and for assisting me with last minute experiments.

I have been fortunate to have the opportunity to work with most of the members of the Stem Cell and Cancer Research Institute (SCC-RI). Thank you to all those who helped me overcome technical issues, for sharing meaningful conversations about life stories, experimental procedures, and sharing hours of laughter. I especially want to thank Minomi Kalpana

Subapanditha for keeping me sane during my grad school experience. Thanks also to Andrew Allen for your technical expertise and for facilitating smooth operations at the SCC-RI.

Lastly, I am thankful to my family and friends for their support, guidance, and encouragement. I feel lucky to have parents that gave me unconditional love and made incredible sacrifices for me. My older sister has always been supportive.

This thesis and the results presented herein could not have been attainable without the funding support received from the Canadian Institutes of Health Research (CIHR) and from the Department of Biochemistry and Biomedical Sciences at McMaster University.

TABLE OF CONTENT

LIST OF FIGURES

LIST OF TABLES

LIST OF ABBREVIATIONS

ADSCs	Adipose tissue derived stem cells
AD	After differentiation
Ang-1	Angiopoietin-1
AT	Adipose tissue
a-iPSCs	Induced pluripotent stem cells derived from ADSCs
BD	Before differentiation
bFGF	Basic fibroblast growth factor
BM	Bone marrow
BM-MSCs	Bone marrow derived mesenchymal stem cells
CCNB1	G2/mitotic-specific cyclin B1
CD	Cluster of differentiation
CDX1	Caudal type homeobox1
CEBP	CCAAT/enhancer-binding protein
CFU-F	Colony forming units-fibroblastic
DMEM	Dulbecco's Modified Eagle Medium
DMEM-F12	Dulbecco's Modified Eagle Medium- nutrient mixture F-12
DNA	Deoxyribonucleic acid
DPBS	Dulbecco's Phosphate Buffered Saline
EGF	Epithelial growth factor
EAE	Experimental autoimmune encephalomyelitis
EB	Embryoid bodies

EDTA	Ethylenediaminetetraacetic acid
EMT	Early epithelial to mesenchymal stem cells
FABP4	Fatty acid binding protein 4
FBS	Fetal bovine serum
FGF	Fibroblast growth factor
GNL3	Guanine nucleotide-binding protein-like 3
GLUT4	Glucose transporter 4
HGF	Hepatocyte growth factor
HSC	Haematopoietic stem cells
HSL	Hormone sensitive lipase
KGF	Keratinocyte growth factor
Klf4	Kruppel like factor 4
KO-DMEM	Knock-out Dulbecco's Modified Eagle Medium
LIF	Leukemia inhibitory factor
LPL	Lipoprotein lipase
M-CSF	Macrophage colony-stimulating factor
MEF	Mouse embryonic fibroblast
MEF-CM	Mouse embryonic fibroblast conditioned medium
MHC II	Major histocompatibility class II
MOI	Multiplicity of infection
Myf5	Mayogenic factor 5
MSCs	Mesenchymal stem cells

MSX1	Msh homeobox1
NCAM1	Neural cell adhesion molecule-1
hESCs	Human embryonic stem cells
hiPSCs	Human induced pluripotent stem cells
IBMX	3-Isobutyl-methylxanthine
ICAM1	Intercellular adhesion molecule-1
IL-1β	Interleukin 1β
IGF-1	Insulin growth factor-1
ISCT	International Society for Cellular Therapy
Oct4	Octamer-binding transcription factor 4
ORO	Oil Red O
PDGF	Platelet-derived growth factor
PPARγ2	Peroxisome proliferator-activated receptor-γ2
POU5F1	POU domain, class 5, transcription factor 1
PSCs	Pluripotent stem cells
RA	Retinoic acid
RNA	Ribonucleic acid
RT- qPCR	Reverse transcriptase quantitative polymerase chain reaction
SCF	Stem cell factor
SCID	Severe combined immune-deficient
SDF-1	Stromal cell derived factor-1
Sox2	(Sex determining region Y)-box 2

SSEA3	Stage specific embryonic antigen 3
SSEA4	Stage specific embryonic antigen 4
TGFβ	Transforming growth factor-b
TNFα	Tumor necrosis factor α
VCAM1	Vascular cell adhesion molecule-1
VEGF	Vascular endothelial growth factor
VIM	Vimentin

1. INTRODUCTION

1.1. What are stem cells?

Stem cells are defined by their ability to undergo numerous cell divisions while retaining their stem cell identity, called self-renewal, and, depending on external or internal stimuli, can differentiate into any cell type of the human body. During the process of differentiation, stem cells become restricted towards specific lineages (i.e. endoderm, ectoderm, and mesoderm)[1,2]. Their ability to self-renew and the number of lineages to which they can differentiate towards, dictates their placement in the hierarchy of stem cells. At the top of the hierarchy are totipotent stem cells followed by pluripotent stem cells (PSCs), which lose their potency in the process of differentiation to specific cell lineages. Further downstream are multipotent stem cells, such as mesenchymal stem cells (MSCs)[3], and stem cells that are lineage restricted, for example hematopoietic stem cells[4] and neural stem cells[5] that are limited to giving rise to the different blood cell types and all cell types of the nervous system, respectively (Figure 1). The exception is the MSC which can differentiate into at least three lineages, osteocytes, chondrocytes, and adipocytes (Figure 2)[6].

Another source of PSCs is the induced pluripotent stem cells (iPSCs). Recent studies have shown that virtually any adult somatic cells can be reprogrammed into iPSCs with equal differentiation potency to ESCs using integrative (lentivirus) and non-integrative (i.e. RNA based methods; Sendai virus) reprogramming techniques (Figure 1)[7].

1.2. Pluripotent stem cells

Theoretically, pluripotent stem cells (PSCs) have the ability to produce copies of themselves indefinitely without signs of replicative senescence[10] through the process called self-renewal. Self-renewal in PSCs is governed by a complex networks of transcription factors,

including Oct3/4, Nanog and Sox2, which have been shown to maintain PSCs' pluripotent state [8, 9, 10]. In addition, PSC are also defined by the presence of cell surface markers, such as stage-specific embryonic antigen-3 (SSEA3), stage-specific embryonic antigen-4 (SSEA4), TRA antigens (TRA-1-60), which have been shown to be specific to PSCs, however their functional role remains to be delineated[11, 12].

Importantly, PSCs are able to differentiate into all cell types of the body[2]. Therefore, various potential sources and approaches have been used to generate human PSC lines of both embryonic and non-embryonic origin to identify factors and conditions that regulate both self-renewal processes and differentiation towards specific lineages.

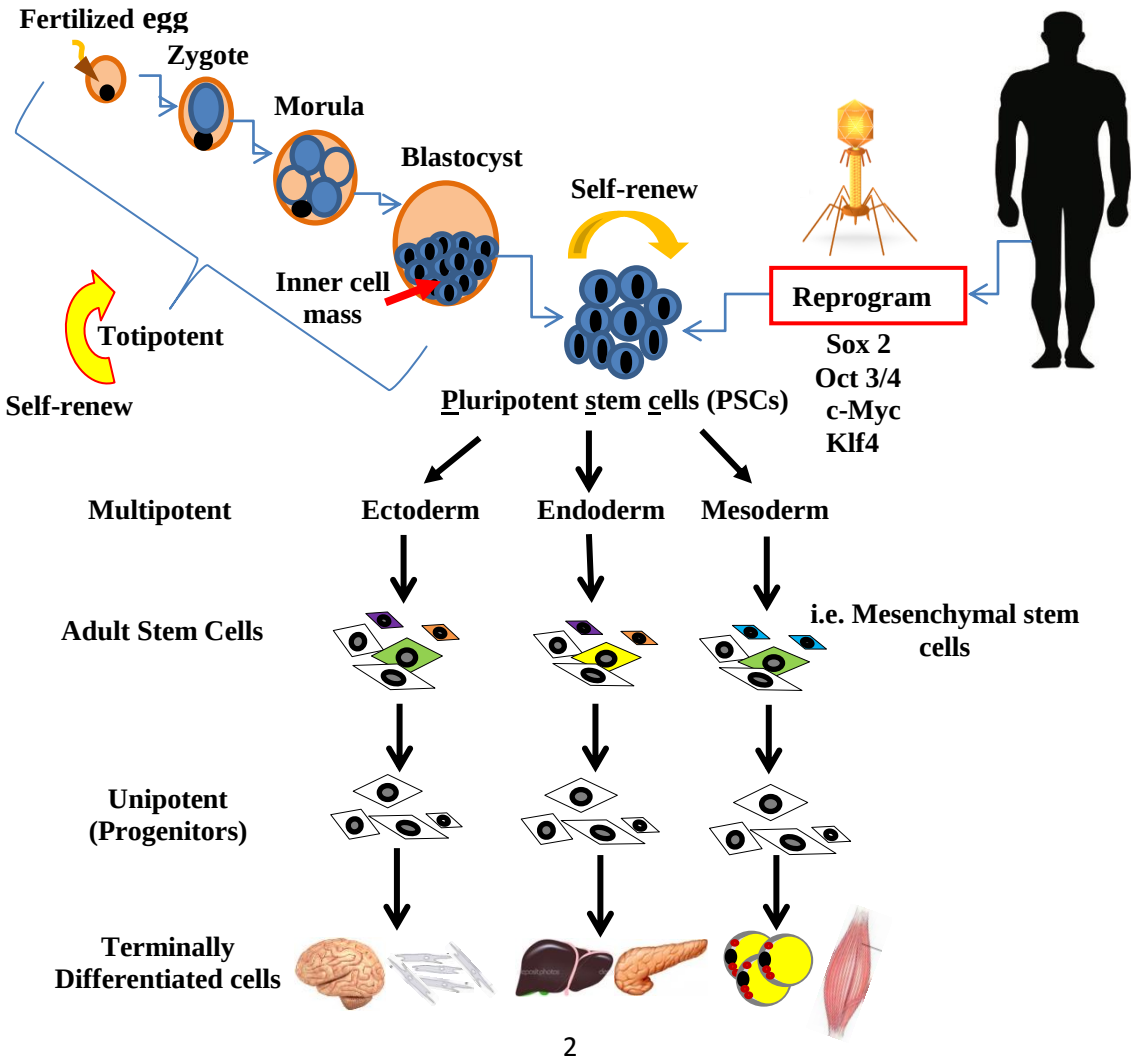

Figure 1: **Hierarchy of stem cells differentiation**. Pluripotent stem cells (PSCs) can be derived from either the inner cell mass of a blastocyst or adult human somatic cells via reprogramming using Oct4, Sox2, c-Myc, and Klf4. These cells can be further differentiated into the three germ layers (ectoderm, endoderm, and mesoderm). Subsequently, these cells lose pluripotency and differentiate to adult stem cells that are even more lineage-restricted. These cells then give rise to progenitor cells which have limited proliferation and differentiation capacity. The progenitors give rise to mature post-mitotic terminally differentiated cells.

1.2.1. Human PSCs from embryonic origin

Initially, PSCs were isolated from teratocarcinoma and grown in cell culture as stem cells, which are now known as embryonal carcinoma (EC) cells[13]. These cells were initially used for *in vitro* modeling of early mouse development[14]. However, EC cells harbor genetic mutations and have an abnormal karyotype, which hampers their use in understanding normal development[15]. In 1981, a new era for stem cell biology was initiated by the isolation of embryonic stem cells (ESCs) from the inner cells mass (ICM) of a mouse blastocysts stage embryo, which is formed during early embryogenesis[16]. It was noted that the outer layer of the blastocyst stage embryo, called trophectoderm forms extra-embryonic tissue, which give rise to the placenta, chorion, and umbilical cord[16]. The researchers also reported optimized culture conditions to propagate mouse ESCs (mESCs) *in vitro* for at least 100 passages without noticeable lose in self-renewal capacity and maintain differentiation capacity towards the three germ layers[16, 17].

Subsequently, the techniques used to derive mESCs were applied to derive ESC lines from non-human primates (e.g. rhesus monkey[18] and Callithrix jacchus[19]). This was followed by derivation of human ESCs line in 1998 by Thomson and coworkers from the ICM of a human *in vitro* fertilized (IVF) embryo, which, similar to undifferentiated nonhuman primate ES and human EC cells, were able to self-renew and differentiate into the three germ layers, expressed similar surface markers (SSEA3, SSEA4, Tra-1-60 and Tra-1-81); and were karyotypically stable over passages[20]. Additionally, hESCs were able to give rise to teratomas, which include tissues representing all three germ layers, *in vivo* when injected subcutaneously or intra-testicularly into severe combined immunodeficient (SCID)[20]mice lacking both B and T cells[21], making the study of hESC behaviour feasible to study *in vivo*[22] without the need for immunosuppressant drug[23]. Subsequently, in 2000 Benjamin Reubinoff and colleagues, showed ability of human blastocyst derived ICM to expand on mouse embryonic fibroblast (MEFs) while maintaining same characteristics as previously mentioned undifferentiated hESCs over passages and further characterized these cells by showing expression of octamer-binding transcription factor 4 (Oct4) in the undifferentiated hESCs[24]. Human ESCs derived in this study were also able to differentiate into all three embryonic germ layers (endoderm, ectoderm and mesoderm) and spontaneously differentiate into neural progenitor cells when cultured *in vitro* at high density [24].

Another method for generating human PSC line was published in 1998 by John Gearhart and coworkers, who isolate specialized cells known as primordial germ cells (PGCs) from 5-7 week old embryo, which are destined to become either oocytes or sperm cells, depending on the sex of the developing embryo[25]. The resulting cells in culture are called embryonic germ cell lines, which share many properties with hESCs. However, compared to hESCs, PGCs present

challenges with sustained growth in culture, as PGCs spontaneously differentiated to other cell types *in vitro*, which hindered the isolation of pure clonal lines[26]. Therefore, the application of these cells requires a more complete understanding of their derivation and maintenance *in vitro*[25, 26, 27].

The methods explained above involve destroying a living preimplantation embryo that has potential to develop into a human being. Therefore, significant ethical issues exist in use of ESCs for therapeutic purposes[28]. This has lead exploration of other strategies for derivation of hESC lines. For example, in 2006 Robert Lanza isolated single cell from a pre-implantation cleavage-stage embryo, thus preventing destruction of a live human embryo. The single cell was then expanded to a hESC line, which behaved like PSCs, including making proteins critical for stemness and having the capacity to give rise to all three germ layers [29, 30]. Another method for deriving tissue-matched hESCs that does not require destruction of a fertilized embryo is hESCs isolated from an embryo created without fertilizing an egg with a sperm through a process called parthenogenesis, giving ability to generate tissue-matched cells for transplantation to treat women who are willing to provide their eggs[31, 32].

While the hopes for hESCs is their use for regenerative therapies, the issue of histocompatibility in the recipient individual remains a concern regardless of the method used to derive PSCs[33]. To overcome this issue, somatic cells have been reprogrammed to pluripotent state through a process called somatic cell nuclear transfer (SCNT), which involves replacing nucleus of an oocyte with the nucleus of a somatic cell (a differentiated adult cell from elsewhere in the body)[34]. These cells develop into a the blastocyst stage embryo after alteration of the state of the mature nucleus to pluripotent state by factors present in the oocyte cytoplasm through a

process called nuclear reprogramming[35]. ICM from the blastocyst stage embryo is then removed and cultured as hESCs[34, 35]. Another method of reprogramming somatic cells to pluripotent state is by fusion of a somatic cells with hESCs, which indicated that factors provided by PCSs can reprogram somatic nulei[36].

1.2.2. Human PSCs from non-embryonic origin

More recently the reprogramming was revolutionized by the discovery of induced pluripotent stem cells (iPSCs)[37]. These iPSCs were derived by reprogramming skin fibroblast to pluripotent state by ectopically overexpressing of a cocktail of transcription factors using retroviruses or lentiviruses. The most common transcription factors used for reprograming purpose are OCT4 (also known as POU5F1, POU domain, class 5, transcription factor 1), Sry-box containing gene 2 (SOX2), myelocytomatosis oncogene (MYC) and Krüppel-like factor 4 (KLF4) (Figure 1)[37]. Other pluripotency transcription factors such as Nanog and Lin28 also have been used for reprogramming somatic cells to a pluripotent state[38]. In the process of reprogramming somatic cells to pluripotent state, these transcription factors have been shown to alter senescence-associated DNA methylation (DNAm) acquired during *in vitro* expansion[39] and age-related DNAm, accumulated during aging of the organism[40], to resemble those of hESCs[41] and regulate genes involved in maintaining hESC-like pluripotency[42].

1.2.3. Properties and applications of PSCs

The establishment of PSCs have provided a biologically relevant *in vitro* model for studying early human development and the molecular mechanisms involved in early stages of cellular commitment towards various lineages[43,44,45]. These mechanisms include epigenetic changes (traits that may be inherited that do not arise from changes in the DNA sequence) to the chromatin[34, 37], developmental changes in gene expression[37], response to growth factors, and

interactions between adjacent cells[35]. Understanding these basic mechanisms may enable future scientists to mobilize and differentiate endogenous populations of pluripotent cells to replace a cell type ravaged by injury or a disease. Moreover, PSCs derived from genetically abnormal embryonic or somatic cells provide a disease model that allows understanding of the genetic-bases of the specific disease and the abnormal cellular processes that drive disease development.

Additionally, since, iPSCs can be derived by reprograming any somatic cells of a patient derived through either SCNT, cell fusion, or use of reprogramming transcription factors, iPSCs can be used to develop human cell based disease models *in vitro* and screen for patient specific drugs [34, 35, 37] . For example, iPSCs derived from William-Beuren Syndrome (WBS) patient's skin fibroblast have been used to model and develop the drug (rapamycin) as potential treatment for WBS, which is caused by a microdeletion that removes elastin, resulting in elevated vascular stromal muscle cells proliferation and stenosis[46]. Similarly, differentiation of diabetic patient's foreskin fibroblast derived iPSCs to pancreatic lineage and endothelial cells can be used to better understand the mechanisms responsible for defective insulin production or vascular dysfunction[47]. Moreover, vascular cells derived by differentiating iPSCs from reprogramming skin fibroblasts of type-I diabetes patient have been shown to repair vascular tissue in mouse model[48].

Regardless of the method used to derive PSCs, each of the embryonic or non-embryonic origin has limitations, which hinders their use clinical applications.

1.2.4. *Limitations of PSCs*

PSCs (hESCs and iPSCs) are grown either directly on feeder cell layer of mouse embryonic fibroblasts (MEFs)[20] or indirectly as a source of MEF conditioned medium[49], increasing the risk of contamination with murine viruses or other proteins that hinder their use

for transplantation therapies. In the case of embryonic germ cell lines derived from PGCs, the issue is that these cells differentiate spontaneously *in vitro,* restricting sustained growth in culture and thus hindering the isolation of pure clonal lines. Therefore, more complete understanding of EGCs derivation and maintenance *in vitro* is needed[26, 27] before these cells can be used for clinical applications. Additionally, while hESC lines derived from single cell embryo biopsy possess properties of PSCs, they may lack capacity to differentiate into all mature cell type of a human being[30]. The limitation for the use of PSCs derived by SCNT method lies in the fact that the mitochondrial genome carried by the oocyte used to hold the donor somatic cell's nucleus increases the chances of tissue rejection and thus preventing use of these cells for transplantation therapies[50]. Moreover, somatic cells reprogrammed through cell fusion contain four copies of the cellular DNA rather than the normal two copies, making PSCs derived using this technique difficult to use for clinical applications, unless an extra set of chromosome is removed[36]. Furthermore, reprogramming somatic cells to pluripotent state using retroviruses and lentiviruses may result in viral genome integration into the host genome and possible re-expression of the ectopic genes following differentiation[7].

Regardless of the method used to derive PSCs, from embryonic[51] or non-embryonic[52] origin, these cells have a tendency to form teratoma *in vivo,* which hinders their direct application towards regenerative therapies. Additionally, differentiation of PSCs to a specific lineage requires the correct stimuli and culture conditions, an aspect of PSC biology that is difficult to control. This is because detailed molecular analysis of pathways necessary to obtain pure population of the mature adult cell types is largely unknown[53, 54]. Furthermore, the growth factors (e.g. bone morphogenetic factor 4 (BMP4) and Wnt proteins) that are known to drive

early commitment of PSCs to specific cell type are used across multiple lineages, therefore it remains unclear what concentration and timeline of exposure is required for directed differentiation to a specific lineage [55, 56, 57]. As such, instead of PSC, many studies are using adult multipotent stem cells, given that they have a more restricted number of lineages that they can differentiate towards and the differentiation conditions required are better defined.

1.3. Adult multipotent stem cells

Adult multipotent stem cells differentiate into limited lineages and are also more limited in their self-renewal and proliferative capacities compared to PSCs. Theoretically, multipotent stem cells reside in almost all organs of a human body[58] for the maintenance of the corresponding tissues over a lifespan of an individual[59]. Multipotent stem cells were first isolated in 1976 by Friedenstein et al. from the bone marrow (BM) based on their differential adhesion properties. These cells, called haematopoietic stem cells (HSCs), were a mixture of cells that had clonogenic and non-phagocytic capacity, and were fibroblastic in nature with the ability to give rise to colony forming units-fibroblastic (CFU-F)[60]. However, while HSC can be functionally defined, their isolation remains challenging in humans, since surface markers only enriches for them, but do not allow exact identification of a bonafide HSC.

Alternatively umbilical cord blood has also been used as a source of multipotent stem cells, since these cells can be isolated with minimal invasive procedures without any harm to the mother or infant [61]. Adipose tissue (AT) is another source that can be used to obtain multipotent stem cells with similar properties as bone-marrow (BM) derived counterparts. Stem cells derived from AT are called adipose-tissue derived stromal cells (ADSCs)[62]. Multipotent stem cells or

multipotent stromal cells were further characterized by an international consortium and named collectively as mesenchymal stem cells (MSCs)[63].

1.4. Mesenchymal stem cells

Mesenchymal stem cells (MSCs) can be theoretically found in almost all postnatal organs and tissues (i.e. BM[64] and AT[6])[58]. During human development, MSCs can arise from all three germ layers: mesoderm, endoderm, and ectoderm[65]. These MSCs represent prenatal multipotent stem cells with ability to self-renew and give rise to the cell types of corresponding germ layers or trans-differentiate into cell types of other germ-layers, depending on the stimuli received from the surrounding cells[65].

1.4.1. Properties of MSCs

Postnatal MSC preparation and their differentiation potential into certain lineages varies greatly and is affected by their origin, such as BM or AT, as well as cell-culture media used to expand them[66, 67]. This makes characterization of MSCs and comparison between studies difficult to achieve. Regardless of the source of MSCs, they must meet three of the criteria set by *International Society for Cellular Therapy (ISCT) or International Federation of Adipose Therapeutics and Science (IFATS)*[68]. The first criterion is MSCs should be able to adhere to plastic tissue culture plate and have fibroblast-like morphology. Second, although the markers used to define MSC are not very specific, there are certain patterns of surface marker expression that MSCs possess, such as being positive for CD90, CD73 and CD105 and negative for hematopoietic markers (CD45 or CD117), endothelial markers (CD31), and major histocompatibility complex class II (MHC class II) surface molecules (Figure 2)[59, 69]. In addition to the *ISCT criteria*, studies have proposed that MSC should also express a set of cell surface

antigens, including stromal precursor antigen 1 (STRO1), vascular cell adhesion molecule 1 (VCAM-1)[70], Src homology 2 (SH2), SH3, SH4), CD271, ganglioside 2 (GD2), and stage-specific embryonic antigen-4 (SSEA4)[9]. The third criterion set out by *ISCT* is that MSCs should be able to differentiate into osteogenic, chondrogenic, and adipogenic lineages (Figure 2), proving their multipotency[4].

1.4.2. *Application of MSCs*

Even though MSC differentiation potential is less broad than that of ESCs or iPSCs, MSCs have been used in many pathological and physiological processes, including cellular homeostasis, aging, tissue damage, and inflammatory diseases[71] within the same individual or different individual.

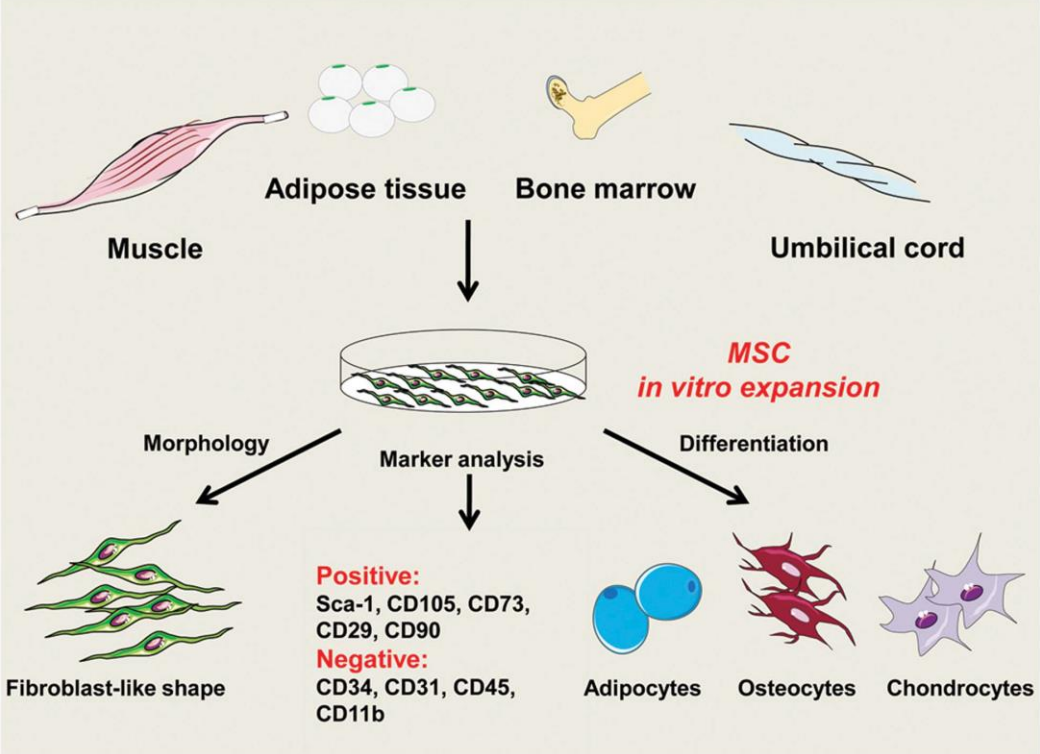

Figure 2: Properties of MSCs. MSCs can be isolated from many different tissues, including adipose tissue, muscles, bone marrow, umbilical cord blood, peripheral blood, etc. MSCs are defined *in vitro* by their ability to adhere to plastic tissue culture plate, have fibroblast-like morphology, express panel of markers: positive for CD90, CD105, CD73, CD29, and sca-1 and negative for CD34, CD31, CD45, CD11b. They have ability to differentiate into at least adipogenic, osteogenic, and chondrogenic lineages.

1.4.2.1. Regeneration and tissue repair for surgeries

Depending on the microenvironment surrounding MSCs, they have been shown to modulate inflammatory responses. At the site of injury, inflammatory mediators, such as TNFα (tumor necrosis factor α), IL-1β (interleukin 1β), free radicals, chemokines, and leukotrienes, are often produced by phagocytes in response to damaged cells[72]. This leads to expression of adhesion molecules, such as CXCR3 ligands, CCR5 ligands, intercellular adhesion molecule-1 (ICAM-1) and vascular cell adhesion molecule-1 (VCAM-1). These adhesion molecules activate T cells and recruit leukocytes to the site of inflammation to suppress immune response[70]. This also leads to mobilization of tissue resident or BM MSCs to the site of injury, where they secrets many growth factors, such as epithelial growth factor (EGF), fibroblast growth factor (FGF), platelet-derived growth factor (PDGF), transforming growth factor-β (TGF-β), vascular endothelial growth factor (VEGF), hepatocyte growth factor (HGF), insulin growth factor-1 (IGF-1), angiopoietin-1 (Ang-1), keratinocyte growth factor (KGF), leukemia inhibitory factor (LIF)[73] and stromal cell derived factor-1 (SDF-1)[74]. These growth factors, promote the development of fibroblasts, endothelial cells and tissue progenitor cells, which carry out tissue

regeneration and trigger tissue repair[71, 75, 76]. Additionally, growth factors such as stem cell factor (SCF), macrophage colony-stimulating factor (M-CSF), SDF-1 , Ang-1 and many chemokines also have been shown to intrinsically trigger tissue repair[71]. HGF, an established growth factor in MSC-based tissue repair, was recently shown to be effective in modulating endogenous neural cell re-myelination, enhancing functional recovery in both experimental autoimmune encephalomyelitis (EAE) and spinal cord demyelination[77]. Therefore, paracrine factors produced by MSCs are shown to provoke tissue-resident progenitor cells or other relevant cells to initiate tissue repair, explaining the beneficial effects of MSCs on tissue repair, even in the absence of local MSC engraftment [77, 78].

1.4.2.2. *Graft vs host disease*

When tissue, an organ, or cells are transplanted from one individual to another individual, the transplanted lymphoid cells mount an immune response against host cells. If the transplanted tissue, an organ, or cells are recognized as non-self, the resulting syndrome is known as graft versus host disease[79]. Primary MSCs are described as MHC II negative cells, lacking molecules such as CD40, CD80, and CD86, which permits allogenic transplantation without immunosuppression[80]. MSC-based treatment for a variety of conditions has been demonstrated in humans. Adipose tissue-derived MSCs (i.e. ADSCs) are currently being investigated in autologous transplantations to improve revascularization and tissue perfusion in ischemic limbs. Additionally, MSCs also have been used for treating many other diseases such as bone defects[81], cartilage degeneration[82], metabolic bone disease[83], ischemic heart disease[84], and cerebral ischemia[85].

1.5. Limitations of primary MSCs

Differences appear between MSC populations from different tissues, representing a challenge to devise a universal definition[86]. Although the criteria to define MSCs are widely accepted, they are imperfect as the three markers (CD90, CD73, and CD105) are co-expressed in a wide variety of cells[67], making identification of a single MSC population *in vivo* difficult[87]. To be able to use MSCs for clinical applications, the cells should be found in abundant quantities, harvested and isolated through a minimally invasive procedure and should be able to differentiate along multiple cell lineages in a reproducible manner[88]. However, there are very few donors who consent to provide tissue for deriving primary MSCs. While stem cells are capable of continuous regeneration and expansion throughout an individual's life, MSCs demonstrate limited proliferative and differentiation capacity over passages *in vitro*[89] due to replicative senescence over passages[90]. In addition, MSCs isolated from older donors demonstrate lower proliferation potential, reducing healing capacity in older patients[91]. The exact anatomical location of MSCs *in situ* is also not clear[88], limiting our capacity to isolate MSCs for autologous cell-based therapy to treat diseases, such as obesity and lipodystrophy. To overcome some of these limitations an alternative source of MSCs are needed and one such source would be from derivation of MSCs from PSC sources.

1.6. Alternative source of MSCs

1.6.1. Current knowledge on derivation of MSCs from PSCs

PSCs have the ability to self-renew extensively in culture without any sign of replicative senescence, and can serve as alternative source for large scale generation of standardized derivatives, such as PSC-derived MSCs. Therefore, several groups of researchers have attempted

to derive MSCs from PSC sources (ESCs and/or iPSCs) using different methods. Most studies utilized uncontrolled differentiation of BMSC-iPSCs to embryoid bodies (EB), culturing them on 0.1% gelatin-coated plate and using EB outgrowths to obtain MSC-like cells[92, 93, 94]. A few other studies simply let skin fibroblast[95] or BM-MSCs[92, 94, 96] derived iPSCs spontaneously differentiate on 0.1% gelatin-coated plate and collagen I coated plates[97, 98] to MSC-like cells or co-cultured BMSC-iPSC derived MSCs with BMSCs[94] or with BMSC conditioned media[94] (Table 1). Similar to primary MSCs, PSC-derived MSCs using these methods had fibroblast-like morphology, > 90% cells expressing MSC markers (i.e. CD90, CD73, CD105, and CD29), and <2% cells expressing hematopoietic markers (i.e. CD45 and CD34). However, they were not able to efficiently differentiate into adipocytes, osteoblasts, or chondrocytes, more specifically these MSC had limited to no adipogenic capacity. In addition, the protocols used are very time consuming, laborious, and expensive as some protocols involve sorting desired population of cells and using primary MSC conditioned media to grow PSC-derived MSCs, taking over 35 days to obtain MSC-like cells[97, 93, 99]. Therefore, a more efficient and effective protocol is required not only for functional and molecular studies to facilitate understanding of the developmental path and downstream differentiation capacity of MSCs, specifically towards the adipogenic lineage, but also to obtain cells for downstream application including regenerative therapies and understand cell biology of a cell type, such as adipocytes.

Table 1: Comparison of methods used and time taken to derive MSC-like cells from different human PSC sources.

hPSC source of MSC-like cells	Method used to obtain MSC-like cells	Matrix used to derive MSC-like cells	Time taken to derive pure MSC-like cells population	Reference
BM-MSCs derived iPSCs	**1**-Spontaneous differentiation **2**-From EB outgrowths	0.1% Gelatin or no coating	35 days	92
Skin fibroblast derived iPSCs	From EB outgrowths	0.1% Gelatin	32 day	93
-H9 hESCs -Skin fibroblast derived iPSCs	Spontaneous differentiation	Collagen I	30 days	97
Gingiva, Lung, and periodontal ligament MSCs derived iPSCs	Spontaneous differentiation	0.1% gelatin for P1 and P2 followed by no coating for subsequent passages	45 days	96
BM-MSCs and amniotic epithelium derived iPSCs	**1**-Spontaneous differentiation **2**-From EB outgrowths **3**-Indirect BM-MSCs co-culture **4**-BM-MSCs growth medium	0.1% Gelatin	**1**- 32 days **2**- 35 days **3**- 45 days **4**- 60 days	94
Skin fibroblast derived iPSCs	Spontaneous differentiation	0.1% gelatin	40 days	95
-Foreskin keratinocytes derived iPSCs -H9 hESCs	Spontaneous differentiation	Collagen I or no coating	36 days	98

1.7. Adipogenesis

Adipogenesis is the process of cellular differentiation by which preadipocytes take on the characteristic of mature adipocytes. Expansion of adipose tissue encompasses two ways: 1)

increase in size of the existing adipocytes due to lipid accumulation or 2) differentiation of new adipocytes from the MSCs residing in adipose tissue[100, 101]. Obesity is due to expansion of adipose tissue by both of these processes resulting in an overall increase in adipocyte number and size[102]. The current obesity epidemic and the resulting metabolic disorders, such as type II diabetes[103, 104] and cardiovascular diseases[101, 105], have made understanding normal and aberrant adipocyte development important towards delineating pathophysiology of obesity[106, 107]. Researchers have used both adult stem cell models and cell lines, such as 3T3-L1 cells, to understand adipocyte development. However, the majority of the studies were conducted using the murine system, thus its direct translation to the human remains unclear. More recently, a few studies have employed human and mouse PSCs to study adipogenesis. This is due to the fact that theoretically PSCs are able to differentiate into any cell type of a human body including adipocytes.

1.7.1. *Adipogenesis from PSCs*

Both mouse and human ESCs and iPSCs have been utilized to obtain adipocytes *in vitro.* Studies using mouse ESCs showed that adipogenesis involves two stages with first being specification of PSCs to MSCs and second being commitment of MSCs to preadipocytes, which later take on the characteristics of mature adipocytes through terminal differentiation. From the studies done on mouse ESCs, several chemical inducers, such as retinoic acid (RA)[108], dexamethasone, rosiglitazone, indomethacin, 3-Isobutyl-methylxanthine (IBMX) and hormonal adipogenic inducers such as insulin, have been shown to facilitate derivation of lipid droplet forming cells[99, 109]. Since microenvironment and biomaterial scaffolds surrounding mouse or human ESCs affect proliferation and differentiation, ESCs have been subjected to adipogenic

differentiation on different substrate, such as 0.1% gelatin[110], collagen II, and matrigel. Of these matrices, ESCs have been shown to most efficiently differentiate on collagen II[81]. To further increase the number of lipid droplet forming cells, different methods such as exiting pluripotency by forming EBs or using outgrowths of EBs prior to subjecting them to adipogenic differentiation have been employed. However, efficiency of adipocytes achieved using any of these methods is only ~9%, preventing use of these cells for modeling a metabolic disorder, or using them for therapeutic purposes[109, 111].

Therefore, given the low yield of adipocytes from ESC sources, many studies have utilized mouse preadipocyte cell lines (3T3-L1) to study cell biology of adipocyte development during commitment stage. From the studies done on immortalized cell lines (i.e. 3T3-L1[112] and 3T3-F442A[113]) [114], it was shown that during the process of adipocyte development cells go through a cell cycle growth arrest at G1/S phase boundary, which is a key event in MSC commitment to a preadipocyte. One factor that has been shown to regulate cell cycle growth arrest in 3T3-L1 preadipocytes is Klf4. This transcription factor inhibits expression of the cell cycle-promoting genes *CCND1* (cyclin D1)[115] and *CCNB1* (cyclin B1)[116]. After few rounds of cell divisions, Klf4 is shown to upregulate expression of transcription factor CCAAT/ element binding protein beta and delta (CEBPβ and δ). Expression of CEBPβ and δ subsequently leads to expression of the main adipogenic regulators peroxisome proliferator activator receptor gamma 2 (PPARγ2). PPARγ2 is shown to upregulate transcription factor CEBPα[117,113], which both are shown to regulate genes involved in glucogenesis, lipogenesis, and lipolysis related enzymes and glucose transporter 4[118].

Due to lack of step wise differentiation of ESCs to adipocyte development, understanding development before preadipocyte commitment remains unclear. Thus, a better understanding of the mechanisms involved in early steps of adipogenesis from ESCs to MSCs and from MSCs to preadipocyte stage is needed to obtain a complete picture of adipogenesis.

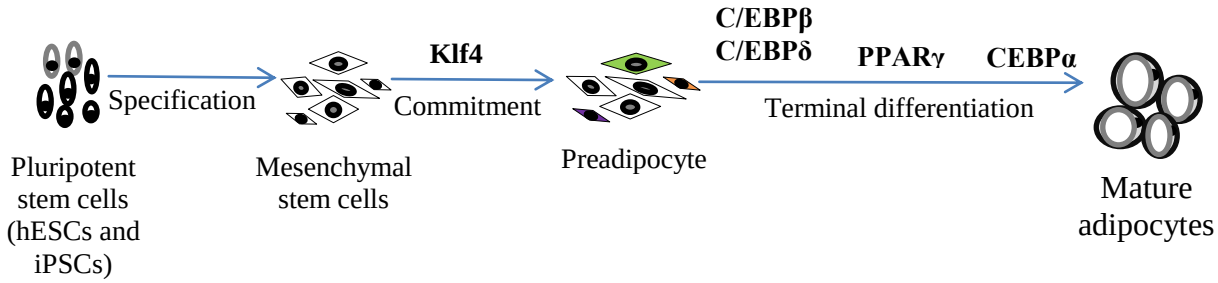

Figure 3: Stages of adipocyte development from PSCs. Differentiation of PSCs to MSCs involves specification following commitment of MSCs to the adipogenic lineages. This is followed by preadipocytes taking on characteristics of mature adipocytes through the process of terminal differentiation. As illustrated detailed analysis of factors involved in the process of adipocyte development, is known for the commitment and terminal differentiation stage. However, very little information is known for the specification stage.

2. Rationale for the project

While human MSCs can be derived from adult sources, such as bone marrow and adipose tissue, they have limited *in vitro* proliferation and expansion capacity along with small donor pool, limiting their use in the clinical and research settings. To address this, one option is to identify an alternative source for MSCs that lacks these limitations, such as PSCs. PSCs have unlimited proliferation capacity *in vitro* and have the potential to differentiate into any cell type of the body, including MSC-like cells. Several groups of researchers have tried to obtain MSC-like cells from PSCs sources using different previously described methods (Table 1). MSC-like cells obtained by these groups met some of the minimal criteria for defining PSC-derived MSC-like cells as MSCs. These criteria were PSC-derived MSCs' have plastic adherent property, fibroblastic shape, expression of the panel of surface markers, (such as CD90, CD73, CD105, CD44, and CD29), lacking expression of hematopoietic, endothelial, and epithelial markers (such as CD45, CD34, and CD13 respectively). However, while they showed some potential to differentiate into osteocytes and chondrocytes, they were severely limited in their capacity to differentiate into adipocytes. Moreover, the methods used to derive MSCs from PSCs were laborious and time consuming, taking over 35 days to obtain MSC-like cells. Given that efficiency of PSC-derived MSCs to differentiate into adipocytes was very low compared to the primary MSCs, a differentiation protocol from PSCs to MSC-like cells is required that is both efficient and less time consuming. Additionally, optimization of conditions to improve adipogenic differentiation potential of PSC-derived MSCs is also necessary.

MSC-like cells will be derived from PSCs, including H9 hESCs and ADSC derived iPSCs (a-iPSCs), to understand human adipogenesis.

3. Hypothesis

The cells surrounding hESCs and iPSCs colonies have fibroblast shape and also form small lipid droplets, suggesting their potential to have MSC properties. Therefore, I hypothesize that fibroblast shaped cells surrounding the PSC colonies have MSC properties.

4. Objectives

1) To characterize the MSC-like properties of fibroblast-like cells isolated from PSC colonies.

To reduce time and labour in obtaining MSC-like cells from the PSC sources (H9 hESCs and iPSCs derived from ADSCs (a-iPSCs)), the fibroblast-like cells surrounding PSC colonies were isolated and expanded until MSC-like population was obtained. To characterize fibroblast-like cells surrounding H9 hESCs and a-iPSCs as MSC-like cells, cell morphology, surface marker expression profile and differentiation capacity was compared to ADSCs. To further characterize MSC-like cells derived from H9 hESCs (H9-MSCs) and a-iPSCs (a-iPSC-MSCs), their gene expression profile was compared to ADSCs.

2) To optimize conditions to obtain functional adipocytes from PSC-derived MSCs.

To improve adipogenic potential of H9-MSCs and a-iPSC-MSCs, effects of known factors involved in inducing adipogenic programs in mouse preadipocyte cell lines were tested in H9-MSCs and a-iPSC-MSCs.

5. METHODS AND MATERIALS

5.1. Cell culture

5.1.1 *Re-establishing of H9 hESCs and a-iPSCs from previously frozen samples*

Previously frozen H9 hESCs of passage 55 (P55) in liquid nitrogen were thawed by diluting in 10 ml of Knock-out Dulbecco's Modified Eagle Medium (KO-DMEM, Gibco) followed by pelleting at 900 rpm for 60 seconds. The supernatant was aspirated and the pellet was re-suspended in 1 ml of mouse embryonic fibroblast conditioned medium (MEF-CM) with 0.8 ng/ml basic fibroblast growth factor (bFGF). MEF-CM was derived by culturing MEFs in MEF media composed of Dulbecco's Modified Eagle Medium (DMEM, Gibco), 10% fetal bovine serum (FBS, HyClone Thermo Fisher Scientific), and 1mM L-glutamine (Life technologies). The re-suspended H9 hESCs were divided into 2 wells of a 4-well tissue culture plate (BD Falcon) coated with 1:15 matrigel (Corning). Media was changed on daily until PSC colonies appeared and were confluent enough to pass into 1 well of a 1:15 matrigel-coated 12-well tissue culture plate. Similar procedure was employed to derive previously frozen a-iPSCs of P17 (a iPSC line that was derived from ADSCs by the Ph.D. candidate (Kanwaldeep Singh) in the lab).

5.1.2 *Maintenance of PSCs*

PSCs (hESCs and iPSCs) were cultured on 1:15 matrigel-coated 6- or 12-well plates and passeged every 6-7 days at 1:4 ratio. One day prior to passaging, tissue culture plate were coated with 1:15 matrigel and stored at 4^0 degree Celsius overnight. Prior to passaging, the PSCs were enzymatically digested for 50-60 seconds with collagenase IV followed by slow scarping of the

PSC colonies in MEF-CM and transfer of the scrapped colonies into matrigel coated tissue culture wells.

5.1.3 *Differentiation and maintenance of MSC-like cells*

Fibroblast surrounding PSC colonies were collected by treating H9 hESCs and a-iPSCs with 0.25% trypsin (Gibco by Life technologies) for 4-5 minutes followed by neutralizing with MSC culture media. The plates were tapped slowly to allow detaching of the cells surrounding the PSC colonies, which were then spun down at 1500 rpm for 5 minutes. The cells pellets were plated in 2 wells of a 6-well plate and this was called passage 0 (P0). The cells isolated from H9 hESCs and a-iPSCs culture were labelled H9-MSCs and a-iPSC-MSCs respectively. The medium was changed at day 1. Upon confluency after 3-4 days, the cells were trypsinized and passaged at 1:3 ratios into 6-well tissue culture plates following the same procedure used to extract cells from H9 hESCs and a-iPSCs cultures. MSC-like cells from both sources were passaged up to passage 7 (P7) and used for analysis and differentiation at P3 and P7.

5.1.4. Maintenance of ADSCs

ADSCs were cultured on tissue culture plastic plates (BD Falcon) in MSC media composed of Dulbecco's Modified Eagle Medium- nutrient mixture F-12 (DMEM-F12, Gibco), 10% FBS and 1 mM L-glutamine (Life technologies). The cells were passaged every 7 to 10 days at the density of 100k cells/well using the same procedure that was used for passaging H9-MSCs and a-iPSC-MSCs. Upon 100% confluency, ADSCs were used for adipogenic differentiation.

5.2. Adipogenic differentiation

5.2.1. ADSCs differentiation

ADSCs were cultured in tissue culture plates and upon reaching confluency, ADSCs were subjected to differentiation using 3ml adipogenic differentiation media per well of a 6-well plate. The differentiation media was composed of MSC media supplemented with adipogenic factors (0.5 µM dexamethasone, 1 µM rosiglitazone, and 10µg/ml Insulin). Subsequently, 50% of the media was changed every 3 to 4 days. At differentiation day 22 the cells were collected for downstream analysis.

5.2.2. H9-MSCs and a-iPSC-MSCs differentiation

Similar to ADSCs, H9-MSCs and a-iPSC-MSCs at P3 (collectively MSC-like cells derived from PSCs) were subjected to adipogenic differentiation when they reached 100% confluency. H9-MSCs and a-iPSC-MSCs were differentiated in 12-well tissue culture plate at the seeding density of 80K cells/well. The media composition was similar the adipogenic media used to differentiate ADSCs. Similar to ADSCs, 50% of the media was changed every 4 to 5 days until day 22nd.

5.2.3. Overexpression of Klf4 in H9-MSCs and a-iPSC-MSCs

H9-MSCs and a-iPSC-MSCs were seeded at 50K cells/well in a 12-well tissue culture plate. The next day cells were infected with *Klf4* containing Sendai viruses at MOI2 (Life technologies) in MSC media. The media was replaced with the fresh MSC media after 24 hours. Following this, the media was changed every 4-5 days until cells were at least 95% confluent. Upon confluency, the cells were subjected to adipogenic differentiation as described for H9-MSCs and a-iPSC-MSCs adipogenic differentiation. The infections were done by a Ph.D. candidate (Alexandrea Afonso) in the lab.

5.2.4. IBMX treatment in H9-MSCs and a-iPSC-MSCs

Similar to H9-MSCs and a-iPSC-MSCs differentiation, the cells were seeded at 80K/well density in 12-well tissue culture plate. Prior to starting differentiation, H9-MSCs were treated with 0.5nM 3-isobutyl-methyl-xanthine (IBMX) for 30 minutes, 1, 2, 6, 12, and 24 hours; and a-iPSC-MSCs were treated with IBMX for 30 minutes, 1 hour and 2 hours. After IBMX treatment, the cells were subjected to adipogenic differentiation with MSC media supplemented with the cocktail of adipogenic factors (0.5 µM dexamethasone, 1 µM rosiglitazone, and 10µg/ml Insulin).

5.3. Oil Red O (ORO) staining

Lipid accumulated in ADSCs, H9-MSCs, and a-iPSC-MSCs differentiated to the adipogenic lineage (at Day 22 of differentiation) were stained with 1 ml of ORO solution/well for 6-well plates and 500 µl of ORO solution/well for 12-well plates. The cells were stained at room temperature for 7-10 minutes followed by washing 3times with water, 2 minutes/wash. To prepare ORO solution, ORO powder was dissolved in 100% isopropanol, followed by dilution in water at the ratio of 6:4 and incubated for 7-10 minutes. The solution was then filtered using 0.22 µm syringe filter and was used immediately to stain lipid accumulated in the differentiated cells to adipogenic lineage. To measure amount of lipid accumulation in H9-MSCs, a-iPSC-MSCs, and ADSCs, ORO dye used to stain lipid was extracted in 500 µl/ well of a12 well plate in 100% isopropanol by gently shaking on a shaker for 30 min. Subsequently, 100 µl from each of 500 µl/ well Isopropanol with the extracted dye was aliquoted to a well of a flat-bottom 96 well plate. Absorbance value of the extracted dye in isopropanol was measured using the FLUOstart®Omega microplate reader software (BMG LABTECH).

5.4. Imaging (BF and ORO)

For the bright field (BF) imaging of ADSCs and PSC-derived MSC-like cells, the images were taken when the cells were ~60% confluent. The images were taken at 10X objective using the olympus phase-contrast microscope. BF images of H9 hESCs and a-iPSCs colonies were taken at 4X objective. Lipid droplets stained with ORO dye were imaged at 20X objective using colour camera of the same microscope under BF settings.

5.5. Flow cytometry

The surface marker (CD90, CD73, CD105, CD45, and SSEA3) expression for ADSCs, H9-MSCs, and a-iPSC-MSCs was tested at P3 and P7. For ADSCs, the cells were trypsinized using 500 µl of 0.25% trypsin/well for 4-5 minutes, followed by neutralization with 500 µl PEF (97% Dulbecco's Phosphate Buffered Saline, DPBS, 1mM Ethylenediaminetetraacetic acid, EDTA, 3% Fetal Bovine Serum, FBS). The detached cells were collected into a 15 ml falcon tube. For H9 hESCs and a-iPSCs, cells were singularised by triturating after partially detaching the cells from the plate using collagenase IV for 30-45 seconds. The cells were slowly scrapped with 5 ml pipette, suspended in 1 ml of PEF, followed by the collection of the cells into 15 ml falcon tubes. The collected cells from all sources were pelleted at 1500 rpm for 5 minutes. The cell pellet was re-suspended in 2 ml of PEF and filtered in a falcon 5 ml round bottom polystyrene test tube with cell strainer snap cap. Subsequently, 200 µl from the strained cells were aliquoted in 5 ml Falcon^{TM} round-bottom polystyrene tubes (Fisher Scientific). The cells were stained for 30 minutes (room temperature) at 1:200 dilution with the following antibodies: FITC-mouse $IgG_{1,k}$ anti-human CD73, PE-mouse $IgG_{1,k}$ anti-human CD105, APC-mouse $IgG_{1,k}$ anti-human CD45, PE-mouse $IgG_{1,k}$ anti-human SSEA3, and at 1:10000 dilution for APC-mouse

$IgG_{1,k}$ anti-human CD90. The cells were washed in 3-4 ml PEF and pelleted at 1500 rpm for 5 minutes followed by re-suspension in 200 µl PEF. The cells were analyzed using BD LSR II flow cytometer. The data was analysed using Flow Jo software.

5.6. RT-qPCR

Total cellular RNA from the frozen (-80^{o} C) palette of the trypsinized cells was isolated with the Qiagen RNeasy Plus Mini kit according to the manufacturer's instructions. Complementary DNA was generated using SuperScript III Reverse Transcriptase Kit in accordance with the manufacturer's instructions (Invitrogen). The expression of genes of interest was assessed by reverse transcriptase quantitative polymerase chain reaction (RT-qPCR) using GoTaq® qPCR Master Mix (Promega) using a Bio-Rad CFX96 Real-Time PCR detection system. The cycling protocol used was 95^{0}C for 2 min followed by 40 cycles consisting of 95^{0}C for 15 s, 60^{0}C for 1 minute, and 60^{0}C for 5 s, finished off at 95^{0}C for 5 s with 5^{0}C increment. See the table 2 for the primers used. The primers were obtained from the qPrimerDepot software.

Table 2: Primer sequences for RT-qPCR.

Gene name	5'- Primer sequence -3'	Length of the primer (bp)	GC%	Tm (°C)
PPARγ2-F	GCAGGAGATCTACAAGGACT	20	50	60
PPARγ2-R	CCCTCAGAATAGTGCAACTGG	20	50	60
CEBPα- F	CCACGCCTGTCCTTAGAAAG	20	55	61
CEBPα- R	CCCTCCACCTTCATGTAGAAC	21	55	61
Klf2- F	TTGCAGTGGTAGGGCTTCTC	20	55	60
Klf2- R	ACTCACACCTGCAGCTACG	20	60	61
Klf4- F	CCCCGTGTGTTTACGGTAGT	20	55	60
Klf4- R	GCGGCAAAACCTACACAAAG	20	50	60
Klf9- F	GCGGGAGAACTTTTTAAGGC	20	50	60
Klf9- R	CAGTGGCTGTGGGAAAGTCT	20	55	60
Klf15- F	CACACAGGACACTGGTACGG	20	60	60
Klf15- R	TGTACACCAAAAGCAGCCAC	20	50	59

MSX1- F	ACGGTTCGTCTTGTGTTTGC	20	50	61
MSX1- R	TCCTCAAGCTGCCAGAAGAT	20	50	60
CDX1- F	TGTAGACCACGCGGTACTTG	20	55	60
CDX1- R	GACGCCCTACGAGTGGATG	19	63	61
CD140B- F	CAGGAGAGACAGCAACAGCA	20	55	60
CD140B- R	AACTGTGCCCACACCAGAAG	20	55	61
GNL3- F	CACCACTGTTGGCAATTCTTT	21	43	60
GNL3- R	AGAAGAGGCCATTGTCCAGA	20	50	59
VIM- F	GCAAAGATTCCACTTTGCGT	20	45	60
VIM- R	GAAATTGCAGGAGGAGATGC	20	50	59
GAPDH- F	TCCCTGAGCTGAACGGGAAG	20	45	58
GAPDH- R	GGAGGAGTGGGTGTCGCTGT	20	55	61

F and R denote forward and reverse direction of each of the primers respectively.

5.7. Statistical analysis

For statistical analysis, the unpaired one-tailed Student's t-test was performed using Microsoft Excel. Differences were significant if the p value was <0.05, <0.01, or <0.001, which are depicted by *, **, or *** respectively. The error bars indicate ± standard deviation (± SD) of biological replicates.

6. RESULTS

6.1 Objective 1: To characterize the MSC-like properties of fibroblast-like cells isolated from PSC colonies

6.1.1. Aim 1. Differentiation of PSCs to MSC-like cells

MSC-like cells were derived from H9-hESCs (H9-MSCs) and iPSCs derived by reprogramming human ADSCs (a-iPSCs). As shown in Figure 4, the cells surrounding the H9-hESC colony (Figure 4A) and the iPSC colony (Figure 4B) have a fibroblast–like morphology. Upon closer examination of these cells, I observed that these cells contain small lipid droplets (Figure 4C and D). Therefore, these cells were isolated through trypsinization, and plated onto plastic tissue culture plates in MSC media (Figure 5) to investigate whether these cells: 1. are similar to MSCs, such as the ADSCs (that give rise to adipocytes); and 2. have comparable adipogenic capacity to ADSCs. To expand this population and to obtain a pure culture of MSC-like cells, these cells were cultured until 7 passages, and analyzed every 3rd passage.

To examine whether the MSC-like cells meet the criteria that is set by the International Society for Cellular Therapy (*ISCT*), I initially investigated the first criteria, which includes their capacity to: 1. adhere to tissue culture plastic and 2. having fibroblast morphology. As shown in Figure 6A, the fibroblast-like cells that were isolated from around the H9-hESCs and a-iPSCs colonies (now referred to as, H9-MSCs and a-iPSC-MSCs respectively) adhered to the tissue culture plate. H9-MSCs (Figure 6B) and a-iPSC-MSCs (Figure 5C) maintain fibroblast-like morphology over 7 passages, which is required to meet the first criteria of MSC characterization.

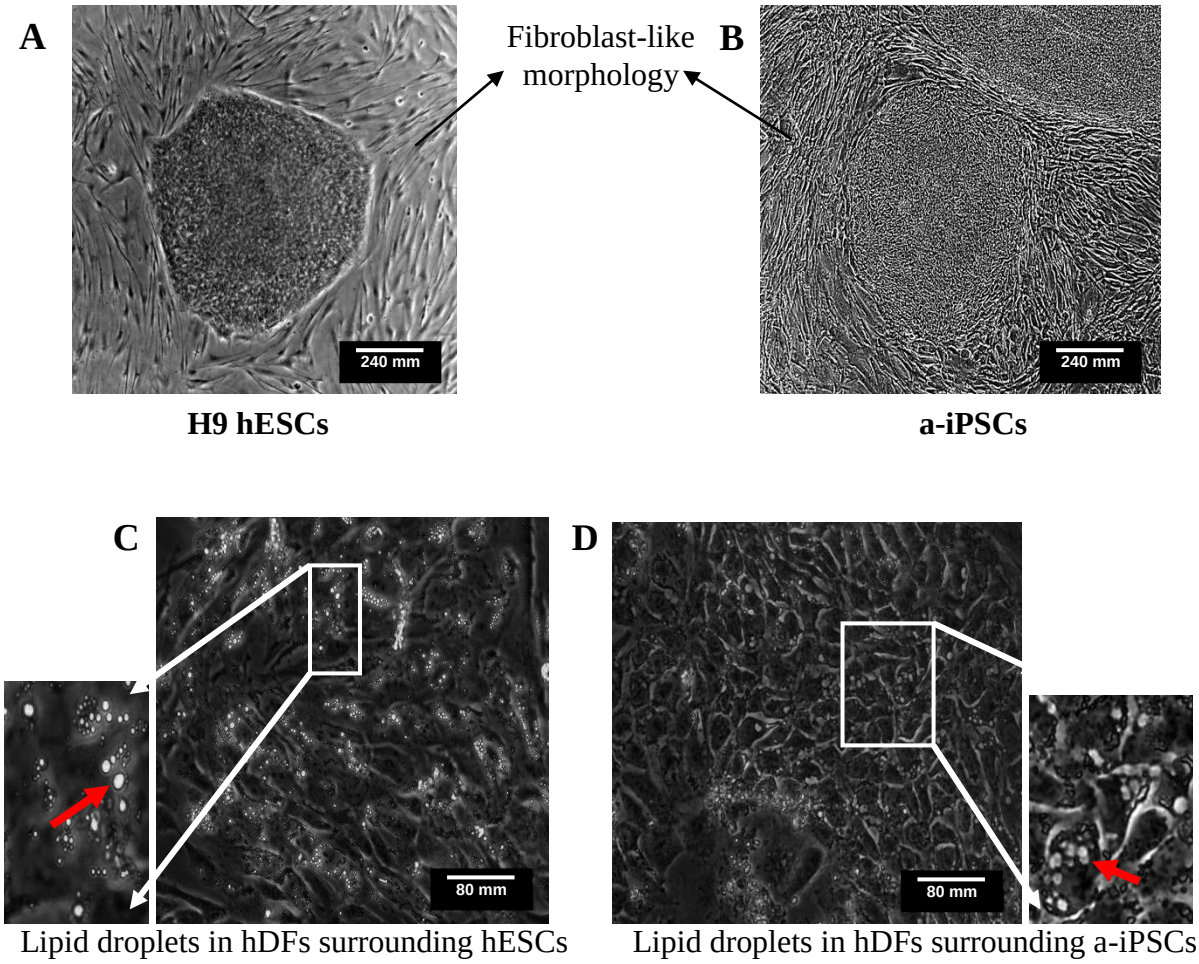

Figure 4: **Images of PSC colonies and representation of lipid droplets in the cells surrounding PSC colonies**. Fibroblast-like morphology of the cells surrounding H9 hESCs (A) and a-iPSCs colonies (B). Red arrow point to lipid droplets in fibroblast-like cells surrounding hESCs (C) and a-iPSCs (D).

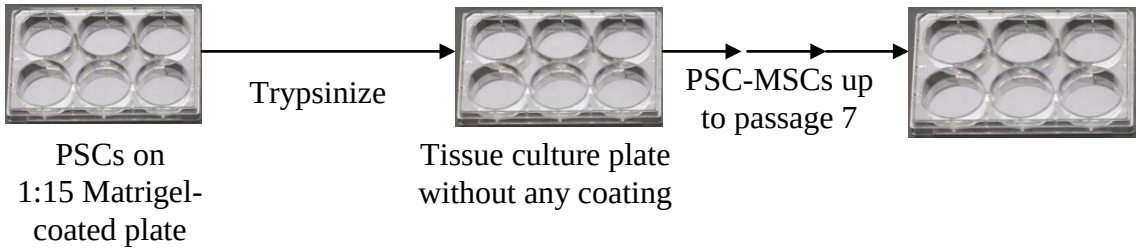

Figure 5: **Schematic representation of method used to isolate fibroblast-like cells surrounding PSCs colony**. Fibroblast-like cells surrounding PSC colony on 1:15 Matrigel were trypsinized and passaged onto tissue-culture plastic plate until passage 7 upon confluency.

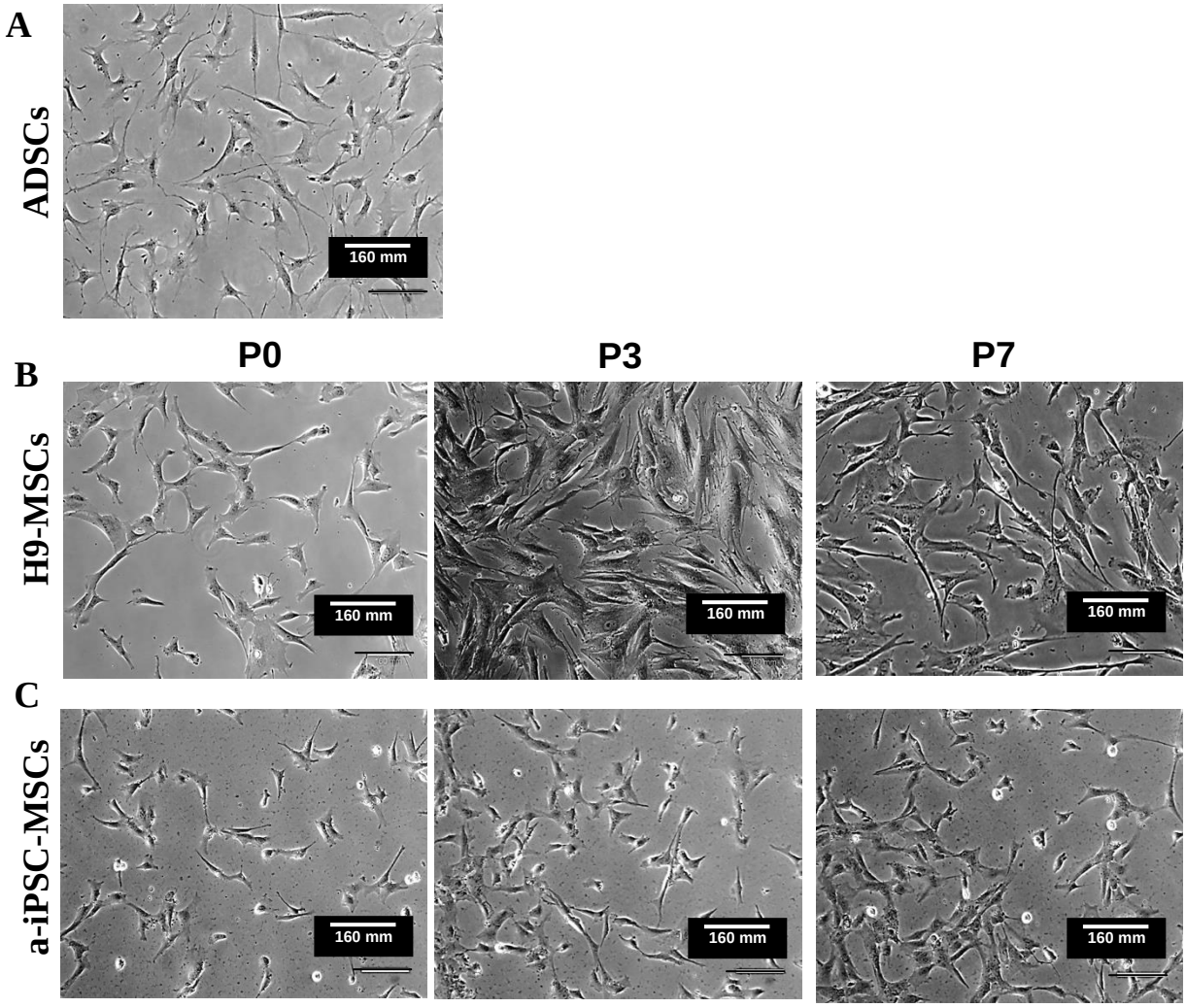

Figure 6: **Morphological comparison of H9-MSCs and a-iPSC-MSCs to ADSCs**. Representative bright field images of MSC-like cells derived from H9 hESC (H9-MSCs) (B) and a-iPSCs (a-iPSC-MSCs) (C) at passages 0, 3, and 7 in comparison to ADSCs (A). The images were taken at 10X. n=5.

6.1.2. Aim 2. Phenotypic characterization of H9-MSCs and a-iPSC-MSCs

To further characterize the H9-MSCs and the a-iPSC-MSCs, analysis of surface marker expression was carried out using flow cytometry. The cells were tested for the presence of MSC markers, such as CD73, CD105, and CD90, < 2% expression of hematopoietic markers (such as CD45), and a decrease in the expression of pluripotency markers (such as SSEA3 and Tra-1-60), as per the second criteria set by *ISCT*. Similar to ADSCs, over 95% H9-MSCs and a-iPSC-MSCs were CD90+CD73+CD105+ (Figure 7, 8 and 9) and negative (<2% positive) for hematopoietic marker, CD45, as early as passage 3 and this was maintained through passage 7. Expression of the pluripotency marker SSEA3 was approximately 1.5% in H9-MSCs and a-iPSC-MSCs (Figure 8 and 9) as compared to ~28% SSEA3 positive cells in H9s and a-iPSCs. Therefore, pluripotency capacity is reduced in these cells as indicated by the reduced SSEA3 expression, while expression of MSC markers is comparable to the criteria set out by *ISCT* both MSC-like cells. Since no significant difference in CD90+CD105+CD73+ between P3 and P7 was observed for either H9-MSCs or a-iPSC-MSCs (Figure 9), further experimentation was carried out at only P3 for both cell types.

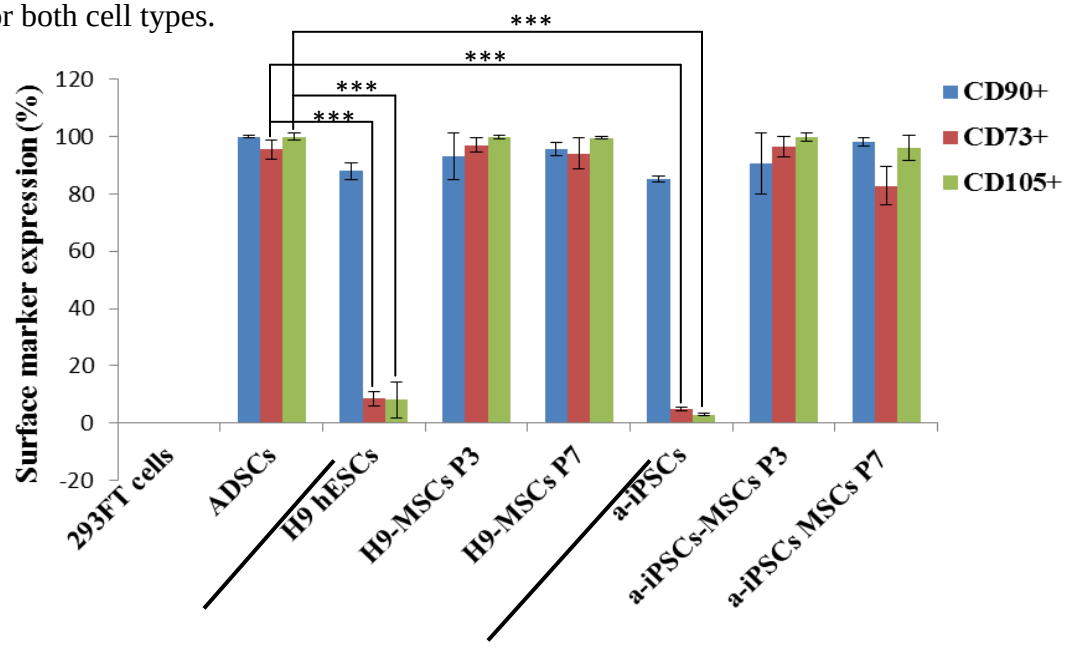

Figure 7: **MSC surface marker expression profile of MSC-like cells at P3 and P7.** Comparison of the MSC surface marker (CD90, CD73, and CD105) expression in H9 hESCs, a-iPSCs, and MSC-like cells derived from H9 hESC and a-iPSCs at passages 3 and 7 to ADSCs (positive control). n=3. The data represent the mean expression value in the form of percentages (%), and error bars indicate ± standard deviation (± SD), Statistical differences *** ($p<0.001$).

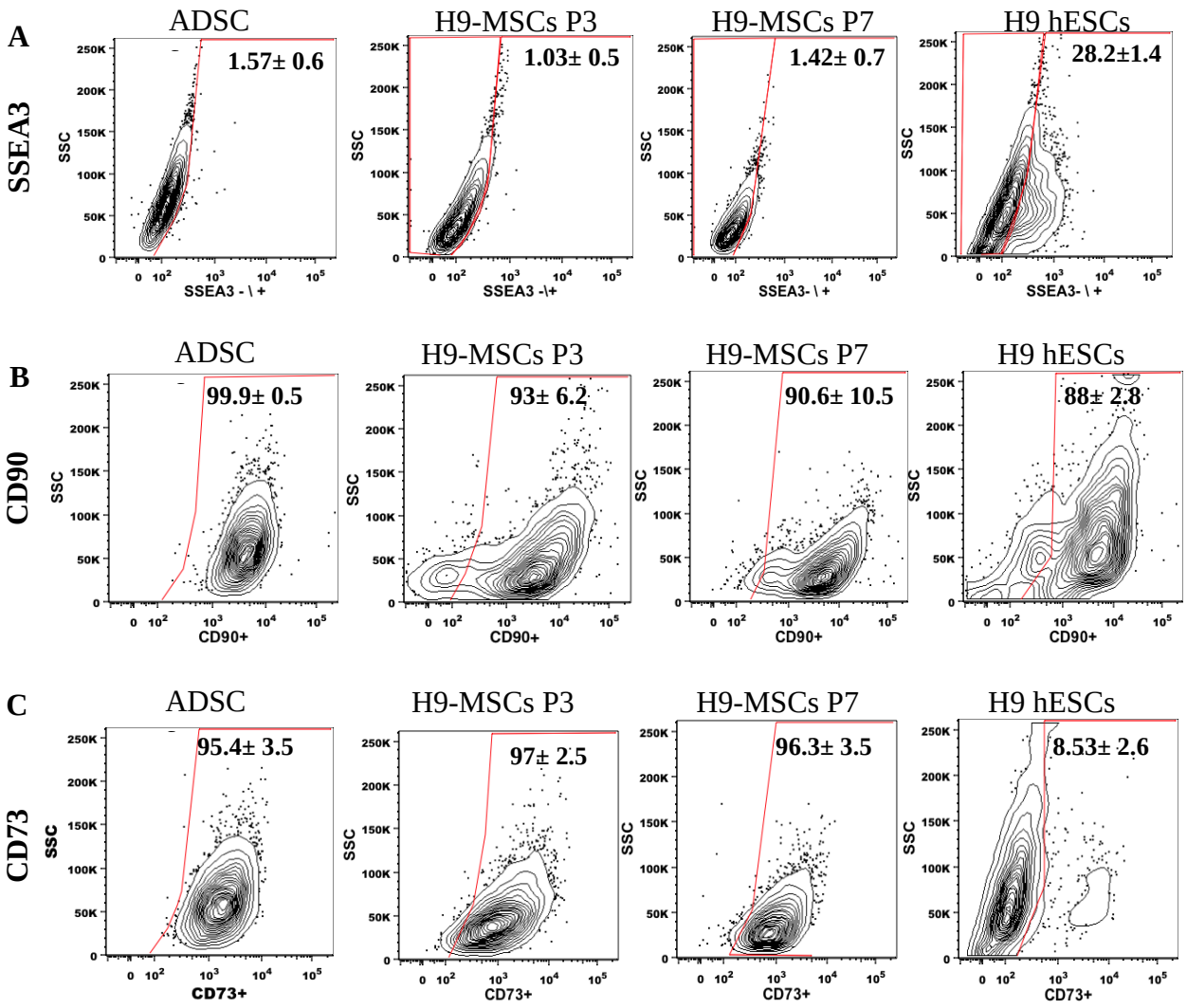

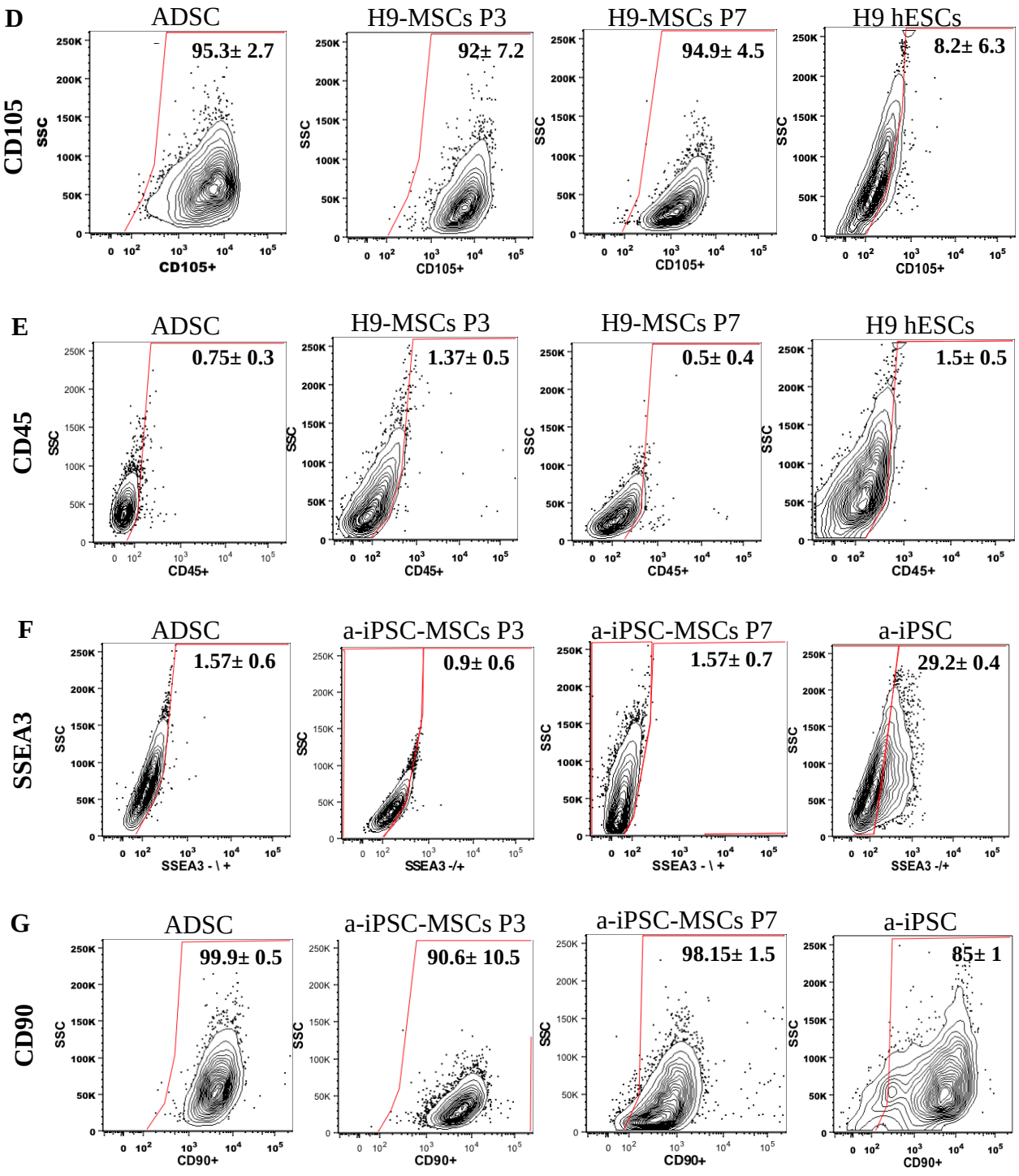
D
CD105
ADSC
95.3± 2.7
H9-MSCs P3
92± 7.2
H9-MSCs P7
94.9± 4.5
H9 hESCs
8.2± 6.3
SSC
CD105+
E
CD45
ADSC
0.75± 0.3
H9-MSCs P3
1.37± 0.5
H9-MSCs P7
0.5± 0.4
H9 hESCs
1.5± 0.5
CD45+
F
SSEA3
ADSC
1.57± 0.6
a-iPSC-MSCs P3
0.9± 0.6
a-iPSC-MSCs P7
1.57± 0.7
a-iPSC
29.2± 0.4
SSEA3 - \ +
SSEA3 -/+
G
CD90
ADSC
99.9± 0.5
a-iPSC-MSCs P3
90.6± 10.5
a-iPSC-MSCs P7
98.15± 1.5
a-iPSC
85± 1
CD90+

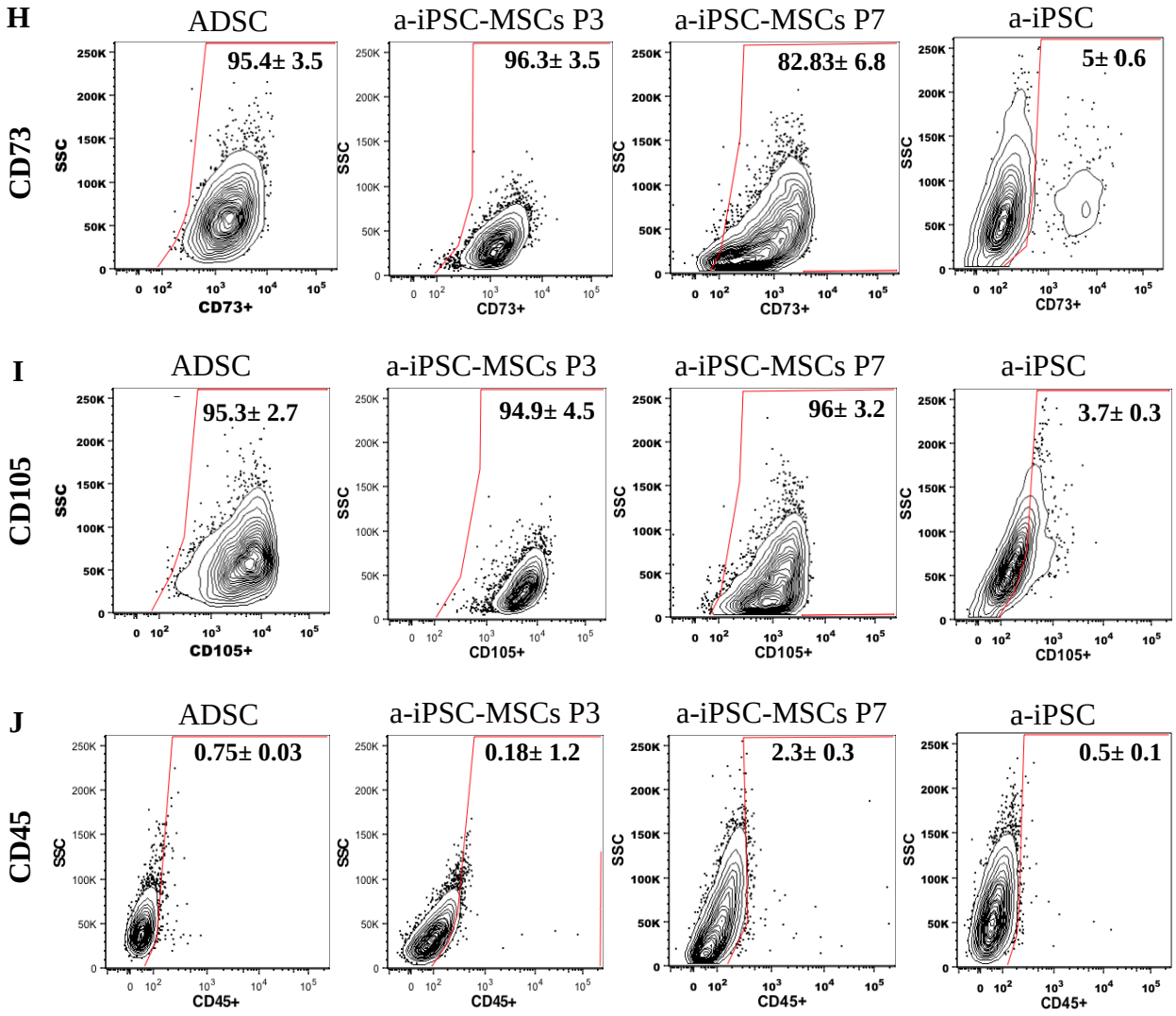

Figure 8: **MSC-like cells have similar MSC and hematopoietic marker profiles to ADSCs**. Representative flow plots for MSC markers (CD90, CD73, and CD105), hematopoietic markers (CD45), and pluripotency marker (SSEA3) for H9 hESCs, H9-MSCs P3, H9-MSCs P7, a-iPSCs, a-iPSC-MSCs P3, a-iPSC-MSCs P7, and ADSCs. The first value represent mean of the surface markers and the second number indicate ± standard deviation (± SD). The numbers indicate percentages. n=3.

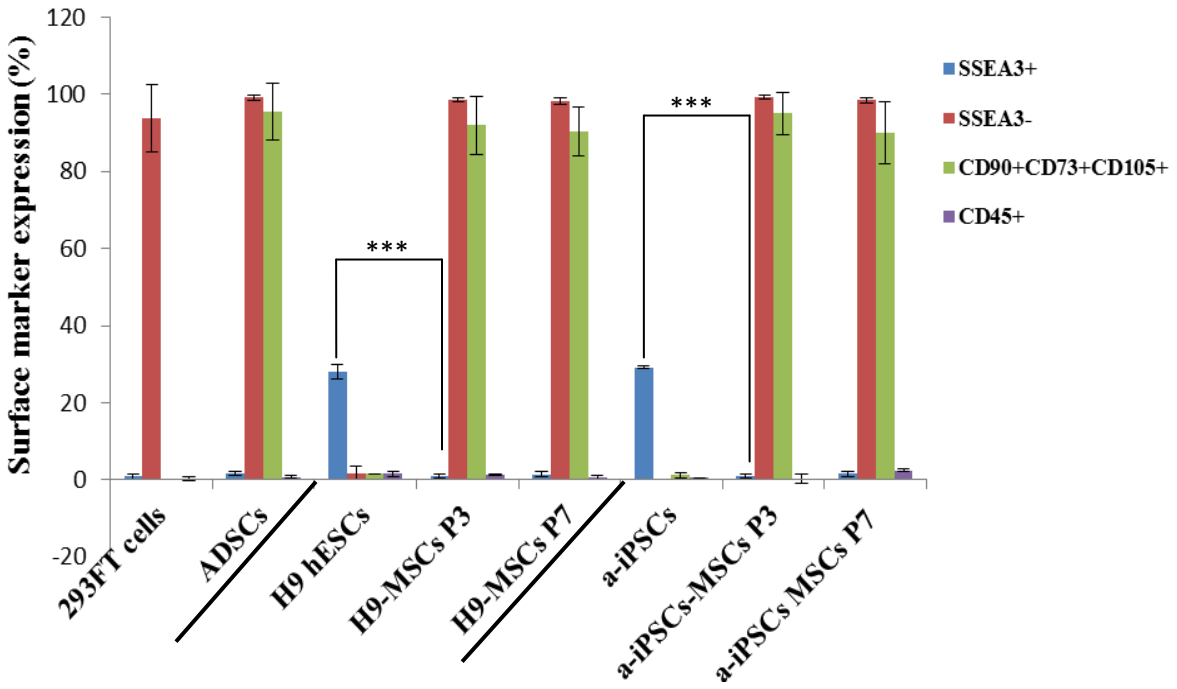

Figure 9: **Level of triple positive MSC-like cells across passages**. Comparison of the cell population positive for the all three MSC markers (CD90+CD73+CD105+), hematopoietic (CD45), and pluripotency (SSEA3) surface marker expressions among ADSCs, H9 hESCs, a-iPSCs, H9-MSCs P3, H9-MSCs P7, a-iPSC-MSCs P3, and a-iPSC-MSCs P7. The data represent the mean surface marker expression values in the form of percentages (%), and error bars indicate ± standard deviation (± SD). Statistical differences of biological triplicates (n=3), *** ($p<0.001$).

6.1.3. Aim 3. To determine the adipogenic differentiation capacity of H9-MSCs and a-iPSC-MSCs compared to bonafide MSCs, such as ADSCs, as a functional output.

MSC-like cells derived from H9 hESCs (Figure 6B) and a-iPSCs (Figure 6C) were differentiated into adipocytes, using MSC media supplemented with a cocktail of differentiation inducing factors (0.1 µM rosiglitazone, 0.5 µM dexamethasone, and 10 µg/ml insulin). Since one

of the main functions of adipocytes is to store energy in the form and accumulate lipid, the differentiated H9-MSCs were stained with neutral lipid staining Oil Red O (ORO) dye. As indicated by fewer ORO stained lipid droplets H9-MSCs (Figure 10B) and a-iPSC-MSCs (Figure 10C) showed reduced lipid formation, thus potential reduced adipogenic differentiation capacity compared to ADSCs (Figure 10A). This indicates that while MSC-like cells derived from pluripotent cells meet at least 2 of the criteria set out by *ISCT*, they are limited in their capacity to differentiate towards the adipocyte lineage, which suggests that their functional capacity (criteria 3) needs to be evaluated and further optimized.

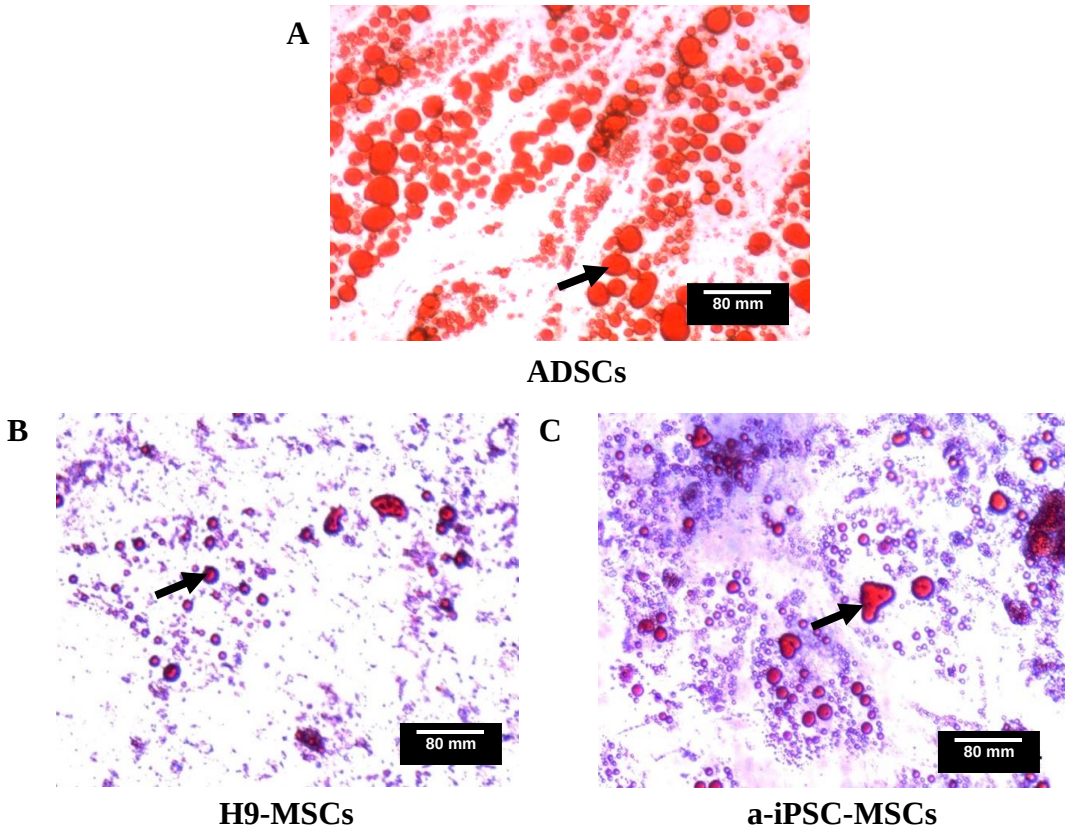

Figure 10: **Comparison of ORO stained differentiated H9-MSCs and a-iPSC-MSCs with ADSCs**. The red areas indicated by the black arrows represent lipid stained with Oil Red O in ADSCs (A), H9-MSCs (B) and a-iPSC-MSCs(C). H9-MSCs (B) and a-iPSC-MSCs(C) formed significantly fewer lipid droplets compared to ADSCs (A) n=3.

6.1.4. Aim 4. Examining gene expression profiles of H9-MSCs and a-iPSC-MSCs compared to ADSCs

Given that the functional capacity of the MSC-like cells derived from PSCs is limited, thus I set out to examine whether their gene expression profiles would be predictive of this differentiation block. Early epithelial to mesenchymal transition (EMT) markers were tested as MSC-like cells are derived from PSC sources and during early human body development PSC go through EMT to produce multipotent stem cells[119]. Therefore, to determine where MSC-like cells derived from H9 hESCs and a-iPSCs fall on the differentiation of PSCs to MSCs trajectory and to further characterize the H9-MSCs and iPSC-MSCs, a panel of MSC specific genes (Guanine nucleotide-binding protein-like 3 (GNL3), Vimentin (VIM), CD140b) and EMT markers (Caudal type homeobox1 (CDX1) and Msh homeobox1 (MSX1))[92] were tested at the mRNA level through quantitative real-time polymerase chain reactions (qRT-PCR).

As shown in Figure 11, gene expression of the MSC markers (GNL3, VIM, CD140b) and the mesenchymal transition markers (MSX1 and CDX1) while similar, it still differs then that observed for ADSCs in both H9-MSCs and a-iPSC-MSCs. Gene expression profiles of H9-MSCs and a-iPSC-MSCs clustered closer for biological replicates n2 and n3 versus n1. This is suggestive of the vast heterogeneity that is observed in the MSCs over different biological replicates. This could also be indicative that only small subpopulation of H9-MSCs and a-iPSC-MSCs have differentiated to MSC-like cells, thus the gene expression profile of the non-MSC like cell dominates, since the q-PCR provides analysis at the population level versus on per cell bases. The results may also indicate that small population of cells within H9-MSCs and a-iPSC-MSCs culture might belong somewhere between PSCs to MSCs differentiation path.

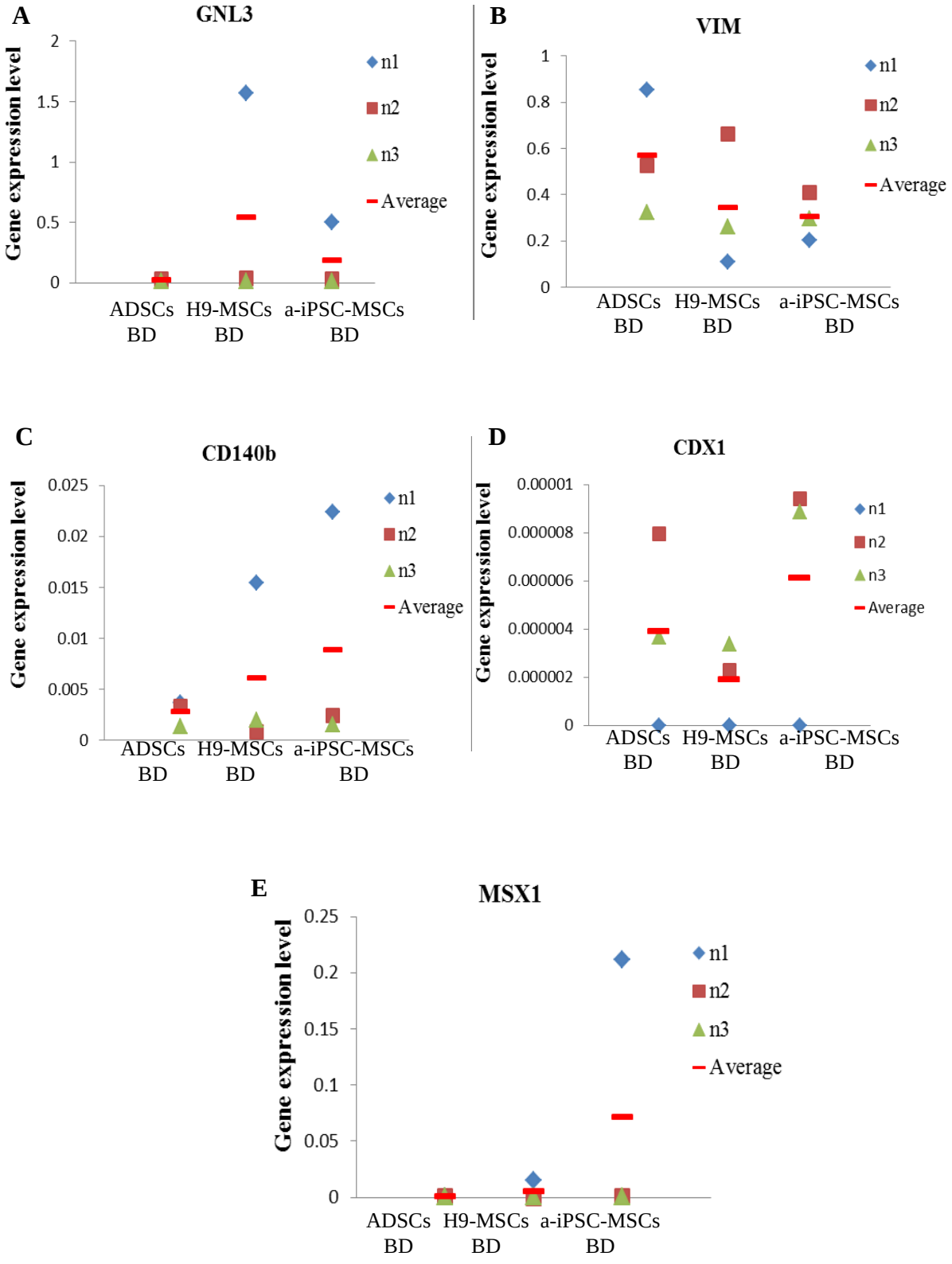
A
GNL3
Gene expression level
2
1.5
1
0.5
0
n1
n2
n3
Average
ADSCs BD
H9-MSCs BD
a-iPSC-MSCs BD
B
VIM
Gene expression level
1
0.8
0.6
0.4
0.2
0
n1
n2
n3
Average
ADSCs BD
H9-MSCs BD
a-iPSC-MSCs BD
C
CD140b
Gene expression level
0.025
0.02
0.015
0.01
0.005
0
n1
n2
n3
Average
ADSCs BD
H9-MSCs BD
a-iPSC-MSCs BD
D
CDX1
Gene expression level
0.00001
0.000008
0.000006
0.000004
0.000002
0
n1
n2
n3
Average
ADSCs BD
H9-MSCs BD
a-iPSC-MSCs BD
E
MSX1
Gene expression level
0.25
0.2
0.15
0.1
0.05
0
n1
n2
n3
Average
ADSCs BD
H9-MSCs BD
a-iPSC-MSCs BD

Figure 11: Gene expression profile of EMT and MSC genes in MSC-like cells compared to ADSCs. Scatter plots of the MSC markers (GNL3, VIM, and CD140b) and the early epithelial to mesenchymal transition (EMT) markers (CDX1 and MSX1) in H9-MSCs and a-iPSC-MSCs compared to ADSCs based on gene expression level at each of the three replicate. From the plots it is apparent that n1 population of both H9-MSCs and a-iPSC-MSCs were very different from n2 and n3 population. Population for n2 and n3 resemble gene expression level to of ADSCs. n=3; done in triplicate.

Overall, MSC-like cells derived from both the PSC sources (H9s and a-iPSCs) meet the first 2 criteria of classical MSCs laid out by *ISCT*. These MSC-like cells derived from hESCs and a-iPSCs adhere to tissue culture plastic plate and maintain fibroblast-like morphology until passage 10; and express MSC markers (CD90+CD73+CD105+) and lack the expression of hematopoietic markers (i.e. CD45). However, neither H9-MSCs nor a-iPSC-MSCs formed as many lipid droplets as ADSCs, indicating lower differentiation capacity of these cells. Additionally, their gene expression profiles also differ from ADSCs, suggestive that these cells are still not as mature or maybe a totally different cell type then bonafide MSCs, such as ADSCs. Therefore, it is important to further characterize and improve adipogenic potential of H9-MSCs and a-iPSC-MSCs. This could perhaps be achieved by providing culture conditions and/or introduction of factors that could enhance gene expression and differentiation capacity of these cells to that observed for ADSCs.

6.2. Objective 2: To establish and optimize conditions that increase the number of adipocytes derived from PSC-derived MSCs

From the results of Objective 1, I observed that MSC-like cells derived from H9 ESCs and a-iPSCs have similar morphology and phenotype in terms of surface marker expression compared to ADSCs. However, their gene expression profiles and differentiation capacity is significantly different compared to primary MSCs. Since the main goal of deriving MSC-like cells from PSCs is to obtain unlimited MSCs that can potentially be used in a clinical setting, it is crucial that PSC-derived MSC-like cells have similar functional abilities as primary MSCs. Differentiation potential of PSC-derived MSC-like cells to osteoblasts and chondrocytes have been shown to be similar to that of primary MSCs[92]. However, they do not differentiate into adipocytes as efficiently as primary MSCs; therefore, adipogenic differentiation of these cells requires further optimization.

The first step in MSCs differentiation towards adipocytes is growth arrest. Current studies using mouse preadipocyte cell lines (i.e. 3T3-L1) have shown that the transcription factor *Klf4* is required to inhibit cell proliferation at G1/S phase boundary of the cell-cycle after mitotic clonal expansion of MSCs, reaching the preadipocyte stage[120]. *Klf4* has also been shown to bind to the promoter of CEBPβ and δ, which are the transcription factors involved in upregulating expression of PPARγ2. PPARγ2 is considered as a master regulator of adipogenesis and has been shown to regulate expression of various downstream genes like glucose transporter 4 (Glut4), Fatty acid binding protein 4 (FABP4), Lipoprotein lipase (LPL) and hormone sensitive lipase (HSL), which finally impart an adipocyte-like phenotype to the cell[118]. Most importantly, since Klf proteins are highly conserved among mammals[121], even though the role of *Klf4* in human cell lines has not been investigated, information obtained from studies on mouse preadipocyte cell lines may be applicable to human cells. Therefore, before ectopically overexpressing *Klf4* in

PSC-derived MSCs, the endogenous *Klf4* level was checked in ADSCs, H9-MSCs and a-iPSC-MSCs by qRT-PCR. As shown in the Figure 12, *Klf4* expression is significantly higher in ADSCs as compared to PSC-derived MSC-like cells.

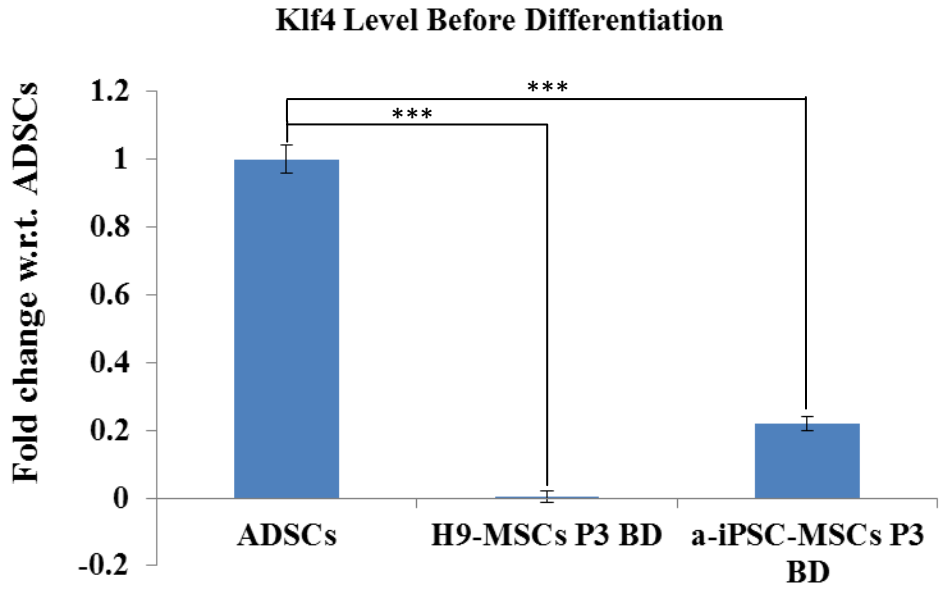

Figure 12: Endogenous *Klf4* expression in ADSCs, H9-MSCs, and a-iPSC-MSCs. Real-time PCR analysis of the endogenous expression of *Klf4* in H9-MSCs, a-iPSC-MSCs, and ADSCs. The data represent fold changes in expression values with respect to ADSC and the error bars indicate ± standard deviation (± SD). Statistical differences of biological triplicates (n=3), *** ($p<0.001$). BD = Before differentiation

6.2.1. Aim 1. To examine how ectopic overexpression of *Klf4* affects adipogenic potential in H9-MSCs.

Given that previous experiments show that *Klf4* expression is important for adipogenesis and I observed that both H9-MSCs and a-iPSC-MSCs have significantly reduced *Klf4* levels compared to ADSCs, I attempted to increase the adipogenic differentiation potential of PSC-

derived MSC-like cells, H9-MSCs by infecting them with *Klf4*-expressing Sendai virus for 24 hours at multiplicity of infection (MOI) 2, 3, and 4. Sendai viruses was chosen as these viruses are enveloped viruses with a non-segmented negative-strand RNA genome vector, which allows a robust and sustained expression of foreign genes[122]. Its life cycle/RNA replication occurs in the cytoplasm without DNA intermediates, minimizing the risk of vector genome (RNA) integration into the host genome[123]. The MOIs 2, 3 and 4 were chosen as MOI 3 was shown to be optimal for reprograming human fibroblasts to iPSCs[124], thus this provided the base line. While the MSC-like cells used in this study have fibroblast like morphologies, they are not bonafide fibroblasts, since they were derived from PSCs, therefore the MOI needed further optimization for H9-MSCs and a-iPSC-MSCs, and so I could attain similar Klf4 expression levels in PSC-derived MSC-like cells to that observed for ADSCs.

H9-MSCs infected with MOI 2 showed similar levels of *Klf4* to that observed in ADSCs after the 24 hour infection (Figure 13A); indicating that *Klf4* infection was successful and the cells are overexpressing *Klf4*. Subsequently, H9-MSCs were differentiated with the cocktail of adipogenic factors (i.e. rosiglitazone, dexamethasone, and insulin) 48 hrs post infection with MOI 2 to investigate their capacity to differentiate to adipocytes.

After 21 days of adipogenic differentiation, *Klf4* infected H9-MSCs showed increased lipid droplet like structures (Figure 13D and I), compared to the uninfected cells (Figure 13E and H). Since one of the main functions of adipocytes is to store energy in the form of lipid, the differentiated H9-MSCs were stained with neutral lipid staining ORO dye. The dye was extracted and quantified to measure degree of adipogenesis in PSC-derived MSC-like cells.

The quantitative analysis of the extracted lipid staining ORO dye from the differentiated H9-MSCs showed that ectopically overexpressing *Klf4* does not significantly improve adipogenic potential of H9-MSCs (Figure 13B). This is in line with gene expression level for the adipogenic regulators, CEBPα and PPARγ2, which also showed no difference upon *Klf4* overexpression versus control conditions after differentiation (Figure 13C). However, it is important to note that *Klf4* expression highly varies between infections, even if MOI 2 is maintained as tested. The decreased adipogenic potential of the cells could have been the result of highly elevated *Klf4* expression (4-fold increase) for this set of differentiation experiments compared to ADSCs. Additionally, after 21 days of adipogenic differentiation, expression level of *Klf4* is negligible in both ectopically overexpressing *Klf4* H9-MSCs and control H9-MSCs compared to expression level of *Klf4* in the differentiated ADSCs to adipocytes. These results indicate that *Klf4* overexpression has to be tightly regulated during adipogenic differentiation of PSC-derived MSC-like cells in order to evaluate its role in human adipogenesis.

Differentiation of a-iPSC-MSCs infected with *Klf4*-expressing Sendai virus, resulted in 95% cell death in two subsequent attempts. Therefore, effect of exogenous overexpression of *Klf4* on adipogenic potential in a-iPSC-MSCs could not be evaluated to the full extent.

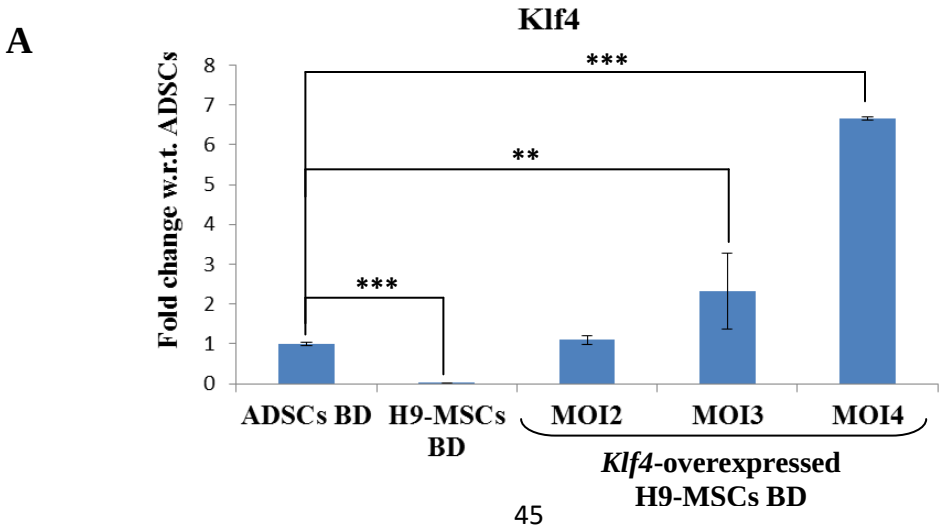

B

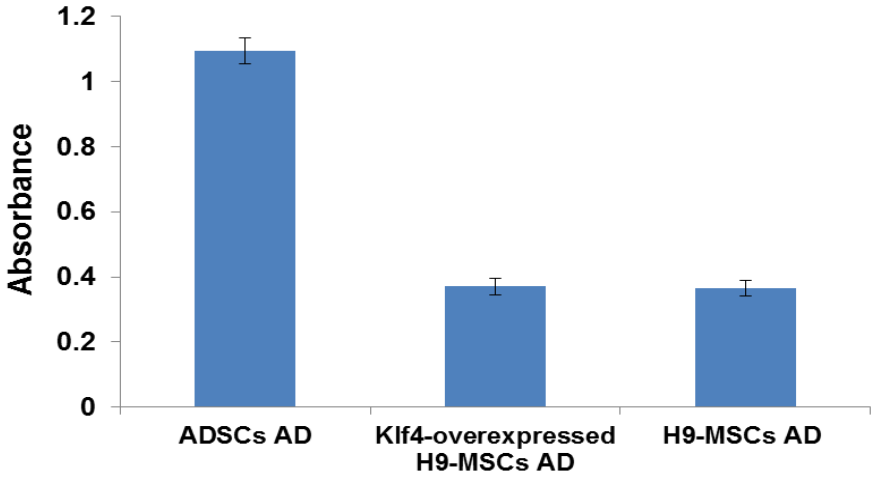

C

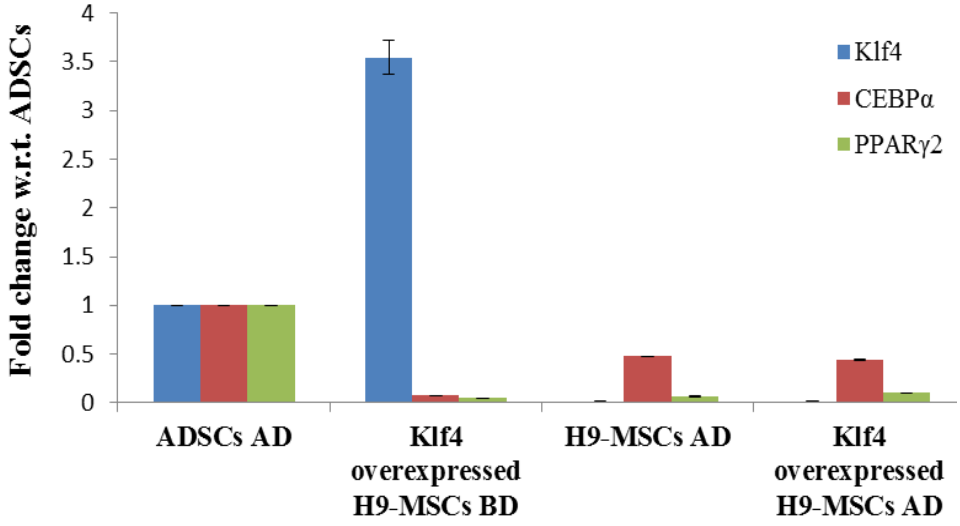

D ***+ Klf4***

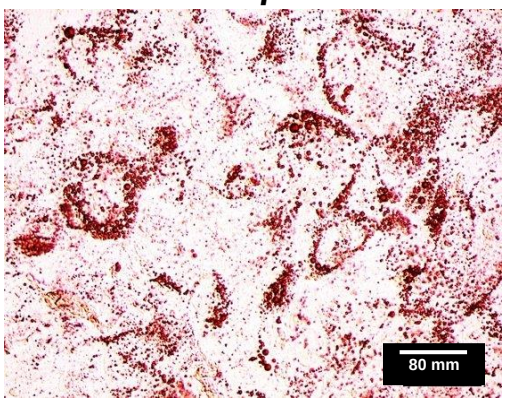

E ***- Klf4***

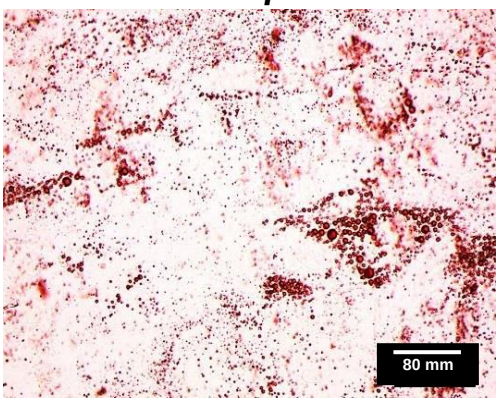

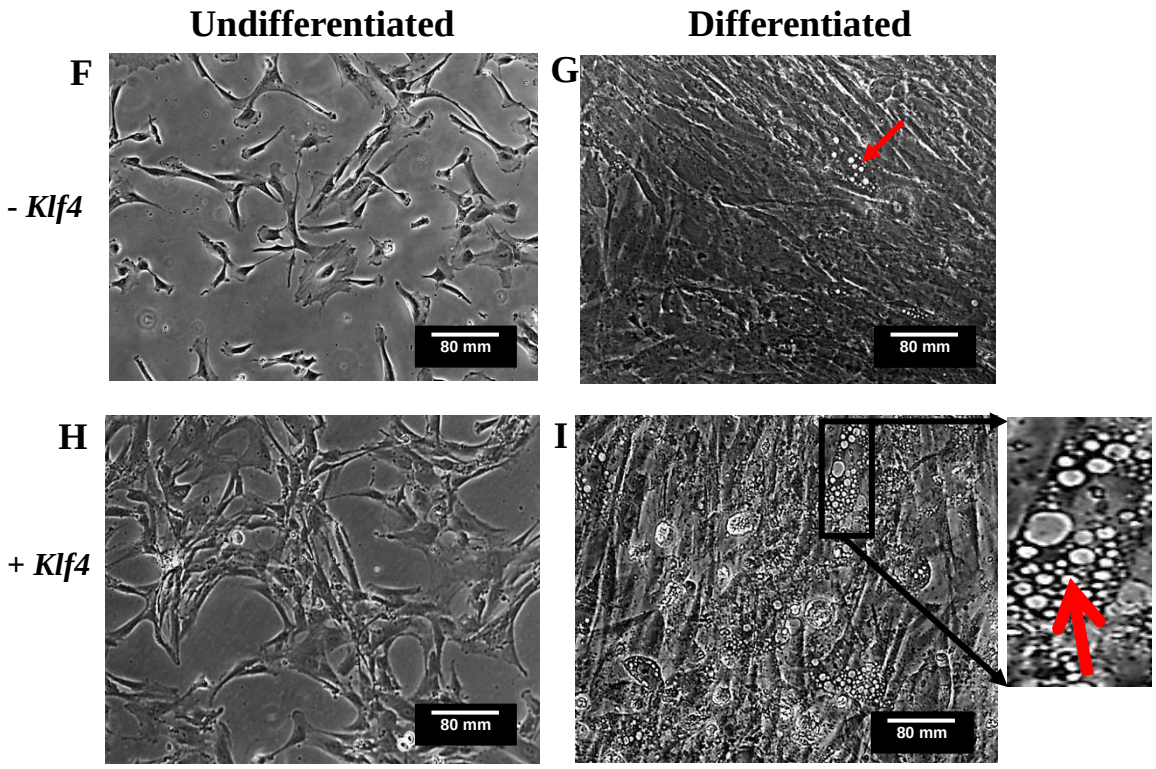

Figure 13: Effect of *Klf4* overexpression on adipogenic potential of H9-MSCs.

Real-time PCR analysis of *Klf4* expression in H9-MSCs infected with Sendai viruses at MOI2, MOI3, MOI4, H9-MSCs before differentiation (BD), and ADSCs The data represent fold changes in expression values with respect to ADSC and the error bars indicate ± standard deviation (± SD) of biological triplicates (n=3), Statistical differences of ** ($p<0.01$) and *** ($p<0.001$) (A). Absorbance value of the extracted ORO dye from the *Klf4* overexpressing Sendai virus infected H9-MSCs and uninfected H9-MSCs after 21 days of adipogenic differentiation. The data represent the mean absorbance values and the error bars indicate ± SD of n=4 (B). Real-time PCR analysis of *Klf4* and adipogenic regulators (CEBPα and PPARγ2) gene expression levels in before and after adipogenic differentiation of *Klf4* overexpressing H9-MSCs, ADSCs, and H9-MSCs BD. The data represent fold changes in expression values with respect to

ADSC and the error bars indicate ± standard deviation (± SD) of biological triplicates (n=3) (C). Representative images of the lipid droplets stained with ORO dye in *Klf4* overexpressing (*+Klf4)* (D) and without *Klf4* overexpression (*-Klf4)* (E). Bright field images of H9-MSCs without *Klf4* overexpression before (F) and after (G) adipogenic differentiation. Bright field images of *Klf4* overexpressing H9-MSCs before (H) and after (I) adipogenic differentiation.

6.2.2. Aim 2. To determine if elevating endogenous *Klf4* through IBMX treatment improves adipogenic potential of H9-MSCs and a-iPSC-MSCs

In mouse 3T3-L1 cells, IMBX has been shown to increase endogenous *Klf4* expression level 30 minutes after treatment, with expression peaking at 2 hour[125]. Therefore, to avoid using *Klf4*-overexpression system that is difficult to control over the different batches of H9-MSCs, H9-MSCs were treated with IBMX for 30 minutes, 1 hour, and 2 hours to elevate endogenous *Klf4* levels. As shown in the Figure 14A, 30 minutes, 1 hour, or 2 hours of IBMX treatment did not lead to an increase in endogenous *Klf4* expression in H9-MSCs to that observed for ADSCs. In previous experiments 24 hours of IBMX treatment led to improved differentiation of H9-MSCs to adipocytes (data not shown). Therefore, H9-MSCs were further treated with IBMX for 6, 12 and 24 hours. For H9-MSCs, 24 hours of IBMX treatment increased endogenous *Klf4* level 3-fold compared to untreated H9-MSCs but it still did not reach *Klf4* level seen in ADSCs (Figure 14A). To minimize the duration of exposure to IBMX and thus reduce chemical stress to the cells, attempts to increase endogenous *Klf4* level by treating H9-MSCs with IBMX for longer than 24 hours were not attempted.

To investigate the effects of increased endogenous *Klf4* expression levels on adipogenic potential of H9-MSCs, the cells were subjected to adipogenic differentiation after treating with IBMX at each of the 6 time points. As shown in the Figure 14B, of the 6 time points, 30 minutes IMBX treatment showed similar amount of lipids to that observed for H9-MSCs without IBMX treatment even though level of *Klf4* was lower in the untreated versus the 30 minutes IBMX treated cells (Figure 14A). Conversely, 24 hours IBMX treatment had significantly lower lipid accumulation compared to H9-MSCs without IBMX treatment (Figure 14B) despite the higher *Klf4* expression compared to the other 6 IBMX treatment durations (Figure 14A). This discrepancy between Klf4 expression and differentiation capacity, as measured by ORO stained lipid accumulation, was further confirmed by my observation that the differentiated H9-MSCs after 30 minutes of IBMX treatment had a higher number and bigger ORO stained lipid droplets (Figure 14E) compared to H9-MSCs treated with IBMX for 24 hours (Figure 14J). Overall, none of the other IBMX treatment durations improved adipogenic potential of H9-MSCs compared to un-treated H9-MSCs (Figure 14B). Therefore, my data suggests that there is no correlation between IBMX treatment timeline and adipogenic capacity in relation to *Klf4* expression in the PSC-derived MSC-like cells.

Next I measured gene expression profile of the main adipogenic regulators, CEBPα and PPARγ2, to evaluate how these factors were regulated by IBMX treatment. The levels of PPARγ2 did not change significantly after any of the 6 IBMX treatment time points compared to the un-treated H9-MSCs. Level of CEBPα significantly decreased with the increasing IBMX treatment duration (Figure 14C). Thus, these results indicate that the level of endogenous *Klf4*

induced by IBMX did not enhance adipogenic regulators, which may explain the lack of effects seen for H9-MSCs in accumulating lipids over the 6 IBMX treatment time durations.

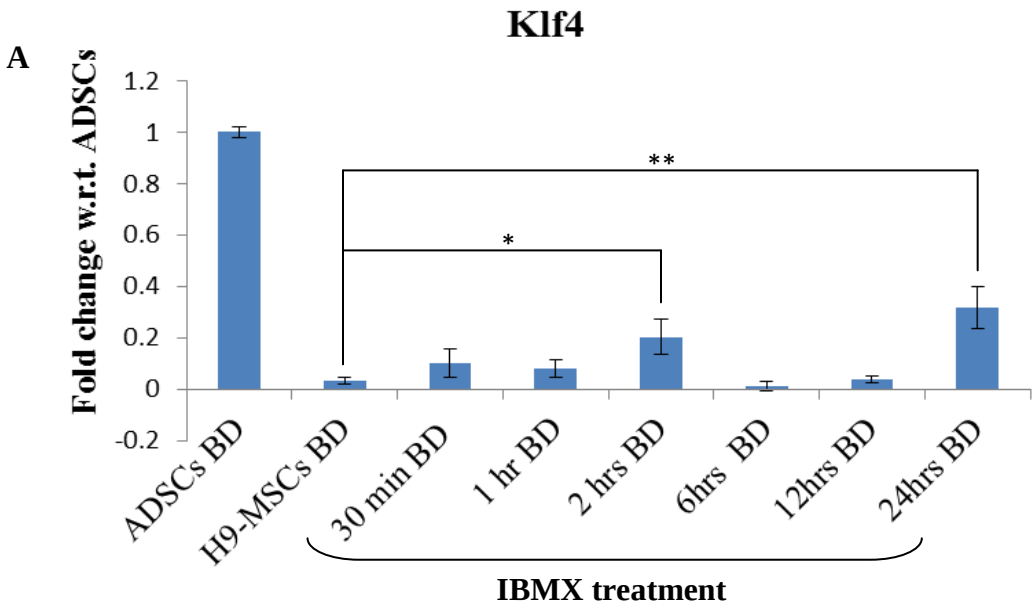

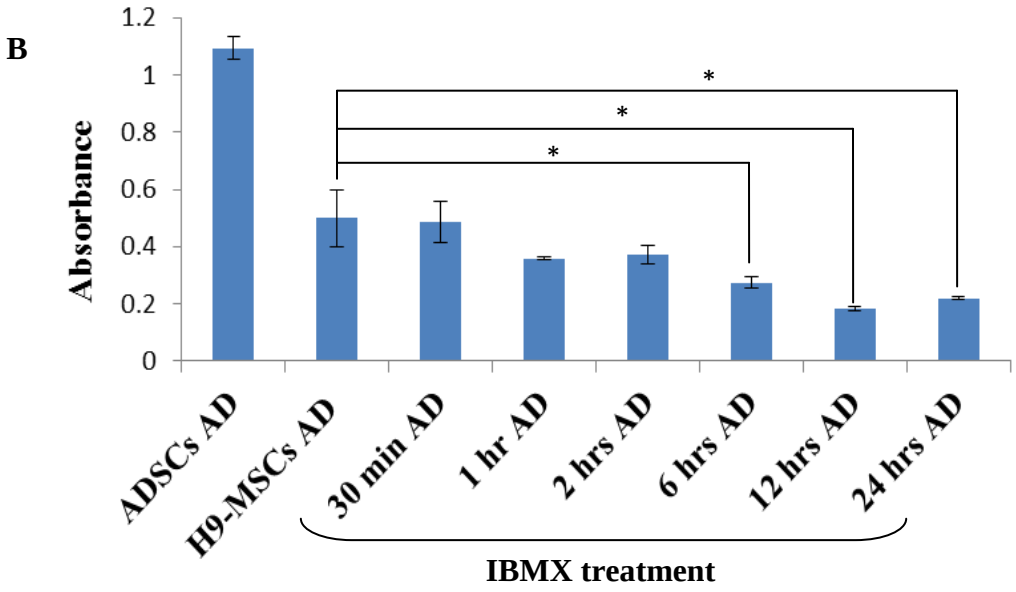

C

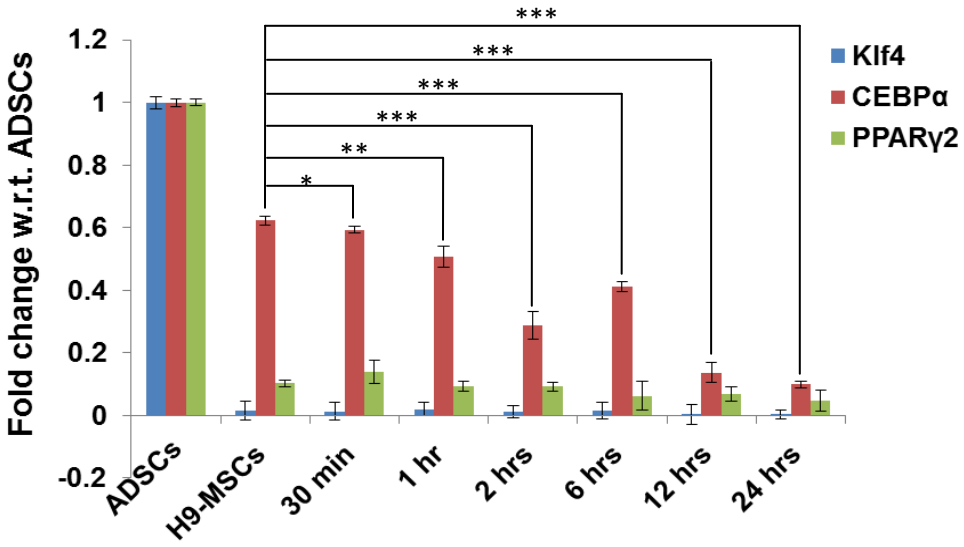

D

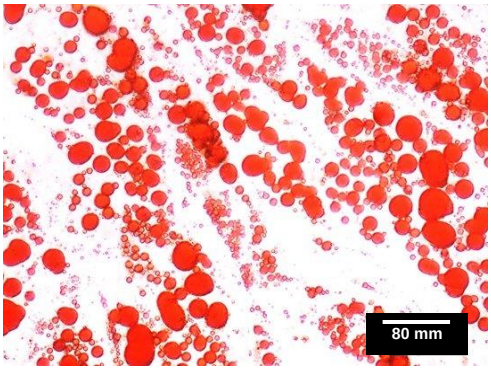

ADSCs

E

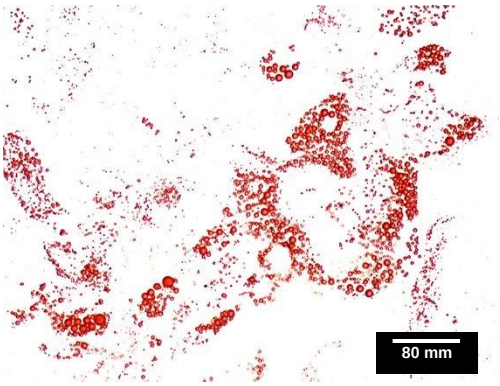

H9-MSCs after <u>30 min IBMX</u>

F

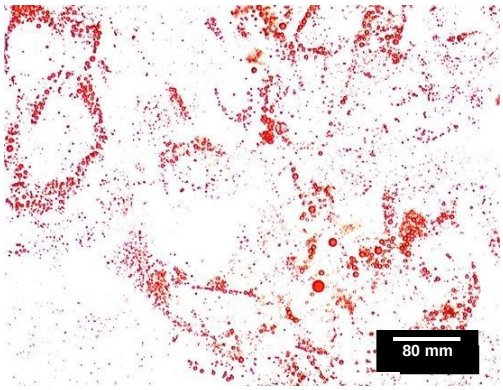

H9-MSCs after <u>1 hour IBMX</u>

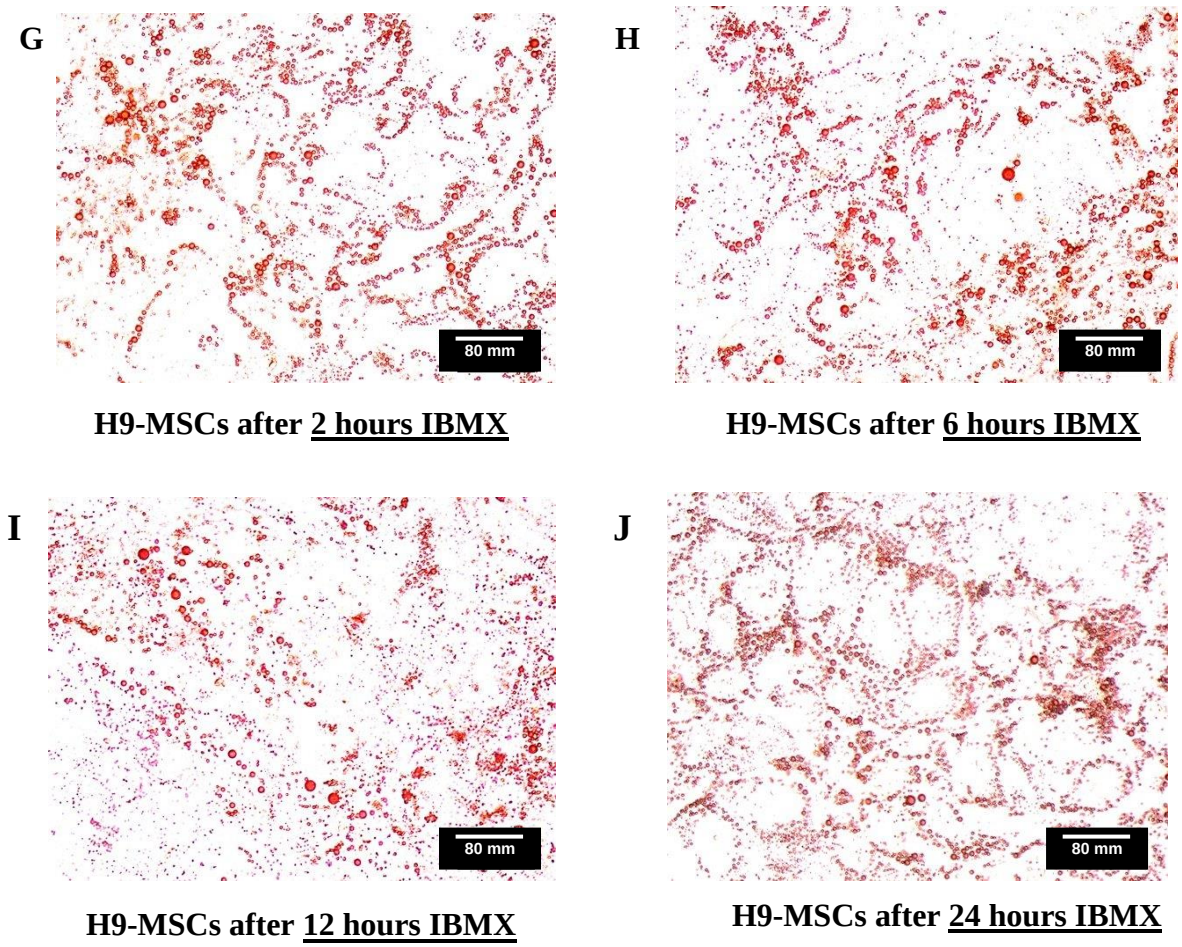

Figure 14: Effect of IBMX treatment on adipogenic potential of H9-MSCs. Real-time PCR analysis of the endogenous expression of *Klf4* in ADSCs, H9-MSCs without IBMX treatment, and in H9-MSCs after IBMX treatment for 30 minutes, 1, 2, 6, 12, and 24 hours. The data represent fold changes in expression values with respect to ADSC (A). The mean absorbance value of the extracted ORO dye from ADSCs, H9-MSCs without IBMX treatment, and in H9-MSCs after IBMX treatment for 30 minutes, 1, 2, 6, 12, and 24 hours after 21 days of adipogenic differentiation (B). Real-time PCR analysis of CEBPα and PPARγ2 and *Klf4* gene expression level after adipogenic differentiation of ADSCs, H9-MSCs without IBMX treatment, and in H9-MSCs after IBMX treatment for

30 minutes, 1, 2, 6, 12, and 24 hours The data represent fold changes in expression values with respect to ADSCs and the error bars indicate ± standard deviation (± SD) of biological triplicates (n=3) (C). Representative images of the lipid droplets stained with ORO dye in ADSCs (D) and H9-MSCs after 30 minutes (E), 1 (F), 2 (G), 6 (H), 12 (I), and 24 (J) hours IBMX treatment followed by 21 days of adipogenic differentiation. The error bars indicate ± SD of n=3, Statistical differences of * ($p<0.05$), ** ($p<0.01$) and *** ($p<0.001$). BD= before differentiation; AD= after differentiation

Similar to H9-MSCs, I investigated whether increased endogenous *Klf4* expression level has an effect on adipogenic potential of a-iPSC-MSCs. These cells were treated with IBMX for 30 minutes, 1 hour, and 2 hours. As shown in the Figure 15A, 30 minutes of IBMX treatment was sufficient to increase expression of endogenous *Klf4* level to that of ADSCs. IBMX treatment for 1 hour increased endogenous *Klf4* expression only 0.5 fold of ADSCs and 2 hours IBMX teatment resulted in 3 fold higher endogenous *Klf4* expression compared to ADSCs. However, of the 3 IBMX treatment durations, degree of adipogenesis was higher for 1 hour of IBMX treatment. But when I compared untreated a-iPSC-MSCs with IBMX treated cells (30 min and 1 hr) there was no significant difference in the degree of adipogenesis, as measured by lipid accumulation (Figure 15B). In fact, the degree of adipogenesis was reduced significantly after 2 hours IBMX treatment compared to the untreated a-iPSC-MSCs (Figure 15B). This lack of change in lipid accumulation can be visualized through the ORO stained images for differentiated a-iPSC-MSCs with no treatemnt, 1 hour IBMX treatment (Figure 15F) versus 30 minutes (Figure 15E) or 2 hours IBMX treatment (Figure 15G).

Effect of increased endogenous *Klf4* expression also did not correspond to increased expression level of the adipogenic regulators, CEBPα and PPARγ2. Expression of CEBPα and PPARγ2 was lower for 30 minutes IBMX treatment compared to 1 hour or 2 hours of IBMX treatment (Figure 15C) even though level of *Klf4* was similar to ADSCs after 30 minutes, lower after 1 hour and was 3 fold higher after 2 hours of IBMX treatment (Figure 15A). Level of endogenous *Klf4* did not have significant effect on expression level of PPARγ2 compared to untreated a-iPSC-MSCs. Expression level of CEBPα was significantly lower after 30 minutes and 1 hour and 0.2 fold higher after 2 hours of IBMX treated compared to the untreated a-iPSC-MSCs (Figure 15C). In addition, expression of *Klf4* reduced significantly in all 3 IBMX treatment conditions after adipogenic differentiation of a-iPSC-MSCs comapred to *Klf4* level in the differentiated ADSCs to adipocytes (Figure 15C).

Thus, the results of effect of increased endogenous *Klf4* epxression level in H9-MSCs and a-iPSC-MSCs through IBMX treatment indicate that level of *Klf4* expression must be regualted tighly in a narrow window during different stages of adipocyte development.

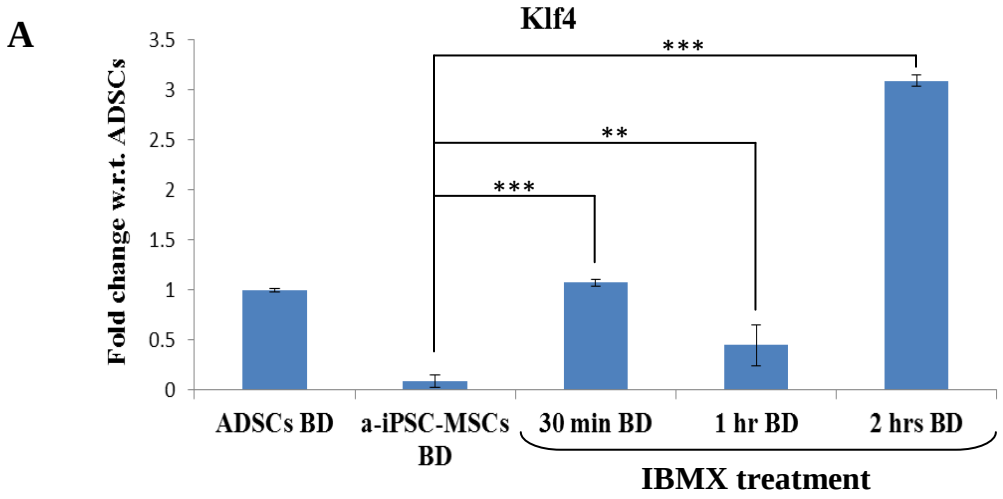

B

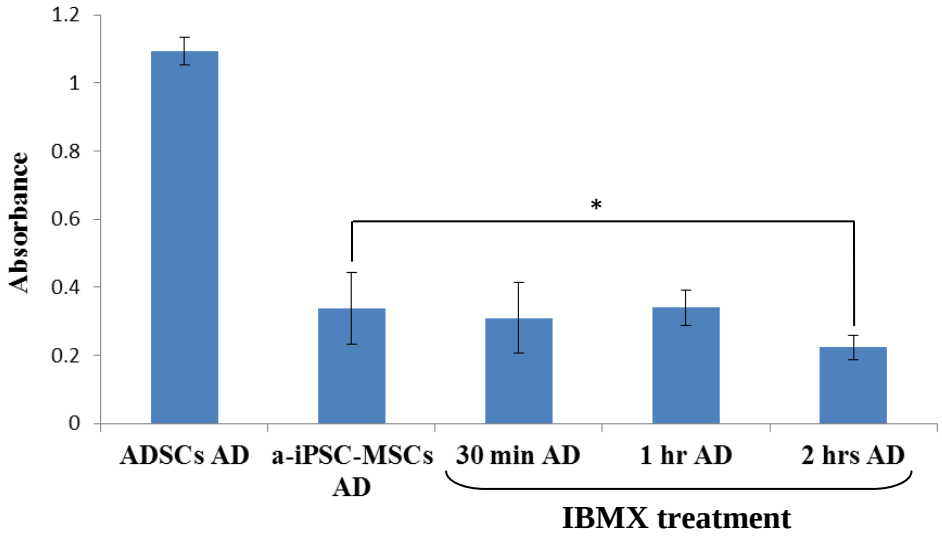

C

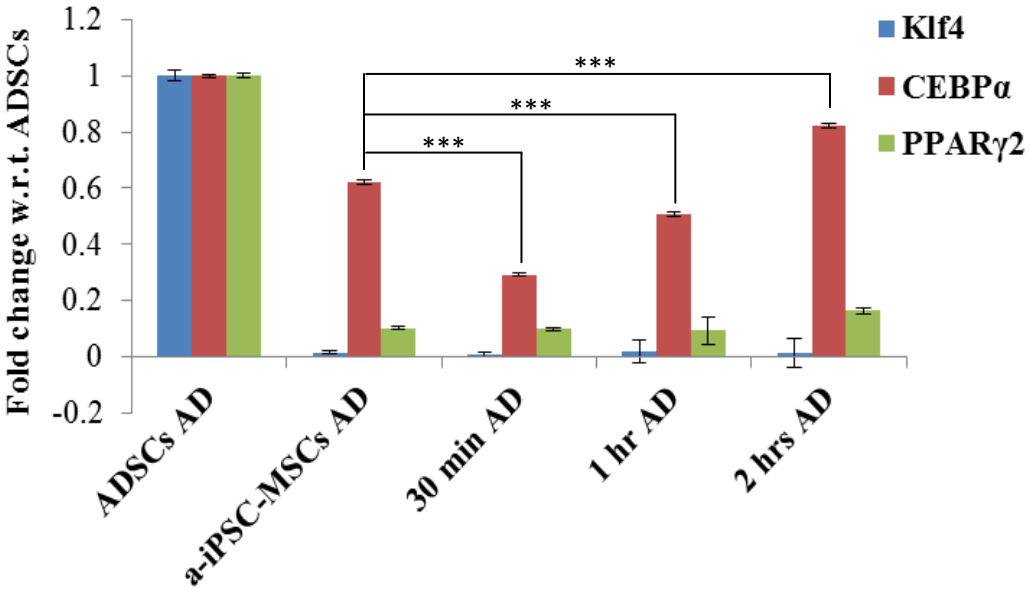

D

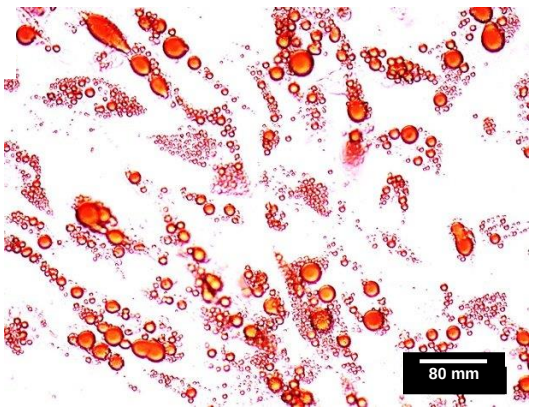

ADSCs

E

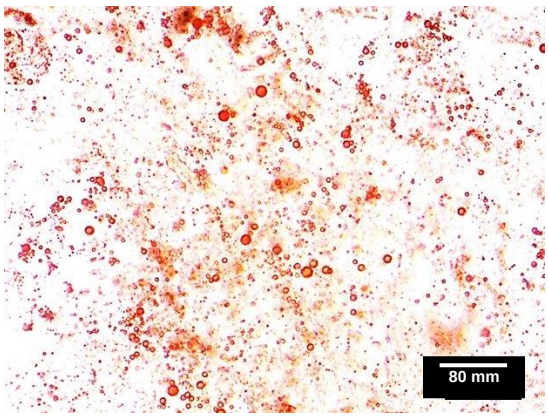

a-iPSC-MSCs after <u>30 min IBMX</u>

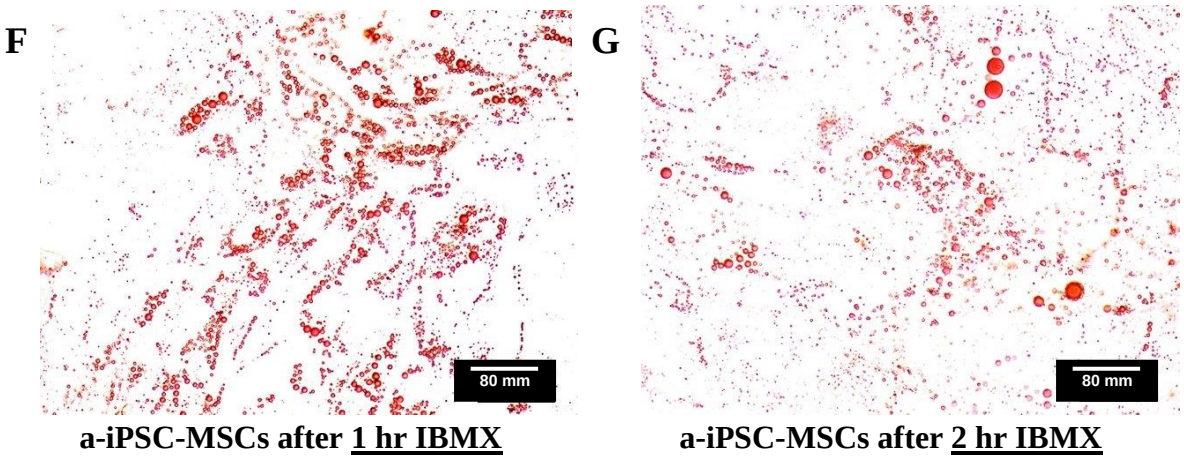

Figure 15: Effect of IBMX treatment on adipogenic potential of a-iPSC-MSCs. Real-time PCR analysis of the endogenous expression of *Klf4* in ADSCs, a-iPSC-MSCs without IBMX treatment, and in a-iPSC-MSCs after IBMX treatment for 30 minutes, 1, and 2 hours. The data represent fold changes in expression values with respect to ADSC and the error bars indicate ± SD of n=3, statistical differences of ** ($p<0.01$) and *** ($p<0.001$) (A). The mean absorbance value of the extracted ORO dye from ADSCs, a-iPSC-MSCs without IBMX treatment, and in a-iPSC-MSCs after IBMX treatment for 30 minutes, 1, and 2 hours after 21 days of adipogenic differentiation. The error bars indicate ± SD of the three biological replicates, Statistical differences of * ($P<0.05$) (B). Real-time PCR analysis of CEBPα and PPARγ2 and *Klf4* gene expression level after adipogenic differentiation of ADSCs, a-iPSC-MSCs without IBMX treatment, and in a-iPSC-MSCs after IBMX treatment for 30 minutes, 1, and 2 hours. The data represent fold changes in expression values with respect to ADSC and the error bars indicate ± standard deviation (± SD) of biological triplicates (n=3) *** ($p<0.001$) (C). Representative images of the lipid droplets stained with ORO dye in ADSCs (D) and a-iPSC-MSCs after IBMX treatment for 30 minutes (E), 1 (F), 2 (G) hours following 21 days of adipogenic differentiation. BD= before differentiation, AD= after differentiation

6.2.3. Aim3. To Examine the effect of dexamethasone on accumulation of lipid

Given that elevating endogenous or exgenous expression of *Klf4*, which influnce the early stage of adipocyte differentaition, did not improve the functional capacity of the H9-MSCs or a-iPSC-MSCs, I then wanted to examine if increasing expression of adipogenic regulators that hallmarks the terminal differentiation stage would bypass this block in differentiation. Importantly, dexamethasone has been shown to increase the main adipogenic regulator (PPARγ2) expression in mouse 3T3-L1 cells. Most researchers have been using 0.5 µM dexamethasone for adipogenic differentiation of mouse 3T3-L1 cells, mouse and human primary MSCs, as well as mouse and human PSCs (ESCs and a-iPSCs)[126, 127, 128]. To determine optimal conncetration of dexamethasone that may have an impact on the adipogenic potential of H9-MSCs and iPSC-MSCs, 0.25 µM, 0.5 µM, and 1 µM concentratios of dexamethsone were tested. Compared to 0.5 µM dexamethasone concentration, 0.25 µM and 1 µM dexamethasone showed significant improvement in lipid accumulation in H9-MSCs but was significantly lower compared to lipid accumulated in the differentiated ADSCs (Figure 16A).

Since studies have shown that expression of the genes involved in acumulation of lipids in preadipocytes are regulated by CEBPα and PPARγ2 transcription factors, I then tested the effect of 0.25 µM, 0.5 µM, and 1 µM of dexamethasone on expression level of these markers. From Figure 16B, it is clear that of the three dexamethasone concentrations I investigated, 0.25 µM of dexamethasone gave the highest PPARγ2 expression compared to 0.5 µM and 1 µM, but all concentrations still resulted in significantly lower levels of PPARγ2 than that observed for differentiated ADSCs (Figure 16B). Gene expression level of CEBPα is also higher at 0.25 µM dexamethasone compared to 0.5 µM and 1 µM, but was lower than that of ADSCs. However,

expression of CEBPα and PPARγ2 did follow the pattern of lipid accumulation for the corresponding dexamethasone concentrations, where lipid accumulation and gene expression level of the adipogenic transcription factors was higher for 0.25 µM and 1 µM dexamethasone concentrations compared to 0.5 µM dexamethasone concentration (Figure 16A and B).

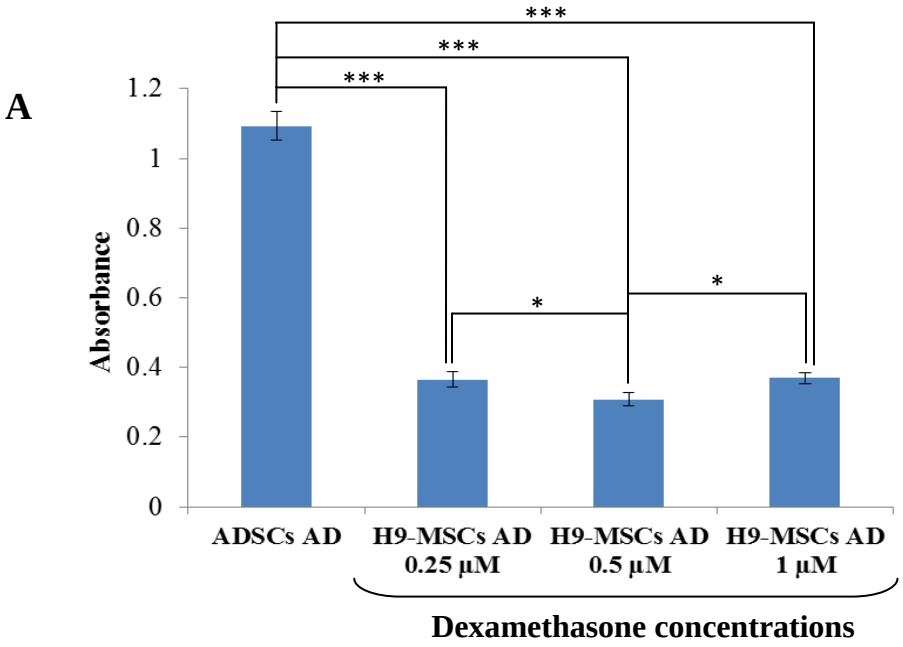

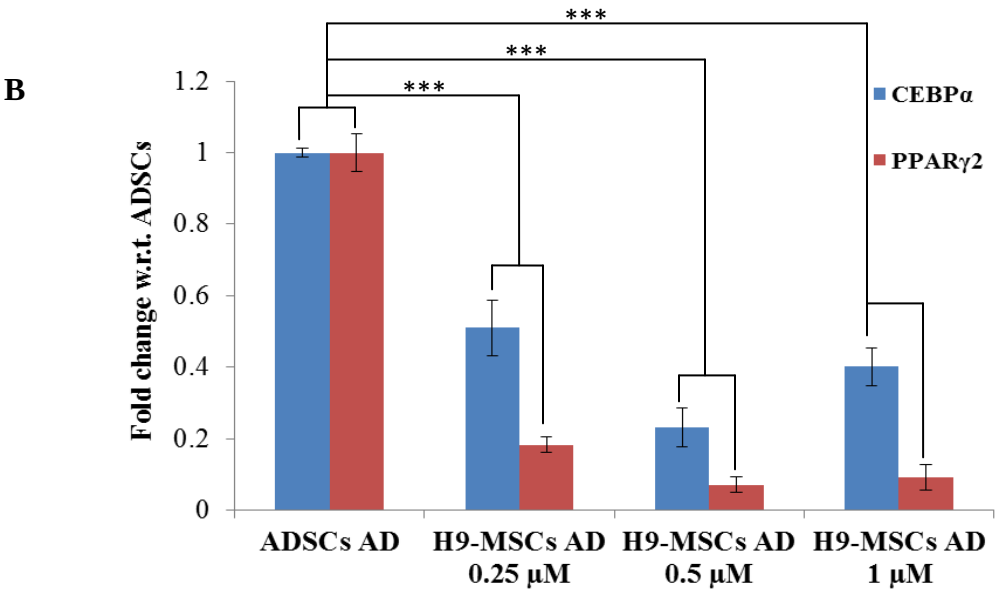

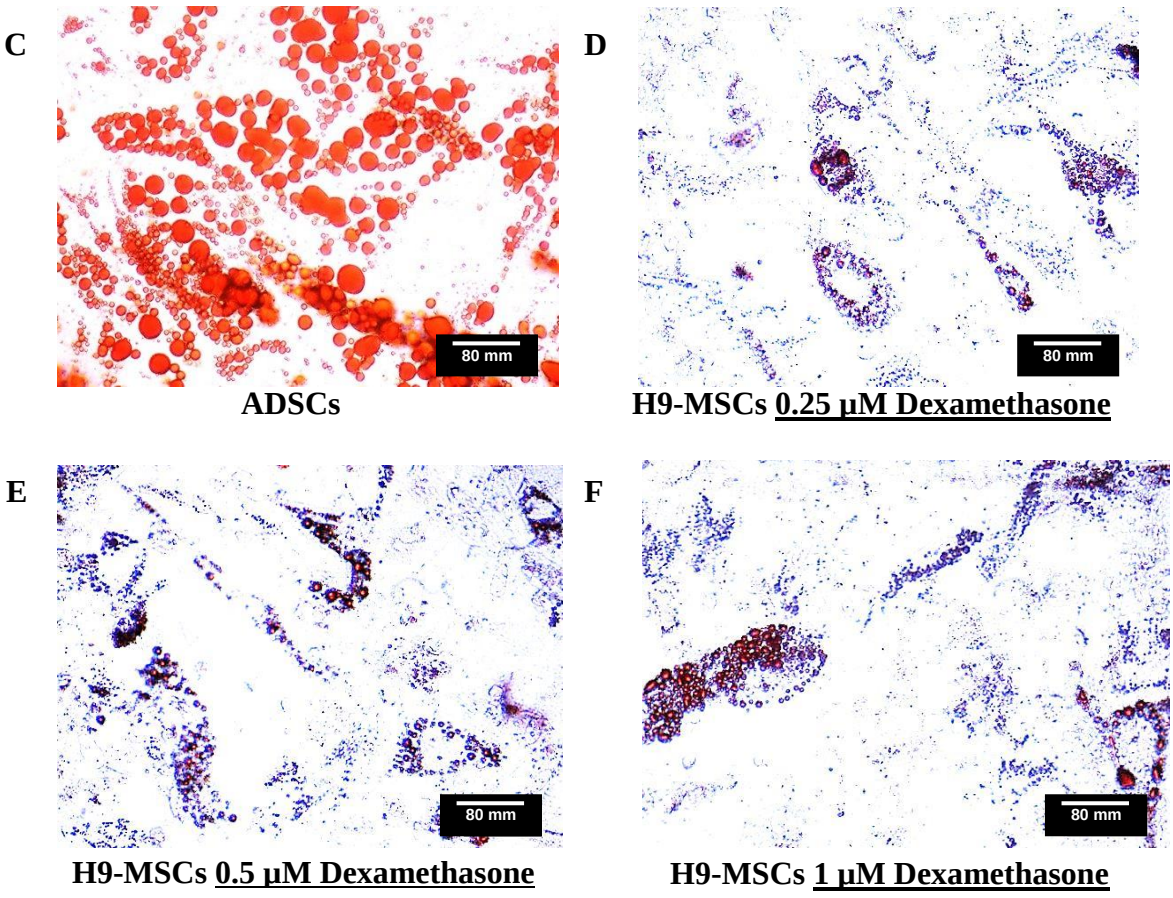

Figure 16: Effect of different dexamethasone concentrations on H9-MSCs. The bar graph represents absorbance value of extracted ORO dye from the differentiated H9-MSCs to adipogenic lineage for 21 days in 0.25 µM, 0.5 µM, or 1 µM dexamethasone concentrations (A). Real-time PCR analysis of CEBPα and PPARγ2 gene expression level after adipogenic differentiation of H9-MSCs. The data represent fold changes in expression values with respect to ADSC and the error bars indicate ± standard deviation (± SD) of biological triplicates (n=3) (B). Representative images of the lipid droplets stained with ORO dye in the differentiated ADSCs to adipocytes (C) and H9-MSCs differentiated to adipocytes in 0.25 µM (D), 0.5 µM (E) and 1 µM (F) dexamethasone concentration, n=3. The error bars indicate ± SD of the three biological replicates, Statistical differences of * ($p<0.05$) and *** ($p<0.001$); AD = after differentiation

When I examined effect of dexamethasone on adipogenic potential of a-iPSC MSCs, the amount of lipid accumulation for a-iPSC-MSCs differentiated in 1 µM dexamethasone was not significantly different from 0.5 µM dexamethasone. However, amount of lipid accumulation was significantly lower for a-iPSC-MSCs differentiated with 0.25 µM compared to 0.5 µM dexamethasone concentration (Figure 17A). The pattern of gene expression level of CEBPα and PPARγ2 in a-iPSC-MSCs mimicked the lipid accumulation pattern in a-iPSC-MSCs differentiated showing no difference in expression of CEBPα and PPARγ2 between 0.5 µM and 1 µM dexamethasone and significantly lower expression for 0.25 µM dexamethasone (Figure 17B). However, the gene expression of CEBPα and PPARγ2 for 0.5 µM and 1 µM dexamethasone concentrations were approximately 5 fold higher than expression levels observed for the differentiated ADSCs, which did not reflective of the amount of lipid accumulated by a-iPSC-MSCs at these two dexamethasone concentrations (Figure 17B).

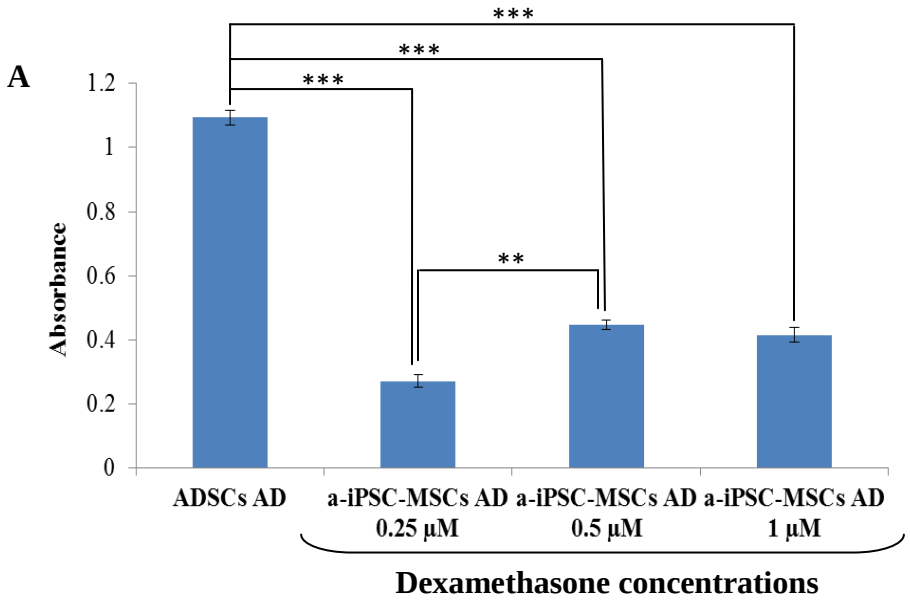

B

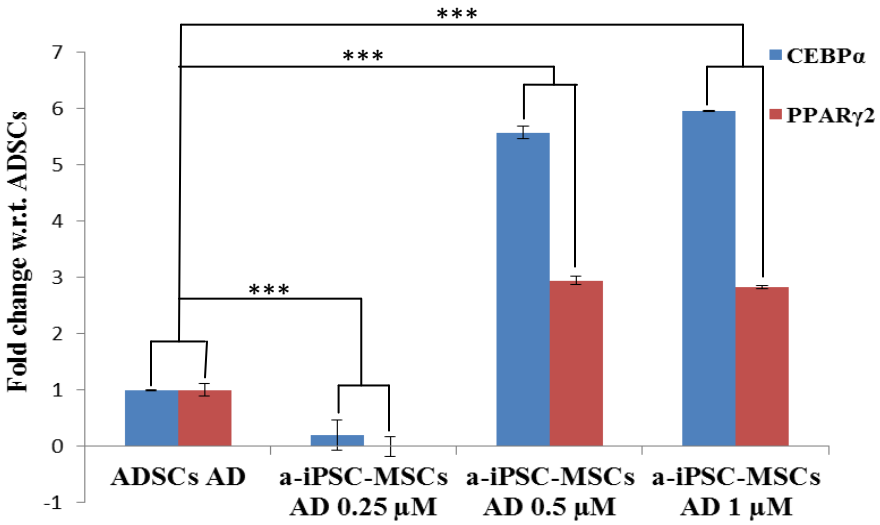

C

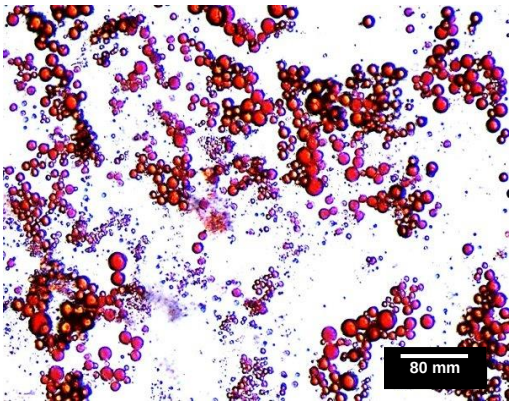

ADSCs

D

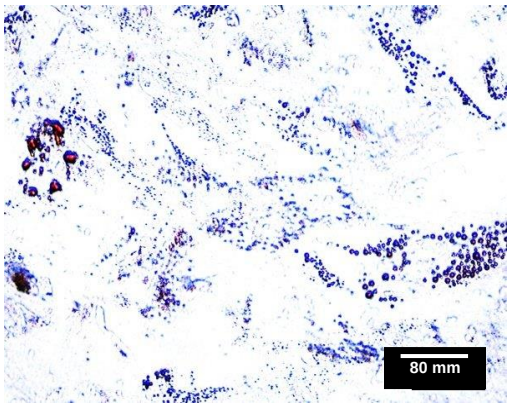

a-iPSC-MSCs 0.25 µM Dexamethasone

E

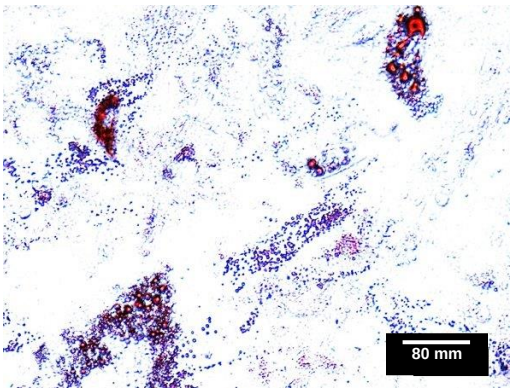

a-iPSC-MSCs 0.5 µM Dexamethasone

F

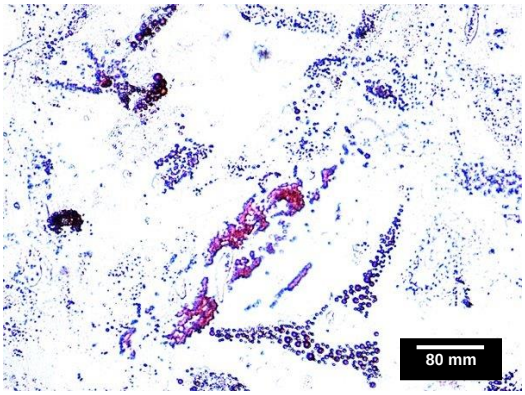

a-iPSC-MSCs 1 µM Dexamethasone

Figure 17: Effect of different dexamethasone concentrations on a-iPSC-MSCs.

The bar graph represents absorbance values of extracted ORO dye from the differentiated a-iPSC MSCs to adipogenic lineage for 21 days in 0.25 µM, 0.5 µM, or 1 µM dexamethasone concentrations (A). (A). Real-time PCR analysis of CEBPα and PPARγ2 gene expression level after adipogenic differentiation of a-iPSC MSCs. The data represent fold changes in the adipogenic gene expression values with respect to ADSC and the error bars indicate ± standard deviation (± SD) of biological triplicates (n=3) (B). Representative images of the lipid droplets stained with ORO dye in the differentiated ADSCs to adipocytes (C) and a-iPSC MSCs differentiated to adipocytes in 0.25 µM (D), 0.5 µM (E) and 1 µM (F) dexamethasone concentration, n=3. The error bars indicate ± SD of the three biological replicates, Statistical differences of ** ($P<0.01$) and *** ($p<0.001$); AD = after differentiation

6.2.4. Aim 4. To examine the effect of MEF-conditioned media (MEF-CM) on adipogenic potential of H9-MSCs

My previous observations indicated that cells surrounding H9 hESCs and a-iPSCs colonies that are cultured in mouse embryonic fibroblast conditioned media (MEF-CM) form tiny lipid droplets. Therefore, I set out to examine whether replacing the MSC media with MEF-CM would improve/retain differentiation capacity of the fibroblast like cells after isolating and passaging these cells. I chose to maintian and passage the cells in MSC media after isolation, because further culturing of these cells in MEF-CM at that stage resulted in remergenace of PSC colonies, which shows that the fibroblast like cells around the colonies are still highly plastic and dynamic. Therefore, I cultured these cells in the MSC media for 3 passages and subjected to

adipogenic differentiation in the different concentrations of MEF-CM in MSC media (i.e. 20%, 40%, 60%, and 80% MEF-CM). H9-MSCs differentiation in 40% and 80% MEF-CM media showed significant increase in lipid accumulation compared to H9-MSCs differentiated in MSC media and 60% MEF-CM media (Figure 18A). Of the H9-MSCs differentiated in 40% and 80% MEF-CM, cells in 80% MEF-CM formed more defined and larger lipid droplets (Figure 18G) compared to ones in 40% MEF-CM media (Figure 18E), indicating that 80% MEF-CM favours adipogenesis, as indiacted by lipid accumulation, to a greater extent. However, no significant difference of overall lipid accumulation was observed between H9-MSCs differentiated in 40% and 80% MEF-CM when lipid accumulation was quantified by ORO extraction (Figure 18A). Regardless of the concentration of MEF-CM used for H9-MSCs adipogenic differentiation, amount of lipid accumulation of increased when compared to H9-MSCs differentiated in the absence of MEF-CM (Figure 18A).

MEF-CM contains knock-out serum replacement (KO-SR) and growth factors secreted by mouse embryonic fibroblasts, while MSC media has a defined formulation with FBS being the only factor that is not defined. Therefore, I wanted to examine which part of the formulation of the MEF-CM would be causal to this increase in adipogenesis. Thus, I first investigated the potential effect of KO-SR on differentiation of H9-MSCs to adipogenic lineage. To this end, the H9-MSCs were differentiated in media containing KO-SR instead of FBS to evalaute whether increase in adipogenic potential of H9-MSCs cultured in MEF-CM is due to KO-SR. As shown in the Figure 18A, differentiating H9-MSCs in media with 20% KO-SR did not improve lipid accumulation as significantly as 40% or 80% MEF-CM or H9-MSCs differentiated in MSC media (Figure 18A). These results indicate that the majority of the increase in lipid accumulation

in H9-MSCs diferentiated in 40% or 80% MEF-CM compared to H9-MSCs differentiated in media containing 20% KO-SR can be due to factors secreted by MEFs.

Upon analysing adipogenic gene expression level of H9-MSCs differentiated in 80% MEF-CM, it is clear that 80% MEF-CM promotes increased lipid accumulation but also increases expression of the two major adipogenic regulators, PPARγ2 and CEBPα, compared to H9-MSCs differentiated in MSC media. A small incremental increase in expression of PPARγ2 and CEBPα was also observed for H9-MSCs differentiated in MSC media but was significantly lower compared to expression of the adipogenic factors in the differentiated ADSCs (Figure 18B). No significant change in expression levels were detected between H9-MSCs differentiated in 20% KO-SR and 80% MEF-CM (Figure 18B).

Thus, the results indicate that factors secreted by MEFs may not have effect on expression level of adipogenic factors but it does improve lipid accumulation in H9-MSCs during adipogenic differentiation.

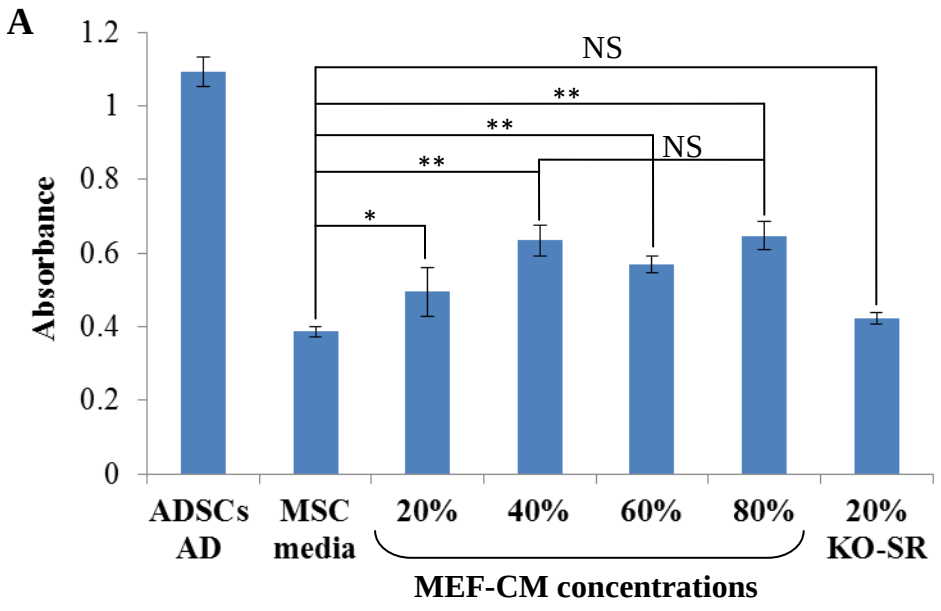

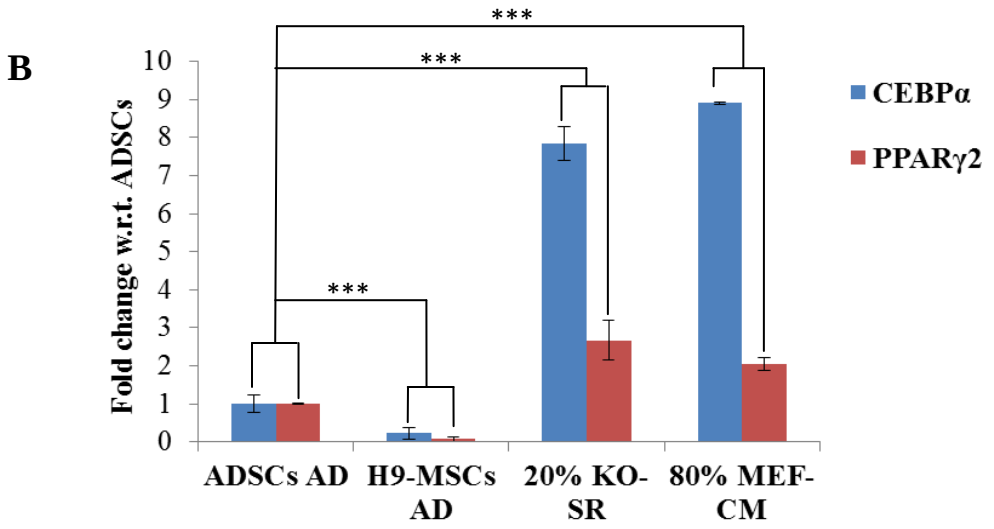

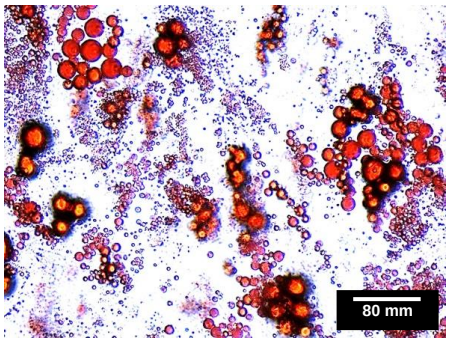

ADSCs

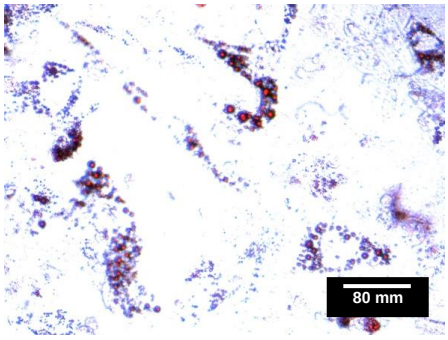

H9-MSCs in MSC media

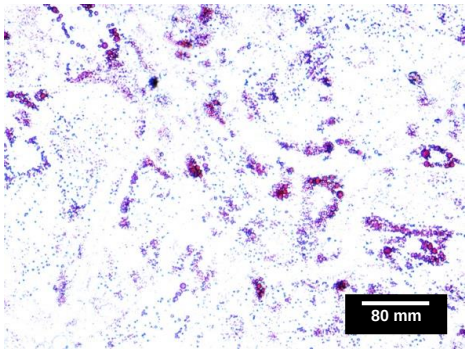

H9-MSCs in 20% MEF-CM

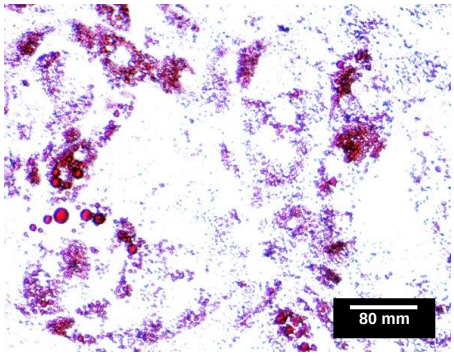

H9-MSCs in 40% MEF-CM

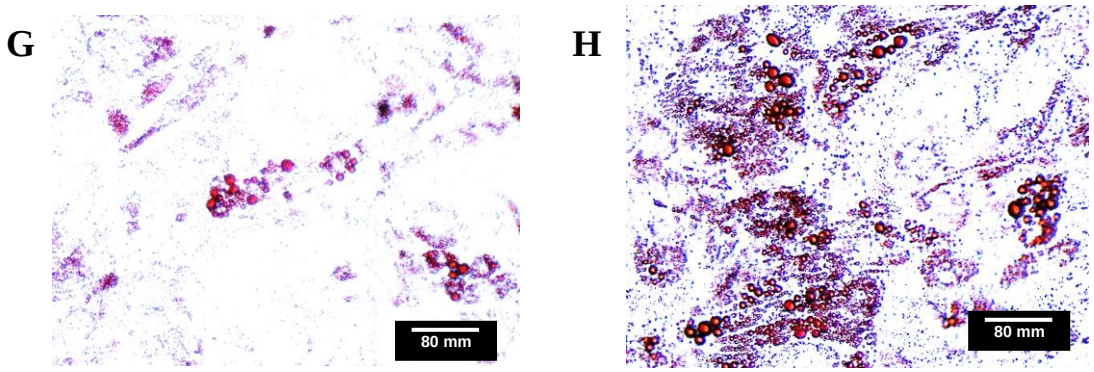

Figure 18: Effect of MEF-CM on adipogenic potential of H9-MSCs. The mean absorbance value of the extracted ORO dye from adipogenic differentiation of ADSCs, H9-MSCs differentiated in only MSC media or in 20%, 40% or 60% MEF-CM, and MSC media made with 20% KO-SR. The error bars indicate ± SD of the three biological replicates, Statistical differences of * ($P<0.05$) and ** ($p<0.01$), NS= not significant (A). Real-time PCR analysis of CEBPα and PPARγ2 gene expression level after adipogenic differentiation of ADSCs, H9-MSCs differentiated in MSC media, H9-MSCs differentiated in MSC media with 20% KO-SR, and in 80% MEF-CM. The data represent fold changes in the adipogenic gene expression values with respect to ADSC and the error bars indicate ± standard deviation (± SD) of biological triplicates (n=3), statistical significance of *** ($p<0.001$) (B). Representative images of the lipid droplets stained with ORO dye in the differentiated ADSCs to adipocytes (C), H9-MSCs differentiated in MSC media (D), 20% (E), 40% (F), 60% (G), and 80% (H) MEF-CM. AD = after differentiation

6.2.5. Aim 5. To examine the effect of ADSC-conditioned media on adipogenic potential of H9-MSCs

The goal of developing a optimized protocol for efficient differentiation of H9-MSCs and a-iPSC-MSCs to adipocytes is to allow us to study human adipogenesis and relevant molecular and functional mechanisms *in vitro* with the hopes that this will provide a novel maens to derive adipocytes and MSCs for regenerative applications. However, MEF-CM contains factors secreted by MEFs, thus it is not xeno-free, which makes the use of this media not competible for cell transplntation purposes in humans. Therefore, conditioned media from the cultured ADSCs (ADSC-CM) were used to differntiate H9-MSCs and a-iPSC-MSCs to adipocytes, since this media is xeno-free.

First the experiment was carried out on H9-MSCs and I initially tested 50% and 100% ADSC-CM on H9-MSCs differenitation. H9-MSCs were cultured in MSC media until passage 3 prior to starting differentiation. H9-MSCs differentiated either in 50% (Figure 19B) or 100% (Figure 19C) ADSC-CM did not accumulate any lipid comapred to ADSCs (Figure 19A).

A

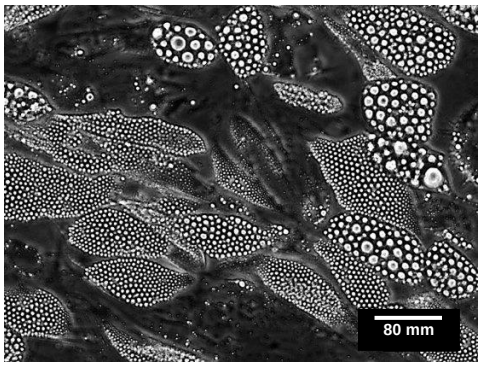

ADSCs

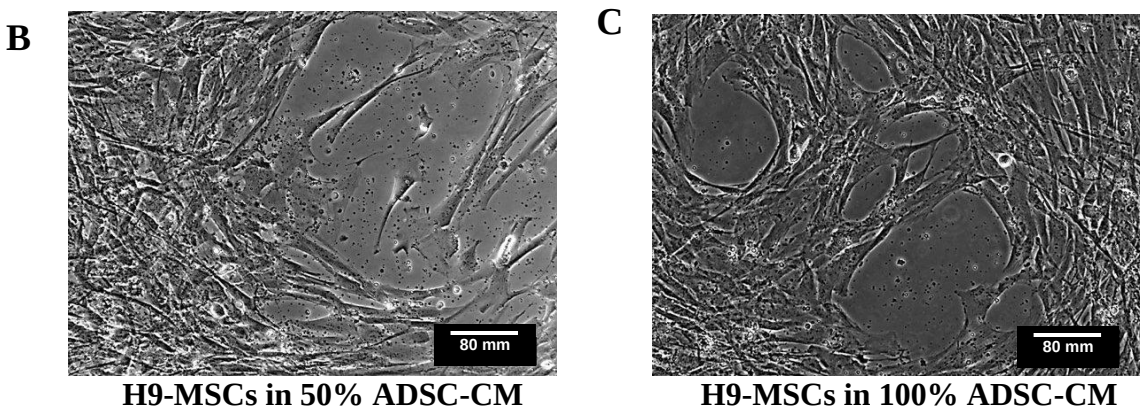

Figure 19: **Effect of ADSC-CM on adipogenic potential of H9-MSCs**. Bright field images of differentiated ADSCs to adipocytes (A) and H9-MSCs differentiated in 50% (B) and 100% (C) ADSC-CM to adipocytes. n=1, done in triplicates

Overall, differentiating MSC-like cells in 80% MEF-CM favours adipogenic differentiation to greater extent than upregulating either ectopic or endogenous *Klf4* in the early stage of adipogenesis or increasing expression of the main adipogenic regulator (PPARγ2) in the later stages of adipogenesis, but it still nowhere near the adipogenic potential of ADSCs.

6.3. Supplementary figures

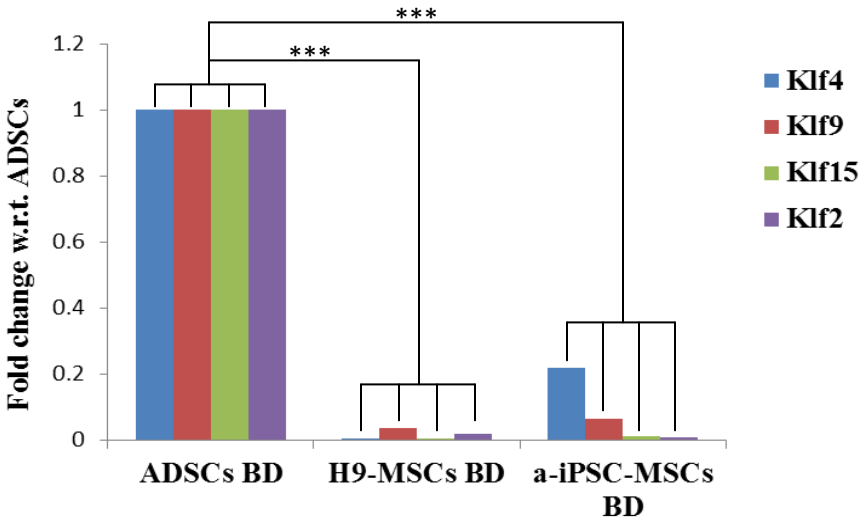

Supplementary figure 1: **Expression of different Klfs in H9-MSCs and a-iPSC-MSCs before differentiation**. Real-time PCR analysis of *Klf4*, *Klf9*, *Klf15*, and *Klf2* gene expression in ADSCs, H9-MSCs, and a-iPSC-MSCs before adipogenic differentiation. The data represent fold changes in the different *Klf* gene expression values with respect to ADSC, n=1 done in experimental triplicates.

7. DISCUSSION

PSCs (i.e. H9 hESCs and iPSCs), due to their capacity to differentiate into any cell type of the body, can be a very good source for the generation of standardized cell types, including MSC-like cells –that the focus of my thesis. However, differentiating PSCs to mature adipocytes remains a major challenge due to our limited understanding of the molecular mechanism involved in specification of PSCs to MSCs and the pathways involved in commitment of MSCs to pre-adipocytes. This may be in part the result of the fact that most studies carried out to optimize differentiation of hESCs and iPSCs to adipocytes involves formation of clumps of PSCs called embryoid bodies (EBs). Subsequently, EBs are subjected to adipocyte differentiation in media supplemented with adipogenic program inducing factors (such as dexamethasone, rosiglitazone, and insulin) for 21 days. During the 21 days of adipogenic differentiation, cells from EBs outgrow and differentiate into adipocytes containing lipid droplets. The differentiated EB cultures are stained with ORO to check for the presence of lipid-engorged adipocytes in these cultures followed by counting EB cultures stained positive for the ORO stain[99,110]. However, the outgrowths of EBs are multilayer and 3 dimensional in structure and can trap ORO dye[99,110]. Thus, these studies do not provide a clear indication of the level of adipogenesis, and moreover, the presence of adipocyte colonies may be grossly overestimated or not reported accurately. In addition, the EB differentiation method provides a highly heterogeneous culture with multiple different cell types, thus providing minimal insight towards human adipocyte development and pathways that regulate this process. Therefore, researchers have used PSC-derived MSC-like cells as intermediate cell type to improve differentiation efficiency by obtaining a more homogenous culture of mature adipocytes.

Over the last 3 years several other groups have used different protocols for generating MSCs from hESCs and/or iPSCs-derived from primary MSCs. However, all the protocols utilized EB formation strategies followed by isolation of EB outgrowths[97,94] and sorting PSC-derived MSC-like cells using the aforementioned MSC markers[95] (CD90, CD105 and CD73). Two studies have also derived MSC-like cells by spontaneous differentiation of PSCs on tissue culture plates in MSC media[96] or BM-MSC conditioned media[94] for extended period (at least 32 days), and/or indirectly co-culturing PSC-derived MSC-like cells with BM-MSCs[94] (Table 1). Similar to the cocktail factors used to differentiate PSCs to adipocytes, PSC-derived MSC-like cells were subjected to adipogenic differentiation using the same factors (0.5 µM dexamethasone, 1 µM rosiglitazone, and 10 µg/ml insulin) followed by staining of these cells with ORO to check for presence of lipid droplet forming cells (adipocytes). According to my studies, the amount of lipid accumulation in differentiated H9-MSCs and a-iPSC-MSCs is higher than that observed for H9 hESCs and human BM-MSC derived iPSCs differentiated directly into adipocytes without the MSC intermediate[99]. Additionally, the quantification of the extracted lipid staining ORO dye is more accurate for my culture conditions as H9-MSCs and a-iPSC-MSCs are differentiated to adipocytes as monolayer, preventing ORO being trapped in multilayered cells, which is one of the limitations in the use of this stain for quantifying lipid accumulation in cultures of clumped cells. Importantly, PSC-derived MSC-like cells allow development of a new *in vitro* model that can be used to study and understand different stages of human adipogenesis.

The protocols used to derive MSC-like cells from different PSC sources are laborious, expensive and time consuming. Additionally, MSC-like cells derived using these protocols show minimal adipogenic differentiation capacity and have not improved significantly the adipogenic

potential of PSC-derived MSC-like cells[96, 129]. In order to use PSC-derived MSC-like cells as a model system to understand human adipogenesis *in vitro*, homogeneous population of PSC-derived MSC-like cells is required.

To overcome some of these limitations, I initially attempted to derive a protocol to obtain MSC-like cells in a shorter time frame. According to the criteria set by *ISCT* to define MSCs, the cells have to be able to adhered to the plastic tissue culture plates and should: 1) have fibroblast-like morphology, 2) express a panel of non-specific surface markers (such as CD90, CD105, and CD73), lack expression of endothelial markers (i.e. CD31) and hematopoietic markers (i.e. CD45), and 3) should differentiate into at least adipogenic, osteoblastic, and chondrogenic lineages[130].

During my studies I have noted that the cells surrounding PSC colonies have fibroblast-like shape and upon confluency are able to form lipid droplets. These observations led me to examine whether the fibroblast-like cells surrounding PSC colonies would be able to provide a faster and more efficient method in deriving MSC-like cells given that these cells already partially satisfied criteria 1 provided by the *ISCT* that refers to fibroblast morphology. Therefore, I proceeded to isolate the fibroblast-like cells surrounding H9 hESCs and a-iPSCs colonies, which lead me to obtain population of PSC-derived MSC-like cells in only 14 days that meet two of the three criteria set by *ISCT* that define MSCs. The H9-MSCs and a-iPSC-MSCs that I derived have fibroblast-like morphology (Figure 6) and express surface markers as outlined by *ISCT* (Figure 7 and 8) at passage 3 and 7. Nevertheless these cells had limited differentiation capacity to adipocytes when compared to their adult MSC counterparts, such as ADSCs (their ability to differentiate into osteoblastic and chondrogenic lineages was not tested). These cells

were not able to differentiate towards the adipogenic lineage as efficiently as ADSCs, depicted by smaller and fewer lipid droplets formed by H9-MSCs and a-iPSC-MSCs compared to ADSCs (Figure 10). This could be due to presence of other cell types within the culture of H9-MSCs and a-iPSC-MSCs. In addition, the panel of surface markers (CD90, CD73, and CD105) used to characterize primary MSCs are also expressed by other cell types, such as pericytes. The PCS derived MSC-like cells may be retaining primitive/embryonic characteristics, thus their molecular and gene expression profiles could be very different from mature adult MSCs[97]. This is a phenomenon that has been reported for many PSC derived cell types, where the differentiated cells lack the functional capacity when compared to adult counterparts[98, 62]. One example is the hematopoietic stem cells (HSC); there are numerous protocols that allow derivation of HSC-like cells from PCS, however their functional capacity, level of maturity (fetal globin to adult globin switch is absent)[131] and molecular profiles[132] differ from that of an adult HSC[133].

Therefore, to validate PSC derived MSC-like cells as an equal counterpart to an adult MSC/ADSC, expressions of some of the genes in primary MSCs (i.e. bone-marrow derived MSCs) were tested[97]. These genes include GNL3, Vimentin, CD140b[97], which have similar but not identical gene expression profile to ADSCs. The differences in gene expression are also observed between batches of PCS-derived MSC-like cells. This result indicated possible heterogeneity between the batches of MSC-like cells derived from different passages of H9 hESCs and a-iPSCs.

During specific steps of embryogenesis and organ development, the cells within certain epithelia appear to be plastic and thus able to move back and forth between epithelial and

mesenchymal states via the processes of EMT and MET[119]. My results imply that the H9-MSCs and a-iPSC-MSCs are not similar to mature adult human MSCs, such as ADSCs. Since H9-MSCs and a-iPSC-MSCs are derived from pluripotent sources, the these cells might be going through on EMT stage, which is defined through the process of MSC formation from the epithelial cells, but have not completely differentiated into a mature MSC and might be trapped at an earlier phase during the specification stage to a MSCs. Therefore, expression of the previously tested early EMT genes, such as MSX1 and CDX1[97], were examined in both H9-MSCs and a-iPSC-MSCs. Similar to gene expression pattern of the MSC markers, gene expression of the early EMT markers of H9-MSCs and a-iPSC-MSCs are close to that of ADSCs, but also show some differences. This is in line with the findings reported by the group who analyzed MSC gene expression profiles between BM-MSCs and MSCs derived from BM-iPSCs. Additionally, in this study only five markers are tested to determine whether H9 hESCs and a-iPSCs derived MSC-like cells have similar gene expression profile as ADSCs. Global gene expression analysis of H9-MSCs and a-iPSC-MSCs with more biological replicates is necessary in order to compare PSC-derived MSCs and ADSCs at the gene expression level.

Since gene expression can be controlled through methylation, close analysis of the DNA methylation status in H9-MSCs and a-iPSC-MSCs in comparison to ADSCs is also required. Previously, DNA methylation of human BM-MSC derived iPSC-MSCs have been shown to have similar DNA methylation patterns to that of human BM-MSCs[97]. In my study, iPSCs were derived from ADSCs, while in other published studies iPSCs are derived from BM-MSC. Only approximately 15% DNA methylation patterns are identical between BM-MSCs and ADSCs. These most significant differences were seen for genes involved in lipid modification and

glucose metabolism, reflecting apparent functional differences of the originating tissues in terms of gene regulation mechanism at the epigenetic level[134]. These findings support need for analysing DNA methylation patterns for a-iPSC-MSCs, H9-MSCs and ADSCs, since BM-MSC experiments may not be applicable to my study given that our starting population is ADSCs or hESCs. Further molecular characterization of the differentiation process will give directions to which genes and signalling pathways need to be regulated to align the profile of PSC-derived MSC-like cells to that of bonafide MSCs and to also improve adipogenic potential of the PSC-derived MSC-like cells.

For my project I used ADSCs as the standard for adipocyte differentiation, and MSC-like cells derived from the PSC sources were continuously compared to these cells on both molecular and functional level. Therefore, in this study, efforts are made to obtain MSC-like cells from H9 hESCs and a-iPSCs with equal lipid accumulation capacity to that of ADSCs. However, the MSC-like cells that I obtained had reduced lipid accumulation capacity compared to ADSCs. This could mean that the PSC derived MSC-like cells are not mature enough or that these cells are on a different developmental trajectory then the ADSCs. Thus, determining the factors that are limiting the PSC differentiation into MSCs that have more adult phenotype or adipogenic potential is difficult to delineate without this in-depth molecular analysis. Accordingly, full characterization PSC-derived MSC-like cells in terms of global gene expression patterns and DNA methylation, will be critical to identify pathways that could aid in differentiation of PSC into more adult like MSCs that can be comparable to MSCs, such as ADSCs.

Moreover, primary MSCs are shown to be devoid of teratoma forming capacity *in vivo.* H9-MSCs and a-iPSC-MSCs both express approximately 1.03± 0.5% and 0.9± 0.6% SSEA3

(Figure 9) respectively, which is expressed by cells with pluripotent and stem cell-like characteristics and thus can give rise to teratoma *in vivo.* Therefore, it is important for us to analyze their *in vivo* teratoma formation capacity before these cells can be used for any future therapeutic applications. However, it is important to note that MSC-like cells derived from human foreskin fibroblast-derived iPSCs and two other commercially available human fibroblast-derived iPSC cell lines have shown to not form teratoma when injected in severe combined immune-deficient (SCID) mice for severe hind-limb ischemia repair[135]. Thus, it is likely that H9-MSCs and a-iPSC-MSCs expressing minimal SSEA3 may induce teratoma formation *in vivo*.

Previous studies have shown MSC-like cells derived from different PSC sources differentiate to osteogenic and chondrogenic lineages efficiently but not to adipogenic lineage[97, 94, 96, 92] . Therefore, despite of the heterogeneity in H9-MSCs and a-iPSC-MSCs, efforts were made to improve adipogenic potential of PSC-derived MSCs using the information known about adipocyte development in mice. In murine adipogenesis it has been shown that: 1. early stages of adipogenesis are regulated by a set of transcription factors, such as Klf4, Klf5, and Klf1[136]; 2. transition to a commitment stage has to allow for mitotic arrest[137]; and 3. transcription regulation through CEBPα and PPARγ2 promotes maturation and lipid accumulation in the final stage of adipogenesis[126]. Therefore, for my thesis project I explored how transcription factors and different culture/media conditions could influence the above 3 aspects towards improving differentiation efficiency of H9-MSCs and a-iPSC-MSCs to adipocytes.

In order to improve adipogenic capacity of MSC-like cells, I initially looked at candidate transcription factors that have been shown to be important in early adipogenesis, such

transcription factor is Klf4. Klf4 regulates key events of arresting cell growth at the MSC stage and upregulating the expression of CEBPα and PPARγ2 transcription factors involved in adipocyte phenotype acquisition in mouse preadipocytes (i.e. 3T3-L1)[125]. Therefore, to control differentiation of PSC-derived MSC-like cells in the beginning of the commitment stage of adipocyte development from PSCs, *Klf4* was over-expressed ectopically.

My results showed that ectopic overexpressing *Klf4* does not lead to more lipid accumulation in H9-MSCs as no difference was observed between absorbance values of the extracted lipid staining ORO dye from the *Klf4* expressing sendai virus infected and uninfected cells. Additionally, ectopically overexpressing *Klf4* also did not lead to increase in adipogenic regulators CEBPα and PPARγ2 (Figure 13C), which are necessary for the cells to undergo maturation of adipocyte progenitors through lipid accumulation to become fully functional adipocytes. Thus, overexpressing *Klf4* also does not increase degree of adipogenesis in H9-MSCs to that of ADSCs. These results can be attributed to the fact that the role of *Klf4* in early cell growth arrest during adipogenesis was shown in mouse 3T3-L1 preadipocyte cells, which have already by passed the commitment stage of MSCs to preadipocyte. On the other hand, the cells used in this study are MSC-like cells derived from human PSC sources. Therefore, the role of Klf4 maybe different at different stages of adipocyte development in MSC-like cells derived from human PSC sources. It is also plausible that the role of Klf4 differs between species, thus direct translation into the human system may not applicable and we should be testing other Klf family members in the human system. Furthermore, PSC-derived MSC-like cells maybe at a different stage (i.e. EMT stage (Figure 11)) of development then the ADSCs or preadipocytes. Klf4 has different roles in different cell types, for example Klf4 regulates a different set of genes

during reprogramming process and pluripotency then adipogenesis. This supports the possibility the MSC-like cells derived in my study are on a different differentiation trajectory then adult MSCs and these differences may influence what genes and pathways Klf4 regulates in MSC-like cells. To test this, future experiments should examine a larger panel of genes that are involved in EMT to show if the differentiation block is the result of the MSC-like cells being stuck in a premature state or in a completely different differentiation pathway.

Furthermore, while Klf4 is expressed in ADSCs, increasing expression in human MSC-like cells may not be sufficient to induce adipogenesis; and it maybe that the presence of other transcription factors and different culture conditions are required before these cells can differentiate towards adipocytes. Controlling Klf4 overexpression levels using a viral system is difficult, since I observed variation in Klf4 expression between batches even when the MOI was maintained. Thus, in order to use this system, the virus has to be titrated for individual biological replicates to achieve the exact levels seen for ADSCs. Therefore, it is plausible that Klf4 expression has to be tightly regulated in order for us to see an effect on adipogenesis. This is also apparent from the cell death of a-iPSC-MSCs infected with *Klf4* expressing sendai viruses at MOI1, MOI2, MOI3, and MOI4. This is possibly because *Klf4* is also one of the transcription factors used to reprogram ADSCs to iPSCs. Thus, *Klf4* genes must be already primed for inducing *Klf4* expression, making it toxic to the cells when overexpressed and thus induce the cells to undergo apoptosis[138, 139, 140]. Therefore, more rigorous optimization of this expression system needs to be conducted in order for me to draw a clear conclusion on the effect of *Klf4* in human adipogenesis. In addition, whether increasing endogenous *Klf4* levels in the PSC-derived MSC-like cells improve adipogenic potential of these cells is need to be investigated.

Given that ectopic expression of *Klf4* is difficult to control, I set out to use IBMX, since IBMX treatment has been shown to increase endogenous *Klf4* expression in 3T3-L1 preadipocyte cell line[125]. To increase *Klf4* levels in H9-MSCs and iPSC-MSCs, I treated the cells with IBMX for varied amounts of time before starting adipogenic differentiation. My results showed that duration of IBMX treatment required to achieve *Klf4* levels similar to that observed for ADSC varied between H9-MSCs and iPSC-MSCs. This difference could be because *Klf4* is one of the transcription factors used to reprogram ADSCs to pluripotent state, making *Klf4* genes primed to be expressed with very small amount of *Klf4* inducing factor, such as IBMX, in a-iPSC-MSCs. However, overall IBMX did not enhance adipogenic differentiation as measured by lipid accumulation in either H9-MSCs or a-iPSC-MSCs. Additionally, the effect of IBMX on expression of the adipogenic regulators, CEBPα and PPARγ2, is not consistent across H9-MSCs and a-iPSC-MSCs. This can be due to the possible different mechanism of how Klf4 acts in ADSCs versus in MSC-like cells derived from the PSC sources.

Moreover, in mouse 3T3-L1 preadipocyte cells, other Klf proteins beside Klf4 have been shown to be involved, where some Klfs (Klf2, Klf6, and Klf9) are shown to inhibit adipogenesis and some, such as Klf5 and Klf15, are shown to regulate Klf4 expression to induce adipogenesis. Role of these Klfs should be investigated in order to examine role of Klf in early or late adipogenesis stage in MSC-like cells derived from human PSC sources, as there may be species differences in the KLfs that are important for human versus murine adipogenesis. As shown in the Figure S1, level of inhibitory Klfs (Klf2 and Klf9) along with Klfs (Klf15) supporting adipogenesis are also down regulated. Thus, increasing expression of adipogenesis promoting

Klfs along with overexpressing or down regulating Klf4 at the right stage of adipogenesis may help improve adipogenic potential of H9-MSCs and a-iPSC-MSCs.

Given that I had limited success with improving adipogenesis by regulation of the early stages of adipogenic differentiation, I next wanted to examine if regulation of the later commitment stages of adipogenesis would improve differentiation capacity of the MSC-like cells. To this end, I used Dexamethasone (a glucocorticoid hormone), which has been shown to lock cells in irreversible post-mitotic growth arrest to prevent cells reverting back to the undifferentiated (adipocyte progenitor) state in the late commitment stage of adipogenesis[137]. Dexamethasone is also shown to increase expression of the main adipogenic regulator, PPARγ2, in mouse preadipocytes and post-mitotic adipocytes[137]. PPARγ2 governs expression of the genes involved in lipogenesis, lipolysis, glucose intake, and insulin sensitivity[126]. These genes collectively lead to maturation of preadipocytes to fully functional mature adipocytes[141]. Studies utilizing 3T3-L1 mouse preadipocyte cell line, mouse ESCs, human ESCs, and human iPSCs consistently use 0.5 µM of dexamethasone in combination with other adipogenic factors (i.e. rosiglitazone, indomethacin, IBMX, and insulin) in their adipocyte differentiation cocktail [127, 128]. In my study the degree of adipogenic potential of PSC-derived MSCs using 0.5 µM dexamethasone was not similar to that of ADSCs (Figure 8 and 14A). Therefore, to determine optimal concentration of dexamethasone to improve adipogenic potential of PSC-derived MSCs, H9-MSCs and a-iPSC-MSCs were subjected to adipogenic differentiation with 0.25 µM and 1 µM dexamethasone in addition to 0.5 µM dexamethasone. Change in dexamethasone concentration had very minimal effect on lipid accumulation or expression level of CEBPα and PPARγ2 (Figure 16B) in H9-MSCs. Nevertheless, it should be noted that while no change in

lipid accumulation was measured at 1μM dexamethasone compared to 0.5 μM dexamethasone, there was significantly lower lipid accumulation at 0.25 μM dexamethasone compared 0.5 μM dexamethasone in a-iPSC-MSCs. Furthermore, 0.5 μM and 1 μM dexamethasone increased expression level of CEBPα and PPARγ2, but was significantly lower at 0.25 μM dexamethasone concentration in a-iPSC-MSCs. This indicates that dexamethasone concentration of 0.5 μM or 1 μM should be chosen for adipogenic differentiation. However, it is important to note that increase in CEBPα and PPARγ2 expression compared to expression of these adipogenic factors in ADSCs did not lead to increase in lipid accumulation at either dexamethasone concentrations. This could be due to post-translational modifications of CEBPα and PPARγ2 RNAs, which may lead to degradation of the RNA, thus measuring RNA levels alone may not be accurate in determining if protein was actually translated. Lack of effect of dexamethasone in H9-MSCs and a-iPSC-MSCs could be due to different effect of CEBPα and PPARγ2 on maturation of PSC-derived MSC-like cells versus mouse 3T3-L1 preadipocyte cells. Additionally, neither H9-MSCs nor a-iPSC-MSCs were similar to mature primary MSCs (i.e. ADSCs) according to the gene expression profile of these cells (Figure 11). This may imply that the differential effect that I observed for dexamethasone treatment of PSC-derived MSC-like cells may be the result of these cells being on an alternative differentiation trajectories that effects their adipogenic differentiation and as a result their response to dexamethasone. Conversely, if the PSC derived MSCs are trapped at an earlier stage of MSC differentiation, then the timeline and concentration of dexamthasone should be further optimized to determine if this would improve adipogenic potential of human PSC-derived MSC-like cells. Furthermore, optimization of the MSC

derivation protocol should also be re-evaluated to ensure that we have bonafide MSCs before we further differentiate using dexamethasone.

While dexamethasone supposed to increases PPARγ2 and promote differentiation, my observation indicate that dexamethasone was not as effective in inducing PPARγ2 and resulted in differential expression of PPARγ2 upon differentiation of PSC-derived MSC-like cells compared to ADSCs. Therefore, different methods that increase PPARγ2 could be also explored to examine effect on adipogenic potential of H9-MSCs and a-iPSC-MSCs. Previously, ectopically overexpressing PPARγ2, using lentiviral vectors containing human PPARγ2, in multipotent progenitor cells derived from H9 hESCs and BM-MSC derived iPSCs has been shown to increase adipogenic potential of these cells up to 60-70%[111]. However, since lentivirus are integrative, similar experiment using non-integrative virus (such as Sendai viruses) should also be conducted, which would reduce the possibility that only ectopic/viral PPARγ2 is expressed versus induction of endogenous PPARγ2.

The main goal of my second objective was to optimize protocol to differentiate H9-MSCs and a-iPSC-MSCs to adipocytes efficiently. Neither increasing *Klf4* levels to drive early stages of adipogenesis, nor induction *PPARγ2* that promote late stage of adipogenesis helped to improve the adipogenic capacity of MSC-like cells derived from PSCs. Thus, I set out to find potential other media formulations that would improve this process. Given that I observed that the cells surrounding H9 hESCs and a-iPSCs form lipid droplets while cultured in MEF-CM, therefore, I then wanted to test whether differentiating these cells in MEF-CM after isolating them from the H9 hESCs and a-iPSCs favours adipogenesis. Initially I tested whether H9-MSCs differentiated to adipocytes using different concentrations (20%, 40%, 60%, and 80%) of MEF-

CM. I discovered that H9-MSCs differentiate efficiently in 80% MEF-CM with 60% lipid accumulation in 80% MEF-CM condition compared to only 35% lipid accumulation for H9-MSCs differentiated in MSC media. Although upregulating *Klf4* through IBMX treatment did not lead to improvement in lipid accumulation in either H9-MSCs or a-iPSC-MSCs, differentiating IBMX treated PSC-derived MSC-like cells may help improve adipogenic potential of these cells. Therefore, H9-MSCs and a-iPSC-MSCs should be differentiated with different MEF-CM concentrations after treating the cells with IBMX for different time durations.

The main defined media component that is difference between the MSC media and MEF media is FBS versus KO-SR respectively. However, in MEF-CM there are also numerous other factors that are secreted by MEFs, which may have different effect on human cells in culture. I initially differentiated H9-MSCs in media containing 20% KO-SR to examine the effect of KO-SR on adipogenesis. The results indicated that differentiating H9-MSCs in media containing 20% KO-SR does not improve lipid accumulation to that obtained in 80% MEF-CM or H9-MSCs differentiated in MSC media (Figure 18A). These results suggest that factors secreted by MEFs must be contributing positively in increasing lipid accumulation in H9-MSCs. To further investigate which factors affect adipogenesis, proteomics of MEF-CM must be carried out followed by testing each factor separately to reduce number of factors needed for differentiation of H9-MSCs and a-iPSC-MSCs to adipogenic lineage efficiently.

If the PSC derived MSCs are to be used for any clinical application, the use of xeno-free media that lacks animal products is required. Accordingly, to prevent use of factors from other species, such as the factors contained in MEF-CM that secreted by MEFs, conditioned media derived from the cultured human ADSCs were used at 50% and 100% concentration for

adipogenic differentiation of H9-MSCs. However, neither of the two concentration led to lipid droplet formation (Figure 19 B and D) in PSC derived MSCs compared to ADSCs (Figure 19A). This could have been because the concentrations tested were not optimal for adipogenic induction in these cells. This experiment was carried out only once. Therefore, more trials with different concentrations of ADSC-CM are necessary. This could also indicate that the PSC derived MSCs are very different and may be at a completely different stage of differentiation or may represent a different cell type then ADSCs.

Most importantly, in my experiments, PSC-derived MSC-like cells differentiated to adipogenic lineages containing small lipid droplets as observed by the ORO stain. Beside mature white adipocytes, most cell types in a human body store lipid in small quantities as an energy resource, such as muscles[142] and leukocytes[143]. In non-adipocyte cells, a lipid droplet' diameter range from 0.1-5 µM compared to a lipid droplet's diameter in white adipocytes that can be more than 100 µM[144]. Thus, lipid droplets forming cells observed in this study could be other cell types. Therefore, to visually determine whether the PSC-derived MSC-like cells have differentiated to adipocytes, the differentiated cells should be stained with BODIPY (fluorescent lipid staining dye) and only the cells with single big lipid droplet per cell should be counted to quantify efficiency of PSC-derived MSC-like cells to adipocytes. Additionally, perilipin A is shown to function as a barrier to protect lipid droplets from hormone sensitive lipase (HSL) to control lipid mobilization specifically only in white adipocytes[145]. Therefore, gene expression and protein levels of HSL and perilipin A along with other adipocyte specific proteins (such as fatty acid binding protein[146], fatty acid translocase (CD36)[147], adiponectin[148]) must be analysed by RT-qPCR and wester blots respectively.

According to the third criteria set by *ISCT,* MSCs should be able to differentiate into at least three lineages (adipogenic, osteogenic, and chondrogenic). The main goal of the study is to obtain functional MSC-like cells from H9 hESCs and a-iPSCs, and in this study efforts are made to differentiate H9-MSCs and a-iPSC-MSCs only to adipogenic lineage. Therefore, H9-MSCs and a-iPSC-MSCs should be differentiated to osteocytes and chondrocytes in order to define these cells as PSC-derived MSCs, which can be used for therapeutic purposes. Moreover, primary MSCs' proliferative and differentiation capacity decreases after passage 14[149]. Therefore, to conclude that PSC-derived MSC-like cells can serve as an alternative infinite source of PSC-derived MSCs, proliferative capacity of H9-MSCs and a-iPSC-MSCs should be tested by expanding these cells until at least passage 20. Additionally, at each passage, rate of proliferation must be calculated to show least change in proliferative capacity of H9-MSCs and a-iPSC-MSCs compared to ADSCs as well as karyotypes at each passage in PSC-derived MSC-like cells must be checked. This is because after passage 4, chromosomes variability is noted in BM-MSCs, which are shown to increase risk for genetic and epigenetic abnormalities that could lead to sporadic malignant cell transformation[149]. Beside differentiation of PSC-derived MSC-like cells to the three lineages, additional functional capability of these cells compared to ADSCs must be carried out. One such main functional role of primary MSCs is their ability to modulate immune response by interacting with T cells and leukocytes through ICAM1 and VCAM1 as well as secreting growth factors (i.e. fibroblast growth factor (FGF), platelet-derived growth factor (PDGF), transforming growth factor-b (TGF-b), vascular endothelial growth factor (VEGF)) to mobilize and trans-differentiate the surrounding cells to that of the injured tissue[71]. Therefore, H9-MSCs and a-iPSC-MSCs must be co-cultured with CD4+ and CD8+ T cells to

investigate whether number of the T cells decrease in the presence of either of the PSC-derived MSC-like cells similar to ADSCs. To further confirm anti-inflammatory property of H9-MSCs and a-iPSC-MSCs, level of the growth factors in the media used for co-culturing T cells and H9-MSCs or a-iPSC-MSCs through ELISA or western blot and gene expression of these factors and the cell adhesion molecules (i.e. ICAM1 and VCAM1) through RT-qPCR.

8. CONCLUSION

My study provides a time and labour efficient protocol to derive MSC-like cells from H9 hESCs and a-iPSCs. These MSC-like cells have similar morphological and phenotypical characteristics to ADSCs, which are bonafide adult MSCs. However, they are not able to differentiate to adipocytes as efficiently as ADSCs. Additionally, these MSC-like cells show differences in some MSC markers at the gene expression level, while having similar gene expressions of early EMT markers. These data suggest that the PSC derived MSC still retain a less mature/more primitive state compared to ADSCs. Therefore, my data indicates that the PSC-derived MSC-like cells should be examined in more in-depth at a global gene expression and epigenetic level to understand what factors and signaling pathways could be responsible for this block in maturation and untimely differentiation into adipocytes. This will also open up avenues to modify genes for more controlled and efficient differentiation of these cells into MSCs and adipocytes that can provide a human cell based platform to model a disease and to obtain in depth knowledge of adipocyte development.

Through my studies, I have explored that endogenous and exogenous overexpression of *Klf4* that acts on early stages of adipocyte development and the late stage factor dexamethasone. However, neither *Klf4* nor dexamethasone improves adipocyte differentiation of the PSC-derived MSC-like cells. To make concrete conclusion on possible effect of endogenous or exogenous *Klf4* overexpression, further optimization of *Klf4* expression levels either by ectopic expression or endogenous induction with IBMX over narrow time periods at different stages of adipocyte development is required, along with a more tightly regulated treatment regimen for dexamethasone that controls the commitment stage of adipogenesis.

In addition, my data also suggest that while the factors that control the different stages of adipogenesis are important, the culture conditions are equally important if not more critical for enhancing adipogenesis. My data indicate that conditioned media significantly enhanced H9-MSCs and a-iPSC-MSCs' lipid accumulation capacity. This increase in adipogenic capacity resulted in more comparable levels of lipid accumulation akin to ADSCs. Nevertheless, it needs to be noted that the PSC derived MSCs may be at a different developmental stage then an adult somatic MSC, thus extensive molecular analysis should be conducted to prove or disprove this notion and to identify factors and pathways that could help specify PSC towards a MSC cell type.

Overall, despite the fact that H9-MSCs and a-iPSC-MSCs are more heterogeneous than ADSCs, my work shows that there is a significant improvement in adipogenic potential of PSC-derived MSC-like cells compared to previous studies. The step-by-step method of deriving MSC-like cells and then differentiating these cells to adipocytes provides an *in vitro* model to study early developmental events in human adipogenesis.

9. REFERENCES

1. Richards, M. *et al.* Comparative evaluation of various human feeders for prolonged undifferentiated growth of human embryonic stem cells. *Stem Cells Dayt. Ohio* **21,** 546–556 (2003).

2. Cowan, C. A. *et al.* Derivation of embryonic stem-cell lines from human blastocysts. *N. Engl. J. Med.* **350,** 1353–1356 (2004).

3. Young, H. E. Existence of reserve quiescent stem cells in adults, from amphibians to humans. *Curr. Top. Microbiol. Immunol.* **280,** 71–109 (2004).

4. Weissman, I. L. Translating stem and progenitor cell biology to the clinic: barriers and opportunities. *Science* **287,** 1442–1446 (2000).

5. Gage, F. H. Mammalian neural stem cells. *Science* **287,** 1433–1438 (2000).

6. Pittenger, M. F. *et al.* Multilineage potential of adult human mesenchymal stem cells. *Science* **284,** 143–147 (1999).

7. Schlaeger, T. M. *et al.* A comparison of non-integrating reprogramming methods. *Nat. Biotechnol.* **33,** 58–63 (2015).

8. Chambers, I. *et al.* Functional expression cloning of Nanog, a pluripotency sustaining factor in embryonic stem cells. *Cell* **113,** 643–655 (2003).

9. Heins, N. *et al.* Derivation, characterization, and differentiation of human embryonic stem cells. *Stem Cells Dayt. Ohio* **22,** 367–376 (2004).

10. Nichols, J. *et al.* Formation of pluripotent stem cells in the mammalian embryo depends on the POU transcription factor Oct4. *Cell* **95,** 379–391 (1998).

11. Wang, Y. *et al.* Induced pluripotent stem cells from human hair follicle mesenchymal stem cells. *Stem Cell Rev.* **9,** 451–460 (2013).

12. Henderson, J. K. *et al.* Preimplantation human embryos and embryonic stem cells show comparable expression of stage-specific embryonic antigens. *Stem Cells Dayt. Ohio* **20,** 329–337 (2002).

13. Kleinsmith, L. J. & Pierce, G. B. MULTIPOTENTIALITY OF SINGLE EMBRYONAL CARCINOMA CELLS. *Cancer Res.* **24,** 1544–1551 (1964).

14. Andrews, P. W. *et al.* Embryonic stem (ES) cells and embryonal carcinoma (EC) cells: opposite sides of the same coin. *Biochem. Soc. Trans.* **33,** 1526–1530 (2005).

15. Martin, G. R. Teratocarcinomas and mammalian embryogenesis. *Science* **209,** 768–776 (1980).

16. Evans, M. J. & Kaufman, M. H. Establishment in culture of pluripotential cells from mouse embryos. *Nature* **292,** 154–156 (1981).

17. Martin, G. R. Isolation of a pluripotent cell line from early mouse embryos cultured in medium conditioned by teratocarcinoma stem cells. *Proc. Natl. Acad. Sci. U. S. A.* **78,** 7634–7638 (1981).

18. Thomson, J. A. *et al.* Isolation of a primate embryonic stem cell line. *Proc. Natl. Acad. Sci. U. S. A.* **92,** 7844–7848 (1995).

19. Thomson, J. A. *et al.* Pluripotent cell lines derived from common marmoset (Callithrix jacchus) blastocysts. *Biol. Reprod.* **55,** 254–259 (1996).

20. Thomson, J. A. *et al.* Embryonic stem cell lines derived from human blastocysts. *Science* **282,** 1145–1147 (1998).

21. Bosma, G. C., Custer, R. P. & Bosma, M. J. A severe combined immunodeficiency mutation in the mouse. *Nature* **301,** 527–530 (1983).

22. Custer, R. P., Bosma, G. C. & Bosma, M. J. Severe combined immunodeficiency (SCID) in the mouse. Pathology, reconstitution, neoplasms. *Am. J. Pathol.* **120,** 464–477 (1985).

23. Swijnenburg, R.-J. *et al.* Immunosuppressive therapy mitigates immunological rejection of human embryonic stem cell xenografts. *Proc. Natl. Acad. Sci.* **105,** 12991–12996 (2008).

24. Reubinoff, B. E., Pera, M. F., Fong, C. Y., Trounson, A. & Bongso, A. Embryonic stem cell lines from human blastocysts: somatic differentiation in vitro. *Nat. Biotechnol.* **18,** 399–404 (2000).

25. Shamblott, M. J. *et al.* Derivation of pluripotent stem cells from cultured human primordial germ cells. *Proc. Natl. Acad. Sci. U. S. A.* **95,** 13726–13731 (1998).

26. Turnpenny, L. *et al.* Derivation of human embryonic germ cells: an alternative source of pluripotent stem cells. *Stem Cells Dayt. Ohio* **21,** 598–609 (2003).

27. Aflatoonian, B. & Moore, H. Human primordial germ cells and embryonic germ cells, and their use in cell therapy. *Curr. Opin. Biotechnol.* **16,** 530–535 (2005).

28. King, N. M. & Perrin, J. Ethical issues in stem cell research and therapy. *Stem Cell Res. Ther.* **5,** 85 (2014).

29. Chung, Y. *et al.* Embryonic and extraembryonic stem cell lines derived from single mouse blastomeres. *Nature* **439,** 216–219 (2006).

30. Klimanskaya, I., Chung, Y., Becker, S., Lu, S.-J. & Lanza, R. Human embryonic stem cell lines derived from single blastomeres. *Nature* **444,** 481–485 (2006).

31. Revazova, E. S. *et al.* Patient-specific stem cell lines derived from human parthenogenetic blastocysts. *Cloning Stem Cells* **9,** 432–449 (2007).

32. Revazova, E. S. *et al.* HLA homozygous stem cell lines derived from human parthenogenetic blastocysts. *Cloning Stem Cells* **10,** 11–24 (2008).

33. Frankel, M. S. In search of stem cell policy. *Science* **287,** 1397 (2000).

34. French, A. J. *et al.* Development of human cloned blastocysts following somatic cell nuclear transfer with adult fibroblasts. *Stem Cells Dayt. Ohio* **26,** 485–493 (2008).

35. Egli, D., Rosains, J., Birkhoff, G. & Eggan, K. Developmental reprogramming after chromosome transfer into mitotic mouse zygotes. *Nature* **447,** 679–685 (2007).

36. Cowan, C. A., Atienza, J., Melton, D. A. & Eggan, K. Nuclear reprogramming of somatic cells after fusion with human embryonic stem cells. *Science* **309,** 1369–1373 (2005).

37. Takahashi, K. *et al.* Induction of pluripotent stem cells from adult human fibroblasts by defined factors. *Cell* **131,** 861–872 (2007).

38. Jung, L. *et al.* ONSL and OSKM cocktails act synergistically in reprogramming human somatic cells into induced pluripotent stem cells. *Mol. Hum. Reprod.* **20,** 538–549 (2014).

39. Koch, C. M. *et al.* Pluripotent stem cells escape from senescence-associated DNA methylation changes. *Genome Res.* **23,** 248–259 (2013).

40. Horvath, S. DNA methylation age of human tissues and cell types. *Genome Biol.* **14,** R115 (2013).

41. Huang, K. *et al.* A Panel of CpG Methylation Sites Distinguishes Human Embryonic Stem Cells and Induced Pluripotent Stem Cells. **2,** 36–43 (2014).

42. Schmidt, R. & Plath, K. The roles of the reprogramming factors Oct4, Sox2 and Klf4 in resetting the somatic cell epigenome during induced pluripotent stem cell generation. *Genome Biol.* **13,** 251 (2012).

43. Zhang, S. C., Wernig, M., Duncan, I. D., Brüstle, O. & Thomson, J. A. In vitro differentiation of transplantable neural precursors from human embryonic stem cells. *Nat. Biotechnol.* **19,** 1129–1133 (2001).

44. He, J.-Q., Ma, Y., Lee, Y., Thomson, J. A. & Kamp, T. J. Human embryonic stem cells develop into multiple types of cardiac myocytes: action potential characterization. *Circ. Res.* **93,** 32–39 (2003).

45. Wang, L., Li, L., Menendez, P., Cerdan, C. & Bhatia, M. Human embryonic stem cells maintained in the absence of mouse embryonic fibroblasts or conditioned media are capable of hematopoietic development. *Blood* **105,** 4598–4603 (2005).

46. Kinnear, C. *et al.* Modeling and rescue of the vascular phenotype of Williams-Beuren syndrome in patient induced pluripotent stem cells. *Stem Cells Transl. Med.* **2,** 2–15 (2013).

47. Stepniewski, J. *et al.* Induced pluripotent stem cells as a model for diabetes investigation. *Sci. Rep.* **5,** 8597 (2015).

48. Samuel, R. *et al.* Generation of functionally competent and durable engineered blood vessels from human induced pluripotent stem cells. *Proc. Natl. Acad. Sci. U. S. A.* **110,** 12774–12779 (2013).

49. Lim, J. W. E. & Bodnar, A. Proteome analysis of conditioned medium from mouse embryonic fibroblast feeder layers which support the growth of human embryonic stem cells. *Proteomics* **2,** 1187–1203 (2002).

50. Sha, H. *et al.* Fates of donor and recipient mitochondrial DNA during generation of interspecies SCNT-derived human ES-like cells. *Cloning Stem Cells* **11,** 497–507 (2009).

51. Hentze, H. *et al.* Teratoma formation by human embryonic stem cells: evaluation of essential parameters for future safety studies. *Stem Cell Res.* **2,** 198–210 (2009).

52. Gutierrez-Aranda, I. *et al.* Human Induced Pluripotent Stem Cells Develop Teratoma More Efficiently and Faster Than Human Embryonic Stem Cells Regardless the Site of Injection. *Stem Cells Dayt. Ohio* **28,** 1568–1570 (2010).

53. Bowers, R. R., Kim, J. W., Otto, T. C. & Lane, M. D. Stable stem cell commitment to the adipocyte lineage by inhibition of DNA methylation: role of the BMP-4 gene. *Proc. Natl. Acad. Sci. U. S. A.* **103,** 13022–13027 (2006).

54. Zehentner, B. K., Leser, U. & Burtscher, H. BMP-2 and sonic hedgehog have contrary effects on adipocyte-like differentiation of C3H10T1/2 cells. *DNA Cell Biol.* **19,** 275–281 (2000).

55. Duggal, G. *et al.* Influence of Activin A Supplementation During Human Embryonic Stem Cell Derivation on Germ Cell Differentiation Potential. *Stem Cells Dev.* **22,** 3141–3155 (2013).

56. Valera, E., Isaacs, M. J., Kawakami, Y., Izpisúa Belmonte, J. C. & Choe, S. BMP-2/6 Heterodimer Is More Effective than BMP-2 or BMP-6 Homodimers as Inductor of Differentiation of Human Embryonic Stem Cells. *PLoS ONE* **5,** (2010).

57. Sudheer, S., Bhushan, R., Fauler, B., Lehrach, H. & Adjaye, J. FGF Inhibition Directs BMP4-Mediated Differentiation of Human Embryonic Stem Cells to Syncytiotrophoblast. *Stem Cells Dev.* **21,** 2987–3000 (2012).

58. da Silva Meirelles, L., Chagastelles, P. C. & Nardi, N. B. Mesenchymal stem cells reside in virtually all post-natal organs and tissues. *J. Cell Sci.* **119,** 2204–2213 (2006).

59. Ma, S. *et al.* Immunobiology of mesenchymal stem cells. **21,** 216–225 (2014).

60. Friedenstein, A. J., Gorskaja, J. F. & Kulagina, N. N. Fibroblast precursors in normal and irradiated mouse hematopoietic organs. *Exp. Hematol.* **4,** 267–274 (1976).

61. Bieback, K. & Netsch, P. Isolation, Culture, and Characterization of Human Umbilical Cord Blood-Derived Mesenchymal Stromal Cells. *Methods Mol. Biol. Clifton NJ* **1416,** 245–258 (2016).

62. Najar, M. *et al.* Proliferative and phenotypical characteristics of human adipose tissue-derived stem cells: comparison of Ficoll gradient centrifugation and red blood cell lysis buffer treatment purification methods. *Cytotherapy* **16,** 1220–1228 (2014).

63. Paiushina, O. V. & Domaratskaia, E. I. [Heterogeneity and possible structure of mesenchymal stromal cell population]. *Tsitologiia* **57,** 31–38 (2015).

64. Friedenstein, A. J., Piatetzky-Shapiro, I. I. & Petrakova, K. V. Osteogenesis in transplants of bone marrow cells. *J. Embryol. Exp. Morphol.* **16,** 381–390 (1966).

65. Wobus, A. M. & Boheler, K. R. Embryonic stem cells: prospects for developmental biology and cell therapy. *Physiol. Rev.* **85,** 635–678 (2005).

66. Covas, D. T. *et al.* Multipotent mesenchymal stromal cells obtained from diverse human tissues share functional properties and gene-expression profile with CD146+ perivascular cells and fibroblasts. *Exp. Hematol.* **36,** 642–654 (2008).

67. da Silva Meirelles, L. *et al.* Cultured Human Adipose Tissue Pericytes and Mesenchymal Stromal Cells Display a Very Similar Gene Expression Profile. *Stem Cells Dev.* **24,** 2822–2840 (2015).

68. Dominici, M. *et al.* Minimal criteria for defining multipotent mesenchymal stromal cells. The International Society for Cellular Therapy position statement. *Cytotherapy* **8,** 315–317 (2006).

69. Dominici, M. *et al.* Minimal criteria for defining multipotent mesenchymal stromal cells. The International Society for Cellular Therapy position statement. *Cytotherapy* **8,** 315–317 (2006).

70. Ren, G. *et al.* Inflammatory cytokine-induced intercellular adhesion molecule-1 and vascular cell adhesion molecule-1 in mesenchymal stem cells are critical for immunosuppression. *J. Immunol. Baltim. Md 1950* **184,** 2321–2328 (2010).

71. Shi, Y. *et al.* How mesenchymal stem cells interact with tissue immune responses. *Trends Immunol.* **33,** 136–143 (2012).

72. Ren, G. *et al.* Mesenchymal stem cell-mediated immunosuppression occurs via concerted action of chemokines and nitric oxide. *Cell Stem Cell* **2,** 141–150 (2008).

73. Nasef, A. *et al.* Leukemia inhibitory factor: Role in human mesenchymal stem cells mediated immunosuppression. *Cell. Immunol.* **253,** 16–22 (2008).

74. Van Overstraeten-Schlögel, N., Beguin, Y. & Gothot, A. Role of stromal-derived factor-1 in the hematopoietic-supporting activity of human mesenchymal stem cells. *Eur. J. Haematol.* **76,** 488–493 (2006).

75. Aguilar, S. *et al.* Bone marrow stem cells expressing keratinocyte growth factor via an inducible lentivirus protects against bleomycin-induced pulmonary fibrosis. *PloS One* **4,** e8013 (2009).

76. Hung, S.-P., Yang, M.-H., Tseng, K.-F. & Lee, O. K. Hypoxia-induced secretion of TGF-β1 in mesenchymal stem cell promotes breast cancer cell progression. *Cell Transplant.* **22,** 1869–1882 (2013).

77. Bai, L. *et al.* Hepatocyte growth factor mediates mesenchymal stem cell–induced recovery in multiple sclerosis models. *Nat. Neurosci.* **15,** 862–870 (2012).

78. Cao, W. *et al.* Leukemia inhibitory factor inhibits T helper 17 cell differentiation and confers treatment effects of neural progenitor cell therapy in autoimmune disease. *Immunity* **35,** 273–284 (2011).

79. Ferrara, J. L., Levy, R. & Chao, N. J. Pathophysiologic mechanisms of acute graft-vs.-host disease. *Biol. Blood Marrow Transplant. J. Am. Soc. Blood Marrow Transplant.* **5,** 347–356 (1999).

80. Igura, K. *et al.* Isolation and characterization of mesenchymal progenitor cells from chorionic villi of human placenta. *Cytotherapy* **6,** 543–553 (2004).

81. Marcacci, M. *et al.* Stem cells associated with macroporous bioceramics for long bone repair: 6- to 7-year outcome of a pilot clinical study. *Tissue Eng.* **13,** 947–955 (2007).

82. Wakitani, S. *et al.* Repair of articular cartilage defects in the patello-femoral joint with autologous bone marrow mesenchymal cell transplantation: three case reports involving nine defects in five knees. *J. Tissue Eng. Regen. Med.* **1,** 74–79 (2007).

83. Horwitz, E. M. *et al.* Isolated allogeneic bone marrow-derived mesenchymal cells engraft and stimulate growth in children with osteogenesis imperfecta: Implications for cell therapy of bone. *Proc. Natl. Acad. Sci. U. S. A.* **99,** 8932–8937 (2002).

84. Dill, T. *et al.* Intracoronary administration of bone marrow-derived progenitor cells improves left ventricular function in patients at risk for adverse remodeling after acute ST-segment elevation myocardial infarction: results of the Reinfusion of Enriched Progenitor cells And Infarct Remodeling in Acute Myocardial Infarction study (REPAIR-AMI) cardiac magnetic resonance imaging substudy. *Am. Heart J.* **157,** 541–547 (2009).

85. Bang, O. Y., Lee, J. S., Lee, P. H. & Lee, G. Autologous mesenchymal stem cell transplantation in stroke patients. *Ann. Neurol.* **57,** 874–882 (2005).

86. Keating, A. Mesenchymal stromal cells: new directions. *Cell Stem Cell* **10,** 709–716 (2012).

87. Lin, C.-S., Xin, Z.-C., Dai, J. & Lue, T. F. Commonly used mesenchymal stem cell markers and tracking labels: Limitations and challenges. *Histol. Histopathol.* **28,** 1109–1116 (2013).

88. Crisan, M. *et al.* A perivascular origin for mesenchymal stem cells in multiple human organs. *Cell Stem Cell* **3,** 301–313 (2008).

89. Vacanti, V. *et al.* Phenotypic changes of adult porcine mesenchymal stem cells induced by prolonged passaging in culture. *J. Cell. Physiol.* **205,** 194–201 (2005).

90. Wagner, W. & Ho, A. D. Mesenchymal stem cell preparations--comparing apples and oranges. *Stem Cell Rev.* **3,** 239–248 (2007).

91. Schäfer, R. *et al.* Age dependence of the human skeletal muscle stem cell in forming muscle tissue. *Artif. Organs* **30,** 130–140 (2006).

92. Frobel, J. *et al.* Epigenetic rejuvenation of mesenchymal stromal cells derived from induced pluripotent stem cells. *Stem Cell Rep.* **3,** 414–422 (2014).

93. Villa-Diaz, L. G. *et al.* Derivation of mesenchymal stem cells from human induced pluripotent stem cells cultured on synthetic substrates. *Stem Cells Dayt. Ohio* **30,** 1174–1181 (2012).

94. Diederichs, S. & Tuan, R. S. Functional comparison of human-induced pluripotent stem cell-derived mesenchymal cells and bone marrow-derived mesenchymal stromal cells from the same donor. *Stem Cells Dev.* **23,** 1594–1610 (2014).

95. Kang, R. *et al.* Mesenchymal stem cells derived from human induced pluripotent stem cells retain adequate osteogenicity and chondrogenicity but less adipogenicity. *Stem Cell Res. Ther.* **6,** 144 (2015).

96. Hynes, K., Menicanin, D., Mrozik, K., Gronthos, S. & Bartold, P. M. Generation of functional mesenchymal stem cells from different induced pluripotent stem cell lines. *Stem Cells Dev.* **23,** 1084–1096 (2014).

97. Liu, Y., Goldberg, A. J., Dennis, J. E., Gronowicz, G. A. & Kuhn, L. T. One-step derivation of mesenchymal stem cell (MSC)-like cells from human pluripotent stem cells on a fibrillar collagen coating. *PloS One* **7,** e33225 (2012).

98. Hewitt, K. J. *et al.* Epigenetic and phenotypic profile of fibroblasts derived from induced pluripotent stem cells. *PloS One* **6,** e17128 (2011).

99. Taura, D. *et al.* Adipogenic differentiation of human induced pluripotent stem cells: comparison with that of human embryonic stem cells. *FEBS Lett.* **583,** 1029–1033 (2009).

100. Lowe, C. E., O'Rahilly, S. & Rochford, J. J. Adipogenesis at a glance. **124,** 2681–2686 (2011).

101. Ali, A. T., Hochfeld, W. E., Myburgh, R. & Pepper, M. S. Adipocyte and adipogenesis. *Eur. J. Cell Biol.* **92,** 229–236 (2013).

102. Lefterova, M. I. & Lazar, M. A. New developments in adipogenesis. *Trends Endocrinol. Metab.* **20,** 107–114 (2009).

103. Das, P., Biswas, S., Mukherjee, S. & Bandyopadhyay, S. K. Association of Oxidative Stress and Obesity with Insulin Resistance in Type 2 Diabetes Mellitus. *Mymensingh Med. J. MMJ* **25,** 148–152 (2016).

104. Wang, C. *et al.* Type 2 diabetes mellitus incidence in Chinese: contributions of overweight and obesity. *Diabetes Res. Clin. Pract.* **107,** 424–432 (2015).

105. Mandviwala, T., Khalid, U. & Deswal, A. Obesity and Cardiovascular Disease: a Risk Factor or a Risk Marker? *Curr. Atheroscler. Rep.* **18,** 21 (2016).

106. Molica, F., Morel, S., Kwak, B. R., Rohner-Jeanrenaud, F. & Steffens, S. Adipokines at the crossroad between obesity and cardiovascular disease. *Thromb. Haemost.* **113,** 553–566 (2015).

107. Lim, R. B. T. *et al.* Anthropometrics indices of obesity, and all-cause and cardiovascular disease-related mortality, in an Asian cohort with type 2 diabetes mellitus. *Diabetes Metab.* **41,** 291–300 (2015).

108. Dani, C. *et al.* Differentiation of embryonic stem cells into adipocytes in vitro. *J. Cell Sci.* **110 (Pt 11),** 1279–1285 (1997).

109. Noguchi, M. *et al.* In vitro characterization and engraftment of adipocytes derived from human induced pluripotent stem cells and embryonic stem cells. *Stem Cells Dev.* **22,** 2895–2905 (2013).

110. Dani, C. *et al.* Differentiation of embryonic stem cells into adipocytes in vitro. *J. Cell Sci.* **110 (Pt 11),** 1279–1285 (1997).

111. Ahfeldt, T. *et al.* Programming human pluripotent stem cells into white and brown adipocytes. *Nat. Cell Biol.* **14,** 209–219 (2012).

112. Green, H. & Kehinde, O. An established preadipose cell line and its differentiation in culture. II. Factors affecting the adipose conversion. *Cell* **5,** 19–27 (1975).

113. Farmer, S. R. Transcriptional control of adipocyte formation. *Cell Metab.* **4,** 263–273 (2006).

114. Tontonoz, P., Hu, E. & Spiegelman, B. M. Stimulation of adipogenesis in fibroblasts by PPAR gamma 2, a lipid-activated transcription factor. *Cell* **79,** 1147–1156 (1994).

115. Shie, J. L., Chen, Z. Y., Fu, M., Pestell, R. G. & Tseng, C. C. Gut-enriched Krüppel-like factor represses cyclin D1 promoter activity through Sp1 motif. *Nucleic Acids Res.* **28,** 2969–2976 (2000).

116. Yoon, H. S. & Yang, V. W. Requirement of Krüppel-like factor 4 in preventing entry into mitosis following DNA damage. *J. Biol. Chem.* **279,** 5035–5041 (2004).

117. Birsoy, K., Chen, Z. & Friedman, J. Transcriptional Regulation of Adipogenesis by KLF4. *Cell Metab.* **7,** 339–347 (2008).

118. Spiegelman, B. M., Choy, L., Hotamisligil, G. S., Graves, R. A. & Tontonoz, P. Regulation of adipocyte gene expression in differentiation and syndromes of obesity/diabetes. *J. Biol. Chem.* **268,** 6823–6826 (1993).

119. Lee, J. M., Dedhar, S., Kalluri, R. & Thompson, E. W. The epithelial-mesenchymal transition: new insights in signaling, development, and disease. *J. Cell Biol.* **172,** 973–981 (2006).

120. Chen, X. *et al.* Krüppel-like factor 4 (gut-enriched Krüppel-like factor) inhibits cell proliferation by blocking G1/S progression of the cell cycle. *J. Biol. Chem.* **276,** 30423–30428 (2001).

121. Brey, C. W., Nelder, M. P., Hailemariam, T., Gaugler, R. & Hashmi, S. Krüppel-like family of transcription factors: an emerging new frontier in fat biology. *Int. J. Biol. Sci.* **5,** 622–636 (2009).

122. Bitzer, M., Armeanu, S., Lauer, U. M. & Neubert, W. J. Sendai virus vectors as an emerging negative-strand RNA viral vector system. *J. Gene Med.* **5,** 543–553 (2003).

123. Li, H. O. *et al.* A cytoplasmic RNA vector derived from nontransmissible Sendai virus with efficient gene transfer and expression. *J. Virol.* **74,** 6564–6569 (2000).

124. MacArthur, C. C. *et al.* Generation of Human-Induced Pluripotent Stem Cells by a Nonintegrating RNA Sendai Virus Vector in Feeder-Free or Xeno-Free Conditions, Generation of Human-Induced Pluripotent Stem Cells by a Nonintegrating RNA Sendai Virus Vector in Feeder-Free or Xeno-Free Conditions. *Stem Cells Int. Stem Cells Int.* **2012, 2012,** e564612 (2012).

125. Birsoy, K., Chen, Z. & Friedman, J. Transcriptional Regulation of Adipogenesis by KLF4. **7,** 339–347 (2008).

126. Tontonoz, P. & Spiegelman, B. M. Fat and beyond: the diverse biology of PPARgamma. *Annu. Rev. Biochem.* **77,** 289–312 (2008).

127. Zebisch, K., Voigt, V., Wabitsch, M. & Brandsch, M. Protocol for effective differentiation of 3T3-L1 cells to adipocytes. *Anal. Biochem.* **425,** 88–90 (2012).

128. Vishwanath, D. *et al.* Novel method to differentiate 3T3 L1 cells in vitro to produce highly sensitive adipocytes for a GLUT4 mediated glucose uptake using fluorescent glucose analog. *J. Cell Commun. Signal.* **7,** 129–140 (2013).

129. Barberi, T., Willis, L. M., Socci, N. D. & Studer, L. Derivation of multipotent mesenchymal precursors from human embryonic stem cells. *PLoS Med.* **2,** e161 (2005).

130. Ma, S. *et al.* Immunobiology of mesenchymal stem cells. *Cell Death Differ.* **21,** 216–225 (2014).

131. Lee, J., Dykstra, B., Sackstein, R. & Rossi, D. J. Progress and obstacles towards generating hematopoietic stem cells from pluripotent stem cells. *Curr. Opin. Hematol.* **22,** 317–323 (2015).

132. Shepard, K. A. & Talib, S. Bottlenecks in Deriving Definitive Hematopoietic Stem Cells From Human Pluripotent Stem Cells: A CIRM Mini-Symposium and Workshop Report. *Stem Cells Transl. Med.* **3,** 775–781 (2014).

133. Lengerke, C. & Daley, G. Q. Autologous blood cell therapies from pluripotent stem cells. *Blood Rev.* **24,** 27–37 (2010).

134. Schellenberg, A. *et al.* Replicative senescence of mesenchymal stem cells causes DNA-methylation changes which correlate with repressive histone marks. *Aging* **3,** 873–888 (2011).

135. Lian, Q. *et al.* Functional mesenchymal stem cells derived from human induced pluripotent stem cells attenuate limb ischemia in mice. *Circulation* **121,** 1113–1123 (2010).

136. Wu, Z. & Wang, S. Role of kruppel-like transcription factors in adipogenesis. *Dev. Biol.* **373,** 235–243 (2013).

137. Shugart, E. C. & Umek, R. M. Dexamethasone signaling is required to establish the postmitotic state of adipocyte development. *Cell Growth Differ. Mol. Biol. J. Am. Assoc. Cancer Res.* **8,** 1091–1098 (1997).

138. Krstic, M., Stojnev, S., Jovanovic, L. & Marjanovic, G. KLF4 expression and apoptosis-related markers in gastric cancer. *J. BUON Off. J. Balk. Union Oncol.* **18,** 695–702 (2013).

139. Zhang, D. *et al.* Sialyltransferase7A, a Klf4-responsive gene, promotes cardiomyocyte apoptosis during myocardial infarction. *Basic Res. Cardiol.* **110,** 28 (2015).

140. Yao, S. *et al.* Down-reguation of Krüppel-like factor-4 by microRNA-135a-5p promotes proliferation and metastasis in hepatocellular carcinoma by transforming growth factor-β1. *Oncotarget* (2016). doi:10.18632/oncotarget.9934

141. Student, A. K., Hsu, R. Y. & Lane, M. D. Induction of fatty acid synthetase synthesis in differentiating 3T3-L1 preadipocytes. *J. Biol. Chem.* **255,** 4745–4750 (1980).

142. Shaw, C. S., Jones, D. A. & Wagenmakers, A. J. M. Network distribution of mitochondria and lipid droplets in human muscle fibres. *Histochem. Cell Biol.* **129,** 65–72 (2008).

143. Bozza, P. T., Magalhães, K. G. & Weller, P. F. Leukocyte lipid bodies - Biogenesis and functions in inflammation. *Biochim. Biophys. Acta* **1791,** 540–551 (2009).

144. Tauchi-Sato, K., Ozeki, S., Houjou, T., Taguchi, R. & Fujimoto, T. The surface of lipid droplets is a phospholipid monolayer with a unique Fatty Acid composition. *J. Biol. Chem.* **277,** 44507–44512 (2002).

145. Londos, C., Brasaemle, D. L., Schultz, C. J., Segrest, J. P. & Kimmel, A. R. Perilipins, ADRP, and other proteins that associate with intracellular neutral lipid droplets in animal cells. *Semin. Cell Dev. Biol.* **10,** 51–58 (1999).

146. Ertunc, M. E. *et al.* Secretion of fatty acid binding protein aP2 from adipocytes through a nonclassical pathway in response to adipocyte lipase activity. *J. Lipid Res.* **56,** 423–434 (2015).

147. Zhou, D. *et al.* CD36 level and trafficking are determinants of lipolysis in adipocytes. *FASEB J. Off. Publ. Fed. Am. Soc. Exp. Biol.* **26,** 4733–4742 (2012).

148. DeClercq, V., d'Eon, B. & McLeod, R. S. Fatty acids increase adiponectin secretion through both classical and exosome pathways. *Biochim. Biophys. Acta* **1851,** 1123–1133 (2015).

149. Binato, R. *et al.* Stability of human mesenchymal stem cells during in vitro culture: considerations for cell therapy. *Cell Prolif.* **46,** 10–22 (2013).